الجمهورية الجزائرية الديمقراطية الشعبية
People's Democratic Republic of Algeria
وزارة التعليم العالي و البحث العلمي
Ministry of Higher Education and Scientific Research

University Mohamed Khider of Biskra
Faculty of Sciences and Technology
Department: Mechanical Engineering
Ref :……

جامعة محمد خيضر بسكـرة
كليـة العلـوم و التكنولوجيــا
قسم: الهندسة الميكانيكية
المرجع: ……..

Thesis submitted for obtaining the degree of

Doctorate in: Mechanical Engineering

Specialty (Option): Mechanical Engineering

Parametric Study of Air / Soil Heat Exchanger Destined for Cooling / Heating the Local in Arid and Semi-Arid Regions.

Presented by:

Samia HAMDANE

Thesis defended publicly 2020/2021

The jury members :

Dr. Nourredine MOUMMI	**Professor**	**Chairman**	**Biskra University**
Dr. Abdelhafid MOUMMI	**Professor**	**Supervisor**	**Biskra University**
Dr. Luis Carlos Carvalho PIRES	**Professor**	**Co-Supervisor**	**Beira Interior University**
Dr. Nourredine BELGHAR	**Professor**	**Examiner**	**Biskra University**
Dr. Zoubir NEMOUCHI	**Professor**	**Examiner**	**Constantine 1 University**

Université Mohamed Khider – Biskra

Faculté des Sciences et de la technologie

Département : Génie Mécanique

Réf : ……

جامعة محمد خيضر بسكـرة

كليـة العلـوم و التكنولوجيــا

قسم: الهندسة الميكانيكية

المرجع:.....

Thèse présentée en vue de l'obtention
Du diplôme de

Doctorat en : Génie Mécanique

Spécialité (Option) : Génie Mécanique

Etude paramétrique d'un échangeur air/sol enterré, destiné au rafraichissement et réchauffement des locaux dans les zones arides et semi arides

Présentée par :

Samia HAMDANE

Soutenue publiquement 2020/2021

Devant le jury composé de :

Dr. Nourredine MOUMMI	**Professeur**	**Président**	**Université de Biskra**
Dr. Abdelhafid MOUMMI	**Professeur**	**Rapporteur**	**Université de Biskra**
Dr. Luis Carlos Carvalho PIRES	**Professeur**	**Co-Rapporteur**	**Université de Beira Interior**
Dr. Nourredine BELGHAR	**Professeur**	**Examinateur**	**Université de Biskra**
Dr. Zoubir NEMOUCHI	**Professeur**	**Examinateur**	**Université de Constantine 1**

Acknowledgements

First of all, thanks to Allah who gives me this chance in working with such gentle and respectful group, that contains elite professors from LGM laboratory - Mohamed Khider University (Algeria) and from Electromechanics department of Beira Interior University (Portugal), during the period of preparation to obtain the Doctorate diploma in Mechanical Engineering.

I would like to direct my sincerest appreciation to my dear parents who gave me moral and material supports. I would like also to extend my gratitude to my family for them help, and special thanks to my ***sisters Abir*** and ***Marwa (Takwa Allah)*** for them effort in supporting me to finish the current thesis.

Thanks to all professors that help in producing this scientific work. I would like to mention Dr. ***Chawki MAHBOUB*** for teaching me the procedures of developing a research and the methodologic of writing a scientific research paper. Thanks to him for his time, efforts and patience thank you so much such a model professor.

I would like also to thank Pr. ***Abdelhafid MOUMMI*** who was a reason in continue my education and reaching what I am in today. Thank you so much for creating such family atmosphere, and that you never hesitate in giving your knowledge in different domains.

Thank you to Pr. ***Luis PIRES***, it was such short period in other nation that I never felt like strange person in. I really appreciate your noble actions in specific condition of Covid 19 pandemic. You were such gentle human, friendly and open mind person. Thank you for the collaboration that gave me chance to learn new knowledge.

Thank you to Pr. ***Pedro SILVA*** for guiding me in developing scientific work. Thank you for the open gate on your scientific knowledge. Thank you for being such open mind, helpful and serious. Also, I would like to pass thanks to the board of examiners.

A special thanks to the jury members Pr. **Nourredine MOUMMI**, Pr. **Nourredine BELGHAR** and Pr. **Zoubir NEMOUCHI** for their rich observations.

I want to thank the ***Mayor of El Kantara Municipality*** and ***My Colleagues*** for helping me in releasing part of the experimental study.

I would like to acknowledge all who was there for me during my academic journey that continue for 20 years since 1999 to 2020. Also, thanks to all who made this research project possible.

Dedication

I, Samia HAMDANE, dedicate my Doctorate degree including the research project and this thesis to every well hard work student. I hope this work redact in list of knowledge that benefits humanity. Also, I have pleaser to dedicate it for the prophet Mohamed (God bless him and grant him peace), my parents and my nation.

Figures list

Tables list

Nomenclature

Glossary	
AST	The apparent solar time (hour)
Cp	Heat capacity ($J.kg^{-1}.K^{-1}$)
$\dot{m}$	Mass flow rate ($kg.s^{-1}$)
r	Radius (m)
D	Diameter (m)
R	Thermal resistance ($m.K.W^{-1}$)
t	Time (week, day or hour)
T	Temperature (ºC)
U	Heat transfer coefficient ($W.m^{-1}.K^{-1}$)
V	Velocity ($m.s^{-1}$)
x	Length (m)
z	Depth (m)
Dimensionless groups	
Re	Reynold number
Pr	Prandtl number
Nu	Nusselt number
Greek letters	
α	Soil thermal diffusivity ($m^{-2}.s$)
k	Heat conductivity ($W.m^{-1}.K^{-1}$)
ρ	Density ($kg.m^{-3}$)
μ	Dynamic viscosity($kg.m^{-1}.s^{-1}$)
ω	Annual angular frequency (rad.week-1)
Abbreviations	
EAHE	Earth air heat exchanger
GHP	Ground heat pump
Subscripts	
tube	Pipe
air	Air
soil	Soil
conv	Convection

outlet	Outlet
inlet	Inlet
min	Minimum
max	Maximum
int, *ext*	Interior and exterior
Undis	Undisturbed temperature
Amp	Amplitude temperature

Contents

General Introduction

1. Introduction

Harsh climatic conditions are very difficult to live in for human, animal and plant. For example, arid and semi-arid climate in north of Africa (Algeria) is characterized by wide temperature swings both daily and seasonally. While generally, it has hot and dry summer (Lane and Nichols, 1999). life in such climate needs to create compromise to get closer for achieving comfort temperatures. For that, air conditioning systems are widely used. Unfortunately, the popular systems are not friendly to the nature.

As an arid region, BELAHYA et al. (2017) declare that more than 63 (%) of total energy consumption in residence and service sectors belong to air conditioning in Ouargla, while more than 80 (%) of Algeria surface including Biskra is in the circle of arid and semi-arid climates (BELAHYA et al., 2017) and more than 41(%) of global world areas belong to arid, semi-arid, hyper-arid and sub-humid climates (Bizikova, 2011).

Nowadays, these regions are facing the challenge of high peak electricity demands due to large residence and service sectors air conditioning penetration. It is possible to considerably reduce this energy consumption using alternative systems, where this last are friendly to the nature. Alternative systems are designed to avoid / decrease the use of classic (popular) systems. Earth to air heat exchanger (EAHE) system is one of the important solutions, where it uses the soil as source / sink of heat in winter / summer respectively, where the options of using soil as heat-source / heat-sink are results of what we call the soil thermal inertia.

Many of researches topics are about: i) soil temperature prediction in shallow depths, where several authors mention that using average annual air temperature of a region allows us predicting soil temperature in shallow depth in that region; ii) outlet air temperature prediction of EAHE system, where authors concerned the most with providing simplified models by neglecting the axial conduction through the soil in comparison with the radial conduction, so that analytical or semi-analytical solutions of these models can be easily obtained.

2. Problematic

- Does the yearly average ambient air temperature always helps in predicting soil temperature in shallow depths?
- How can we create three soil temperature reference years from three years of soil temperature records of three sites? (in Portugal as a case of study)

- What is the best option (pre-heating | pre-cooling) we could benefit by using EAHE system in each site?
- How many types of soil can we find in ten samples of soil took from four cities of Algeria's arid and semi-arid regions? What are their densities?
- During EAHE system operation, is the axial heat conduction through the soil around pipe important? If yes, when does its importance appear?

3. Objectives

Despite the benefits already known, EAHE systems still need for ameliorations studies to reach maximum benefits, especially from the side of defining soil heat distribution in shallow depths to select the correct depth which guarantees a reduced annual thermal variation to install EAHE system. Another important study that should be ameliorated is predicting outlet air temperature for long operation periods to define the correct pipe properties and correct geometric of system, where the EAHE system operation gives maximum benefits with avoiding extra energy consumption and avoiding extra system material (ex: pipe length).

4. Research significance

Research significance lies in the succession and complementation of thesis parts. We start our work by bibliographic studies that contains our principal research topics that exist in the literature, where we used the systematic reviewing method in its redaction. Then, we talked about three important parameters to control the outlet air temperature of EAHE system. After that, we realize experiences that support the present thesis, where the experiences are realized in Algeria and Portugal. Later, a numerical model is developed in term of predicting outlet air temperature of EAHE system. The developed model results demonstrate more precise results as compared with the other models that used one-dimensional heat conduction equation in the soil domain for the relatively long operation duration. This model significance is that it predicts outlet air temperature without need to define the soil around pipe radius that generally all models depend it, what makes the current study to produce results with less relative errors and closer to the heat exchange phenomena logic.

5. Research scope

The information that we include in the research scope covers the following: General purpose of the study which is realizing parametric study about EAHE system distinguished to pre-

cool and pre-heat the habitat. In this work, we highlighted the soil temperature prediction in shallow depths and the outlet air temperature prediction of EAHE system in the horizontal portion. The duration of the study was three years. In this thesis, we will discuss the topics of predicting soil temperature in shallow depths, soil physical analysis and outlet air temperature modeling of EAHE system. The geographical location covered in the study are the arid and semi- arid regions.

6. Thesis outline

This work highlighted several important points about EAHE system, where we touched upon bibliographic study, theoretical study, experimental study (soil analysis and soil temperature record in shallow depths) and system's horizontal portion modeling. The current work has been ranged in four chapters, as defined below.

First of all, we start our work by General introduction that is redacted in 5 pages. It contains introduction about the present work, problematics, objectives, research significance, research scope and thesis outline, where it has been spoke briefly about all chapters.

First chapter is redacted in 23 pages with title: Bibliographic study. We have collected several studies that touch EAHE system and soil temperature prediction, where we present the differences and additions of each research. Then, we highlighted the current study orientations.

Second chapter is redacted in 13 pages with title: Theoretical study. In this part, we have talked about three important parameters that control the outlet air temperature of EAHE system.

Third chapter is redacted in 26 pages with title: Experimental studies. This chapter is divided into two parts. First part is about comparison between using air data and soil data in predicting soil temperature. In this part, authors did an investigation about soil physical analysis and soil temperature records of 1 to 5 meters depths for 3 years (16/05/2016 until 13/05/2019) in 3 different places in Covilhã-Portugal. Second part is about selecting the types of soil and its densities, where the samples belong to Algeria's arid and semi-arid regions. We use 10 soil samples from Elkantara, Tolga, Biskra and Ouargla-Algeria.

Fourth chapter is redacted in 23 pages with title: Modelling study. In this chapter, we aim to model in more details the air thermal behaviour of an EAHE system by investigating the

validity of the hypothesis of dominant radial heat conduction in the soil surrounding the pipe, which is commonly assumed in the study of such system.

Lastly, we have concluded the thesis by conclusion that is redacted in 2 pages with title: General conclusion. This part contains introduction about the present work, overview of thesis, outcomes of thesis, concluding remarks that answer the mentioned problematic in general introduction. We finish this part by suggesting future work that takes one or more subjects of this thesis as bases to develop new studies.

References

BELAHYA, H., BOUBEKRI, A. & KRIKER, A. 2017. A comparative study about the energetic impact of dryland residential buildings with the integration of photovoltaic system *ScienceDirect,* 139**,** 738-743.

BIZIKOVA, L. 2011. Semi-arid Areas. International Institute for Sustainable Development (IISD).

LANE, L. J. & NICHOLS, M. H. 1999. Semi-arid climates and terrain. *Environmental Geology*. Dordrecht: Springer Netherlands.

Chapter I

Bibliographic Study

I.1. Generality

I.1.1. Arid and semiarid regions

Ma and Huete (2016) declared that drought has affected most regions of earth in the 21st century. The consequence of global warming is predicted to increase climate changes. Extreme climatic conditions such as heat waves and drought are very likely to intensify in the coming decades.

Map in Figure I.1 shows the global distribution of climatic zones. More than 41 (%) of land surface is arid including Algeria, where the arid climate cover more than 80 (%) of its surface (BELAHYA et al., 2017). The land surface of these climates is home of more than third of world population (Gaur and Squires, 2018).

Extreme heat waves in general have made arid regions critical places for any type of habitation. This desperate situation is expected to worsen as a result of climate change and changing weather patterns due to human activities (Gaur and Squires, 2018).

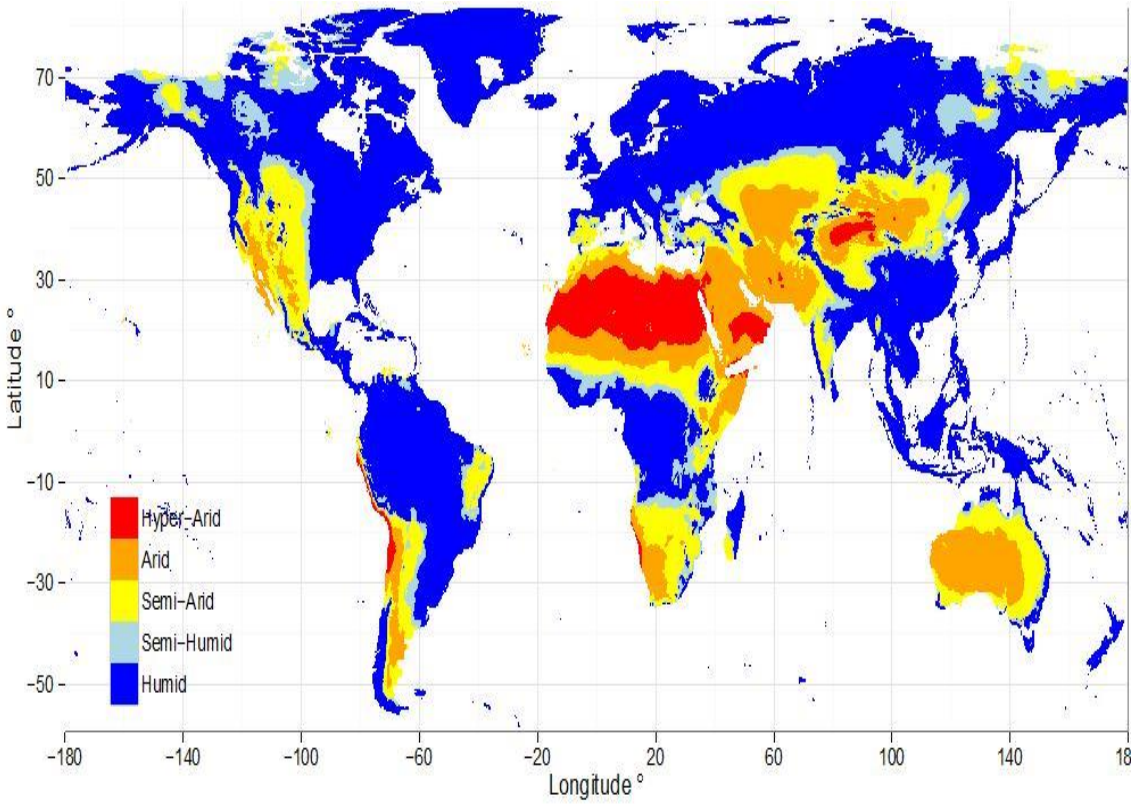

Fig. I.1 Map of global distribution of climatic zones. (Salem., 1992)

I.1.2. Aridity index

Arid environments are extremely diverse in terms of their landforms, soils, fauna, flora, water balances and the human activities that take place there. Because of this diversity, we cannot give a practical definition of arid environments. However, the element common to all arid regions is aridity. This is generally expressed as a function of precipitation and temperature. A useful "representation" of aridity is the following climatic aridity index (Salem., 1992), expressed by the ratio $\frac{P}{ETP}$.

Where P is the precipitation and ETP is the evapo-transpiration potential, calculated by Penman's method, taking into account atmospheric humidity, solar radiation and wind velocity. This index makes it possible to define three types of arid zones: hyper-arid, arid and semi-arid.

Of the total land area of the world, the hyper-arid zone covers 4.2(%), the arid zone 14.6 (%) and the semi-arid zone 12.2 (%). Thus, nearly a third of the total area of the world is made up of arid lands (Salem., 1992).

The hyper-arid zone (aridity index 0.03) includes areas devoid of vegetation, except for a few scattered bushes. A nomadic pastoralism is frequently practiced there. Annual precipitation is low and rarely exceeds 100 (mm). The rains are infrequent and irregular, sometimes non-existent for long periods that can last for several years (Salem., 1992).

The arid zone (aridity index 0.03-0.20) is characterized by pastoralism and the absence of agriculture, except where there is irrigation. Local vegetation is generally sparse, consisting of annual and perennial grasses and other herbaceous plants as well as shrubs and small trees. Precipitation is extremely variable, with annual amounts ranging from 100 to 300 (mm) (Salem., 1992).

The semi-arid zone (aridity index 0.20-0.50) can support rain-fed agriculture with more, lessor regular production levels. Sometimes sedentary breeding is also practiced there. Local vegetation is represented by various species, such as grasses and graminivore plants, non-grasses and small shrubs, shrubs and trees. Annual precipitation ranges from 300-600 to 700-800 (mm), with summer rains, and 200-250 to 450-500 millimetres with winter rains. Arid conditions are also found in the sub-humid zone (aridity index 0.50-0.75).

Fig. I.2 hyper-Arid zones from Algeria. (BELAHYA et al., 2017)

To provide comfort temperature specially for long hot summer in north of Africa, peoples who live in the habitat that exist in the arid zone use the classic air conditioning systems and/or passive cooling systems. We support the use of passive systems as we will clarify the reasons next.

I.1.3. Passive systems:

In such arid and semi-arid climate, it is important to use cooling / heating devices. The passive systems are good alternative to the classical air conditioner systems. There are different kinds of passive systems with significant low energy consumption and that have lower, or none, bad effect on the environment. Several types of passive systems are mentioned by Samuel et al. (2013) next:

a. Cooling by employing natural heat sink
   - a.1 Sky as heat sink: nocturnal radiation cooling
   - a.2 Earth as heat sink: Earth to Air Heat Exchanger (EAHE)
   - a.3 Air as heat sink
     - a.3.1 Ventilation cooling
     - a.3.2 Evaporative cooling
   - a.4 Water as heat sink
     - a.4.1 Hydro-geothermal cooling
     - a.4.2 Deep ocean/lake cooling

b. Cooling by reducing heat transfer
   - b.1 Thermal insulation
   - b.2 Shading

I.2. EAHE systems

I.2.1. EAHE systems significance

EAHE system is a passive system that shares several specifications with passive systems. It is an eco-friendly system, alternative to the classical air conditioning systems that help in the depletion of Ozone layer and global warming by chlorofluorocarbons (CFCs). EAHE system energy consumption is neglected as compared with classical air conditioning consumption. Designing EAHE system is simple as will be shown in the next component. Unlike many passive systems, Earth could be used as heat sink or source. It is significant by undisturbed temperature in certain depth during the year. This undisturbed temperature is usually lower than ambient air temperature in summer and higher than ambient temperature in winter, what makes EAHE system effective for pre-cooling the habitats in hot period (summer) and pre-heating it in cold period (winter) (Bisoniya et al., 2013).

I.2.2. EAHE system designs

EAHE system could be designed in two types: Individual design or integrated design.

I.2.2.1 EAHE system individual designs

In this part, we aim to show several examples of popular EAHE system individual designs that could be designed horizontally or vertically using single pipe or multi pipes (Figure I.3).

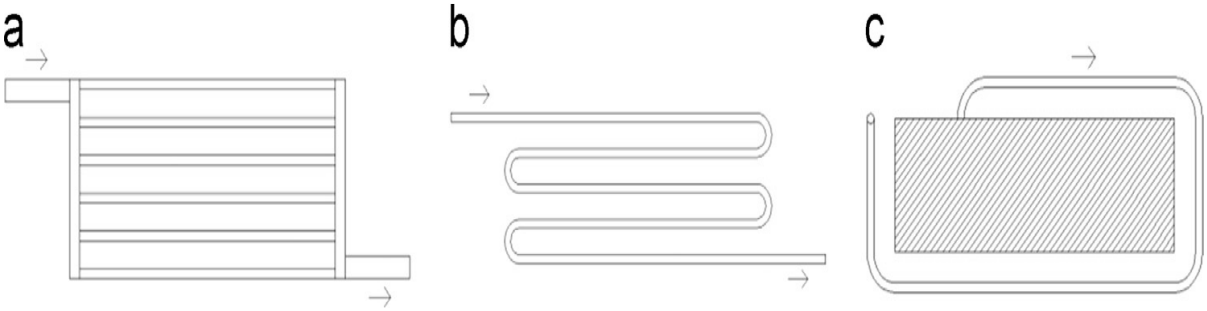

Fig.I.3 Popular EAHE systems individual design (Peretti et al., 2013).

Horizontal (b) design of EAHE system was realized in Biskra university as shown in Figure I.4 in 2008, what helped in producing several studies.

Fig. I.4 Biskra EAHE system design

I.2.2.2 EAHE system integrated designs

EAHE can be integrated to several systems to ameliorate their performance, where the integrated systems could be classic air conditioner or passive cooling / heating as shown in Figures I.5 and I.6.

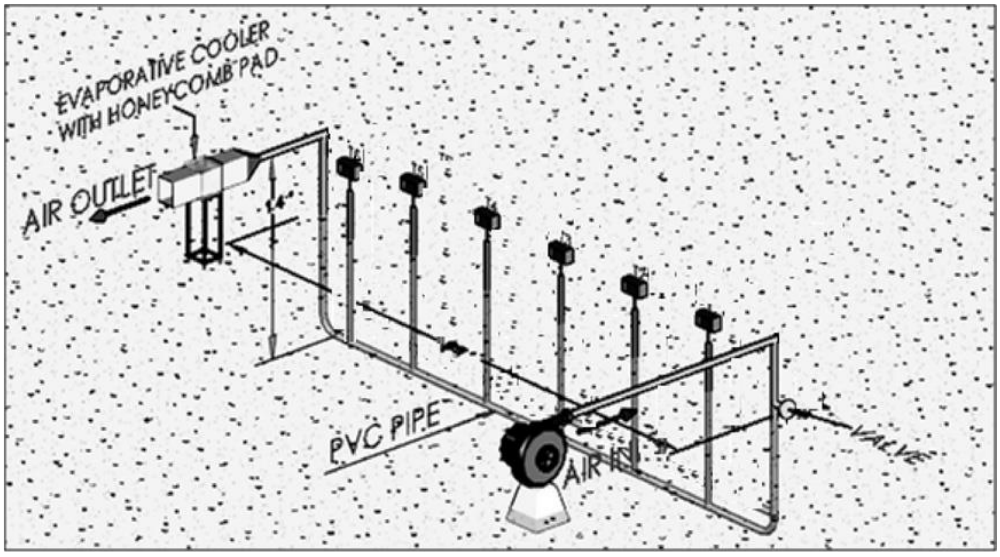

Fig. I.5 EAHE Integrated by passive system – Evaporative cooler with honeycomb pad (Bansal et al., 2012b)

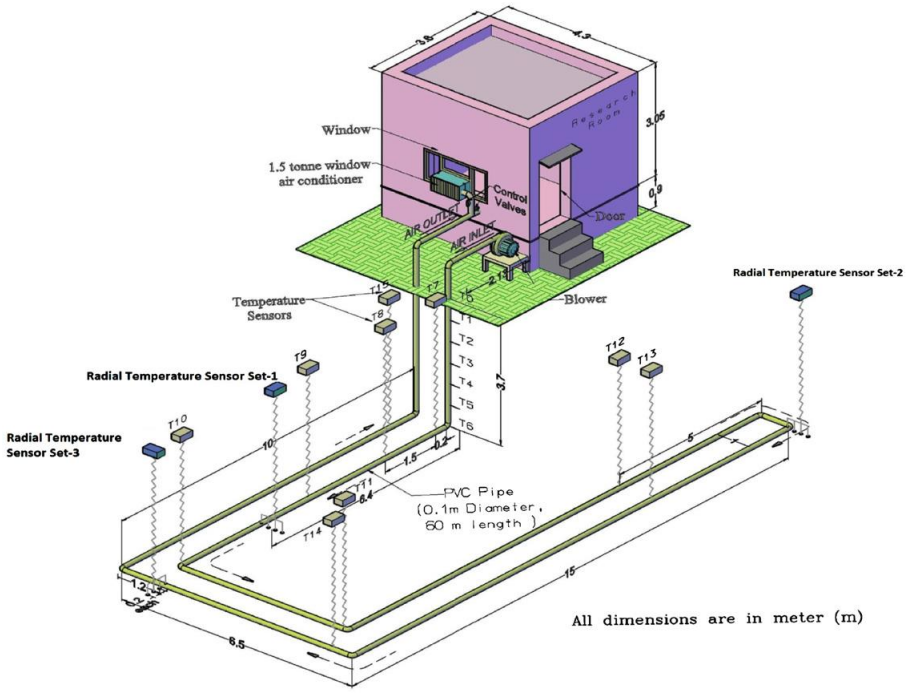

Fig. I.6 EAHE Integrated by classic system – classic air conditioner.
(Misra et al., 2012)

I.3. Bibliographic studies

I.3.1. Experimental studies

Hsu et al. (2018) draw attention to low cost EAHE design that takes up less space in high-density housing. It was about integrated system consisting of air pipes immersed in the water-filled raft foundation. Results indicated that the cooling potential of the integrated system was close to that of the soil-based EAHE at 2 (m) or more of depth (Figure I.7).

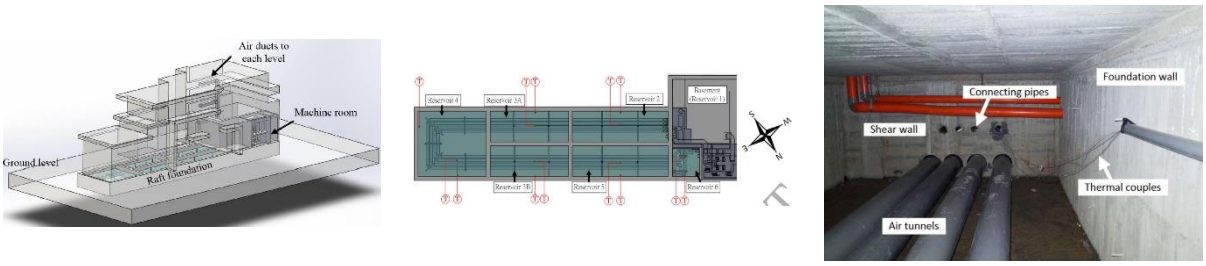

Fig. I.7 EAHE system design in high-density housing. (Hsu et al. 2018)

Bansal et al. (2012b) studied an EAHE integrated by evaporative cooling system economics in reducing / avoiding the use of cooling / heating classic devices, where it has been analysed by evaluating a simple Internal Rate of Return (IRR) on the investment. Authors use three types of electrical blower: high efficiency, middle and low efficiency. Results show that replacement of classic devices with proposed EAHE system is not a technically and

economically applicable option, where IRR value depend highly the blower efficiency (Figures I.8).

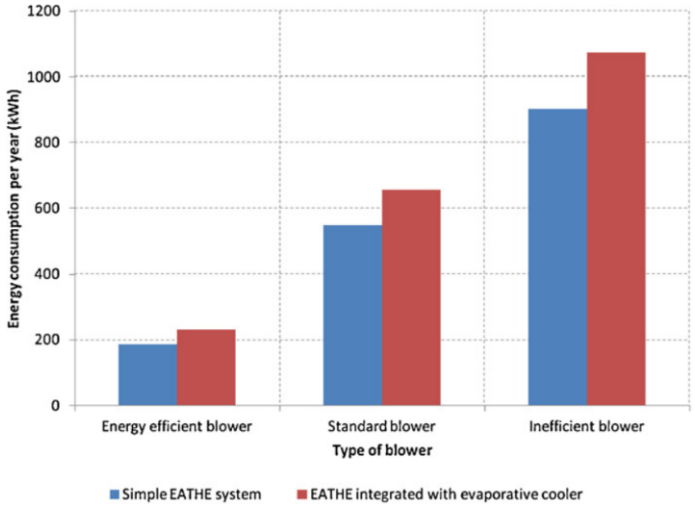

Fig. I.8 Energy consumption per year for different types of electrical blowers. (Bansal et al. 2012b)

Another study was developed by Bansal et al. (2012a) about EAHE that is integrated by evaporative cooler. The study was about analysing the integrated system in hot and dry climatic conditions. They use Computational Fluid Dynamics modelling (CFD) with FLUENT software. Results show that individual EAHE provides 4500 (MJ) of cooling effect during hot months, while the integrated EAHE by evaporative cooler can achieve 3109 MJ of additional cooling effect.

Misra et al. (2012) improve the classic air conditioner performance by integrating it with EAHE system. They declare that the power consumption decreased by 18.1 (%) when refreshed air of EAHE system is completely used by classic air conditioner condenser (Figure I.6).

Ginting et al. (2018) analyse the EAHE system performance using CFD modelling (Figure I.9). They have simulated the 3D results by Ansys software. The results comparison with experimental data of outlet air temperature of EAHE system shows that relative errors is upper than 3 (%).

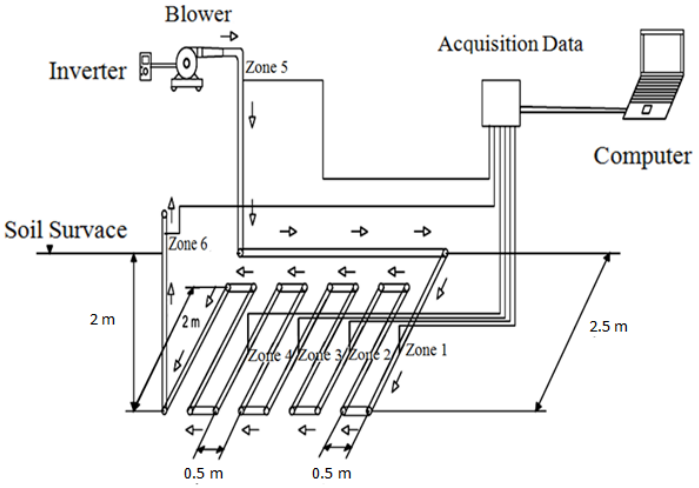

Fig. I.9 Set up experimental of EAHE system. (Ginting et al. 2018)

Singh et al. (2018) have analyzed few parameters effect on EAHE system performance, some of this parameter are velocity, length and drops in inlet air temperature. Results shows that maximum temperature drops in outlet are available in low velocity and greater length. This study has built according to complete details experimental set-up (Figure I.10).

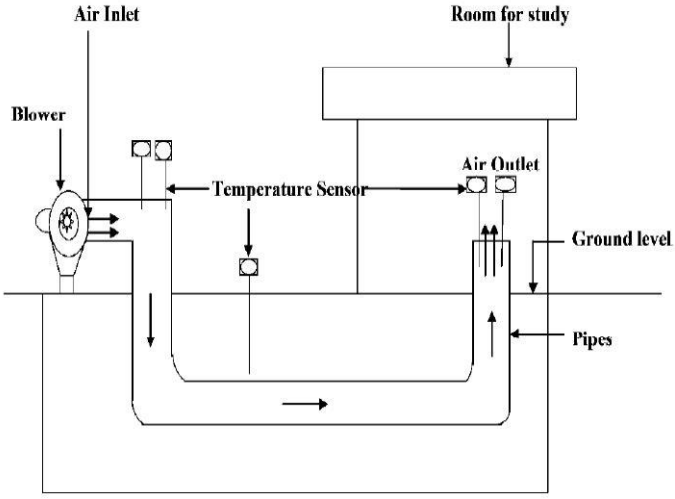

Fig. I.10 Complete setup of the system. (Singh et al. 2018)

Hamdi et al. (2018) realized an experimental investigation in Biskra university for different period from May to September. They declare that the decrease of air temperature could be even higher than 15 (°C) and that the operation duration does not affect outlet air temperature (Figure I.11).

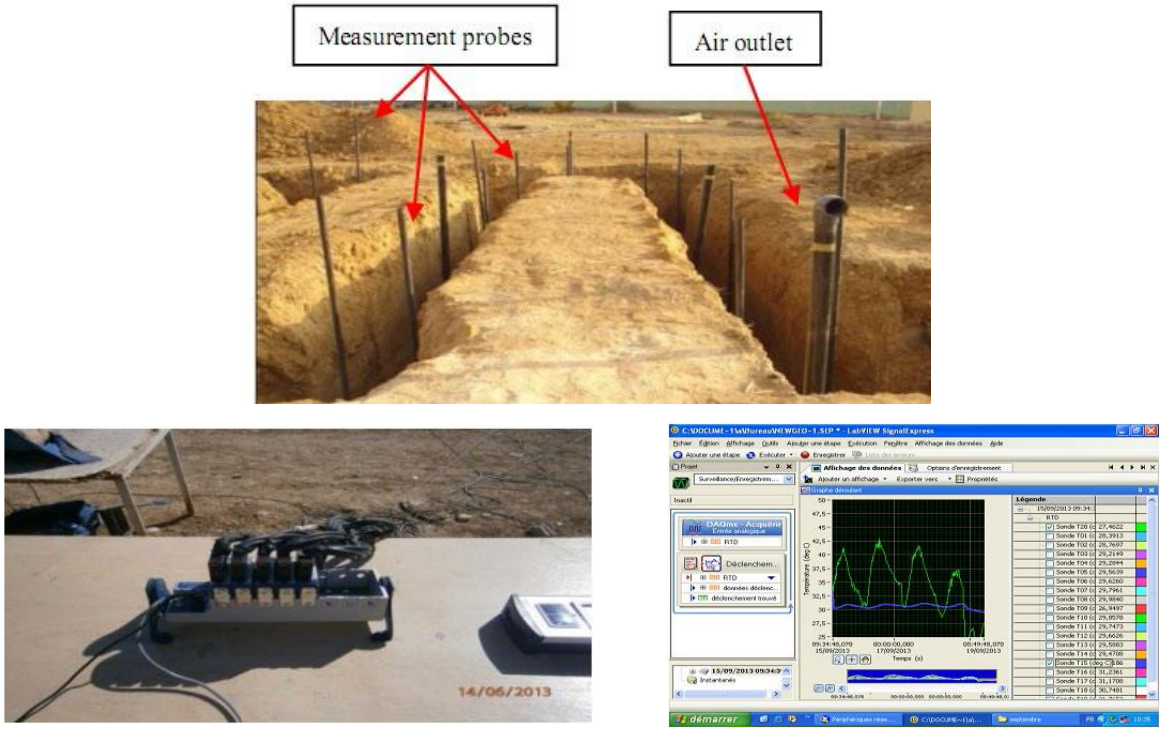

Fig. I.11 System setup and recording air temperature procedure. (Hamdi et al. 2018)

Hatraf et al. (2014) used modelling and experimental investigations to evaluate the performance of horizontal pipe in EAHE system. They conclude that several parameters influence the system performance as: soil diffusivity, depth, pipe diameter and air mass-flow rate (Figure I.12).

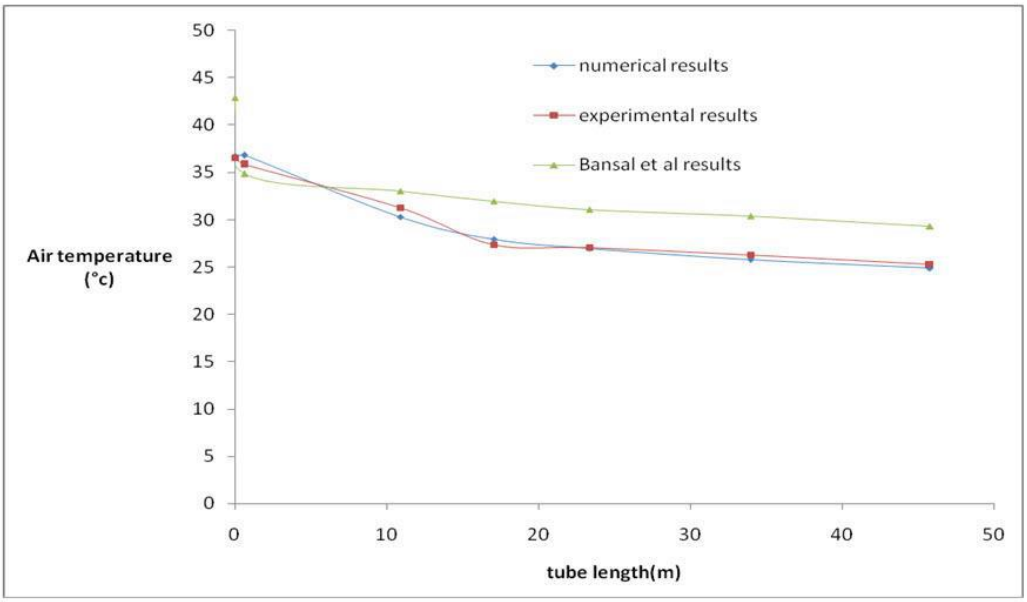

Fig. I.12 Validation and verification of Hatraf et al. (2014) model.

For three seasons since 2009, Ozgener and Ozgener (2013) investigate the exergetic performance (efficiency) of close loop EAHE system in cooling mode (Figure I.13). By the year of 2011 they had more than 40,000 of hourly thermodynamics records in cooling period. Mean cooling exergetic efficiency value was obtained to be 24(%) for 3 (years) of cooling seasons. Later, they mention new exergetic performance of EAHE system in heating mode since 2009. By 2016, more than 80,000 records of measurements have been gathered (Ozgener et al., 2017). Results show that mean heating exergetic efficiency values was 65 (%) for 7 (year) of heating seasons.

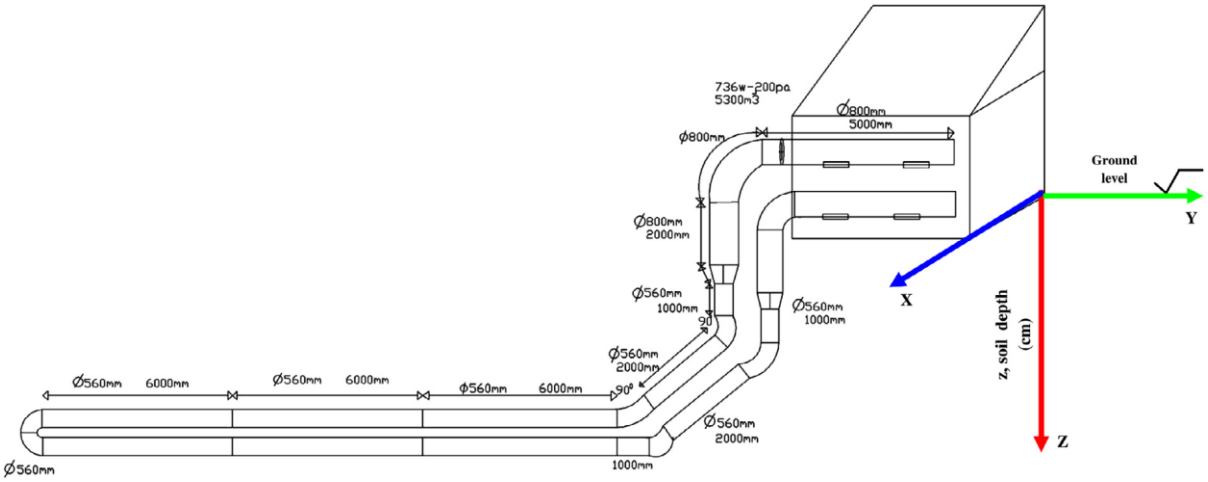

Fig. I.13 Schematic EAHE system. (Ozgener et al., 2017)

Benfatah et al. (2010) realize theoretical analysis of the phenomena through the modelling and simulation of the performance of these systems, where the experimental results allowed them to conclude that the presented model could be improved (Figure I.14).

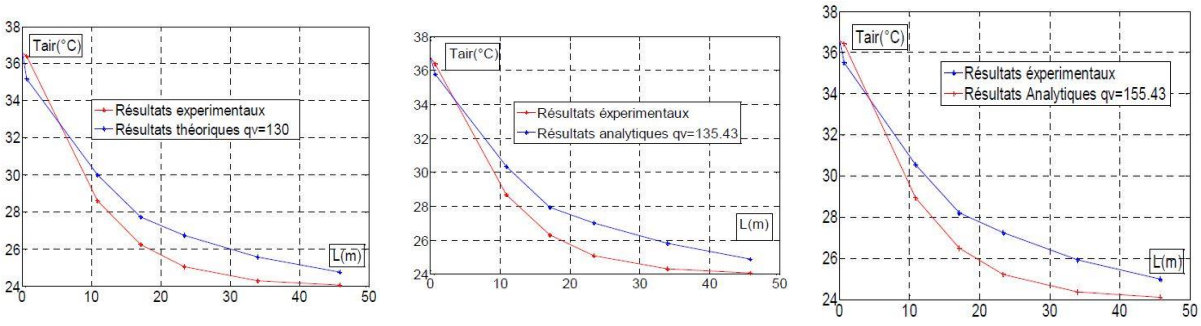

Fig. I.14 Validation of EAHE system mathematical model. (Benfatah et al. 2010)

A transient and implicit model based on CFD modelling have been developed to predict the thermal performance and cooling capacity by Bansal et al. (2010). The model has been developed using Fluent software. They compare the results by experimental investigations,

where good agreement between simulated results and experimental data is obtained. Design of EAHE system is shown in Figure I.15.

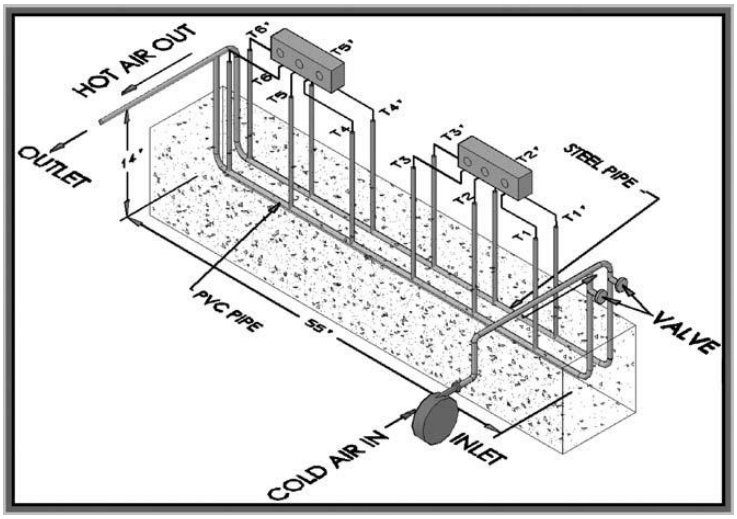

Fig. I.15 EAHE system setup. (Bansal et al. 2010)

I.3.2. Mathematical studies

I.3.2.1. EAHE system modelling

The modeling of EAHE is of huge importance when studying feasibility of such system. Solution of mathematical equation may provide us with useful information for improving the system geometry and selecting the conditions that can lead to optimum system performance. This was the subject of many research papers. Most of proposed models are using the one-dimensional energy equation in the fluid part, while different approaches have been adopted to determine the transient temperature field in the soil surrounding pipe.

Brum et al. (2019) have studied geometric configurations to assemble conduits in order to increase the thermal performance of their installations by performing various simulations with different arrangements of up to five ducts, after having imposed restrictions on the air flow and installation volumes, where they found that significant improvements in EAHE efficiency can be obtained by specific geometric configurations (Figure I.16).

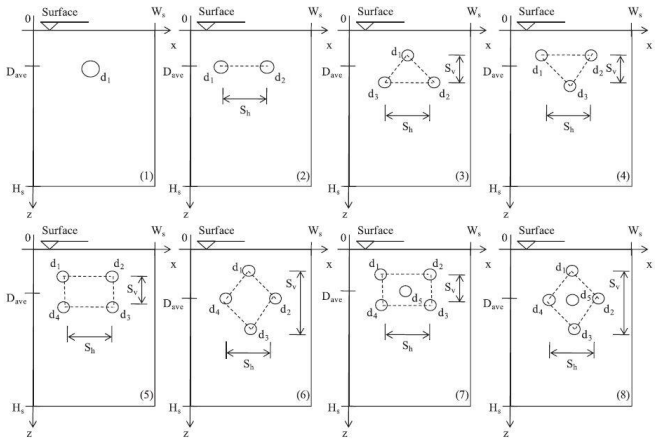

Fig. I.16 Different geometric configurations. (Brum et al. 2019)

Goswami and Dhaliwal (1985), presented heat transfer analysis and developed a computer model to predict the transient outlet air temperature while passing through an underground tube. Authors considered a transient 1D (radial) heat conduction in soil, for which a semi-analytical solution has been given utilizing an integral method (Figure I.17).

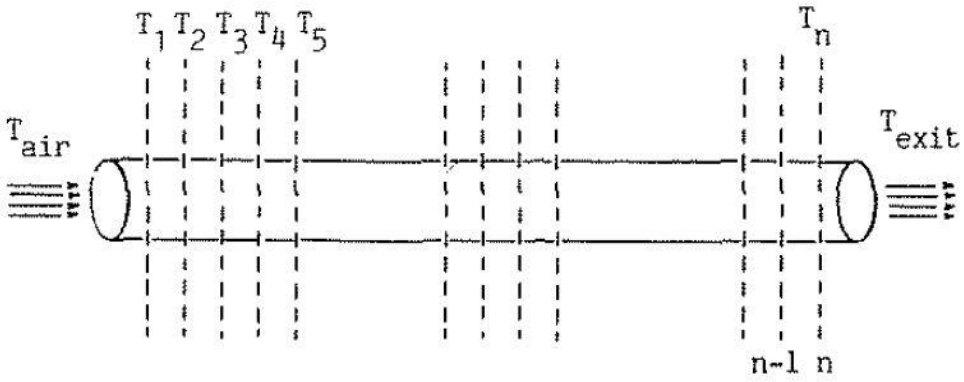

Fig. I.17 EAHE system modeling design. (Goswami and Dhaliwal 1985)

Hollmuller (2003), developed the complete analytical solution for the heat diffusion of a cylindrical air/ground heat exchanger with adiabatic or isothermal boundary condition, submitted to constant airflow with harmonic inlet temperature signal. The results show that depending on available soil radius around pipe, the harmonic signal is subjected to amplitude dampening and phase-shifting as the air passes through heat exchanger (Figure I.18).

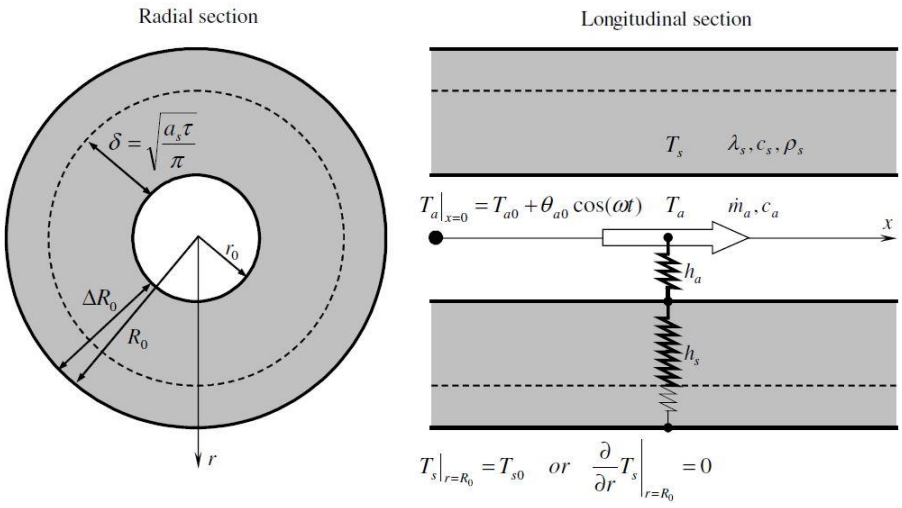

Fig. I.18 Schematic of cylindrical air/soil diffusive heat exchanger. (Hollmuller 2003)

Belatrache et al. (2016) presented the modeling and simulation of ground air heat exchanger used as air conditioning device in climate conditions in south of Algeria. Parametric analysis enabled selecting optimal depth of buried heat exchanger and pipe length allowing air temperature to reach soil temperature (Figure I.19).

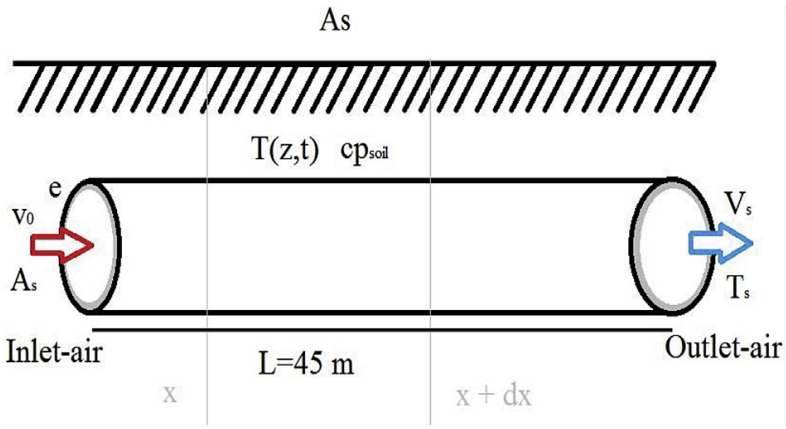

Fig. I.19 Belatrache schematic diagram of simulated EAHE system

Belloufi et al. (2017), investigated thermal performance of ground air heat exchanger in unsteady state conditions for cooling mode. Experimental investigation were performed using PVC tube of 53.16 (m) length and 110 mm diameter buried under 3 (m) depth, continuously for 71 (hours) at summer season in Biskra University-Algeria. Mathematical model for EAHE system was developed to calculate outlet air temperature along pipe horizontal/ vertical portions (Figure I.20).

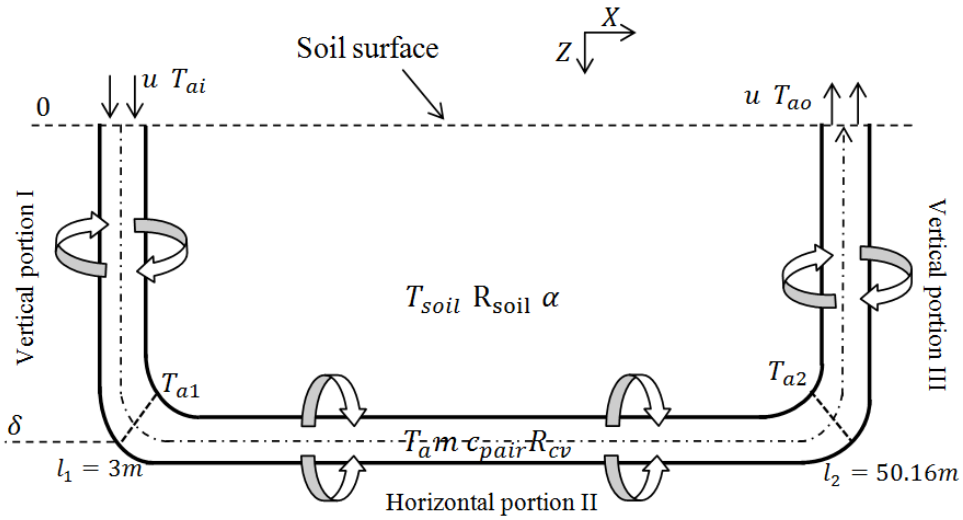

Fig. I.20 Belloufi schematic diagram of simulated EAHE system

Benhammou et al. (2017), examined the impact of thermal insulation of buildings on cooling effectiveness of Ground Air Heat Exchanger systems under hot and arid climate. Transient model was developed for whole system (EAHE+ building) and solved using technique of Complex Finite Fourier Transform (Figure I.21).

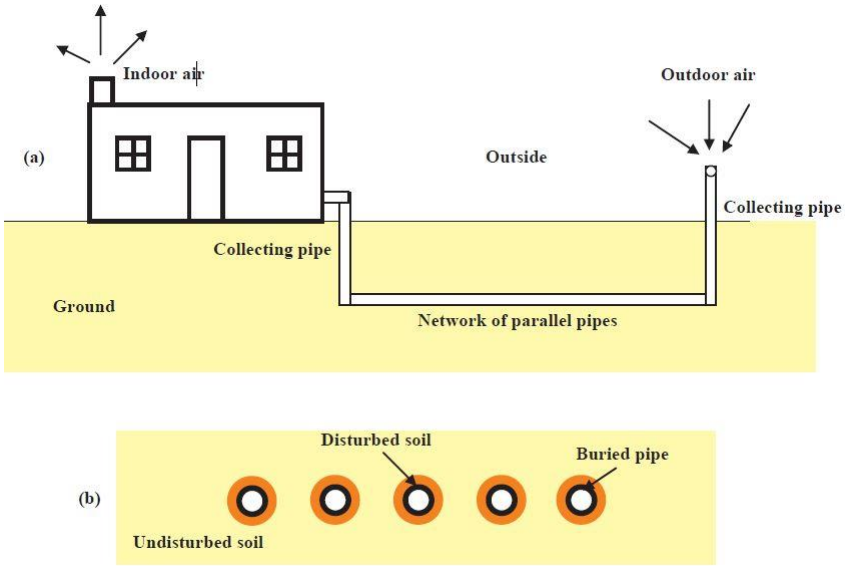

Fig. I.21 Benhammou schematic diagram of simulated EAHE system

Mehdid et al. (2018) developed semi-analytical model to predict thermal performance of EAHE system operating under transient conditions for cooling mode, by subdividing soil and pipe into layers and using a transient semi-analytical model developed earlier by Rouag et al.

(2018), to estimate soil temperature and thermal resistance of the disturbed soil around pipe (Figures I.22 & I.23).

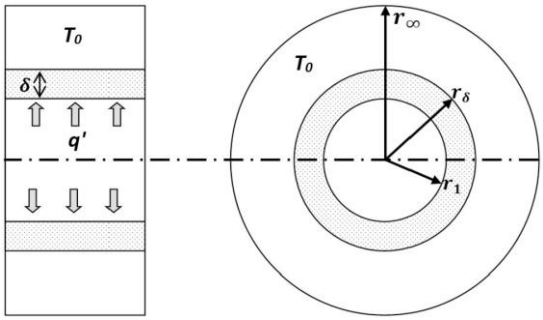

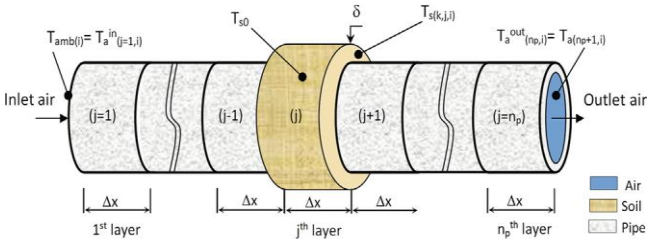

Fig. I.22 Rouag et al. (2018) schematic

Fig. I.23 Mehdid et al. (2018) schematic

Several models of predicting outlet air temperature of EAHE system were developed by previous mentioned authors. We will introduce them in next part.

I.3.2.1.1. Soil temperature

We divide soil thermal modeling in EAHE system for two part. First part is calculating soil thermal distribution in shallow depths. Second part is calculating soil thermal distribution around the pipe of EAHE system. Both 1st and 2nd parts modeling soil temperature are developed using heat conduction equation with different hypothesis. The previous researchers use the heat conduction equation in cartesian coordinates and cylindrical coordinates as shown in Equations I.5 and I.6

$$\frac{\partial}{\partial x}\left(k_s \frac{\partial T_s}{\partial x}\right)+\frac{\partial}{\partial y}\left(k_s \frac{\partial T_s}{\partial y}\right)+\frac{\partial}{\partial z}\left(k_s \frac{\partial T_s}{\partial z}\right)+q=\rho_s C_{p_s} \frac{\partial T_s}{\partial t} \qquad \text{I.5}$$

$$\frac{1}{r}\frac{\partial}{\partial r}\left(k_s r \frac{\partial T_s}{\partial r}\right)+\frac{1}{r^2}\frac{\partial}{\partial \phi}\left(k_s \frac{\partial T_s}{\partial \phi}\right)+\frac{\partial}{\partial z}\left(k_s \frac{\partial T_s}{\partial z}\right)+q=\rho C_{p_s} \frac{\partial T_s}{\partial t} \qquad \text{I.6}$$

Several developed approaches in predicting soil temperature according to depth are mentioned in Table I.1

Table I.1

Approaches to predict soil temperature in shallow depth.

Model	Authors
$-rT_{i-1,j}^{n+1}+(1+2r)T_{i,j}^{n+1}-rT_{i+1,j}^{n+1}=rT_{i,j-1}^{n}+(1-2r)T_{i,j}^{n}+rT_{i,j+1}^{n}$ $-rT_{i,j-1}^{n+2}+(1+2r)T_{i,j}^{n+2}-rT_{i,j+1}^{n+2}=rT_{i-1,j}^{n+1}+(1-2r)T_{i,j}^{n+1}+rT_{i+1,j}^{n+1}$	(Kayaci and Demir, 2018)
$T(z,t)=T_{Undis}+T_{Amp}\sin\left[\frac{2\pi}{P}(t-t_0)-\gamma z-\frac{\pi}{2}\right]$	(Ozgener et al., 2013)
$T(z,t)=T_{Undis}+T_{Amp}\cos\left[\omega(t-t_0)-\frac{z}{d}\right]\exp\left(-\frac{z}{d}\right)$	(Ben Jmaa Derbel and Kanoun, 2010)

Several researchers use the yearly amplitude of average yearly air temperature as an alternative to the amplitude of soil surface temperature. Also, they use the mean yearly air temperature as an alternative to the undisturbed soil temperature T_{Undis} (Larwa and Krzysztof, 2019; Cho and Ihm, 2018, Larwa, 2018).

I.3.2.1.2. Fluid temperature

In the current thesis, authors are aiming to develop a transient approach to predict outlet air temperature that depends on the temperature of soil around pipe in horizontal portion. For that, it has been collected several approaches from literature that has the same subject (Table I.2).

Table I.2

Approach to predict outlet air temperature.

Model	Authors
$T_{f2}=\left(1-\frac{U}{2}T_{f1}\right)+\frac{W_1-W_2}{C_p}H_{fg}+\frac{UT_s}{1+U/2}$ $T_s(r,t)=T_{in}-\frac{q''R/k}{\delta/R}\left(1+\frac{\delta}{R}-\frac{r}{R}\right)^2\left(\frac{1}{\delta/R+2\ln(1+\delta/R)}\right)\ln\left(\frac{r/R}{1+\delta/R}\right)$	Goswami and Dhaliwal (1985)
$T_f(x)=T_{s0}+(T_{f0}-T_{s0})\exp\left(-\frac{2\pi r_0}{C_f\dot{m}_f}hx\right)$ $T_s(x,r)=T_{s0}+\frac{h_f}{h_f+h_s}\frac{\ln\left(\frac{r}{R_0}\right)}{\ln\left(\frac{r_0}{R_0}\right)}(T_{f0}-T_{s0})\exp\left(-\frac{2\pi r_0}{C_f\dot{m}_f}hx\right)$	Hollmuller (2003)
$T_{f\,i,j}+\frac{\Delta t}{\gamma}T_s=-\frac{u\Delta t}{2\Delta l}T_{i-1,j+1}+\left(\frac{\Delta t}{\gamma}+1\right)T_{i,j+1}+\frac{u\Delta t}{2\Delta l}T_{i+1,j+1}$ $T_s=Cst$	Belloufi et al. (2017)
$T_f(x,t)=(T_{in}(x,t)-T_{s0})\exp\left(-\frac{1}{R_{tot}(x,t)\dot{m}C_f}\right)T_{s0}$ $T_s(x,r,t)=\frac{2}{r_\infty^2}\sum_{n=1}^{\infty}\left(\begin{array}{l}\frac{\exp(-\alpha_s\beta_n^2t_m)}{\beta_n^2}\frac{J_0(\beta_n r_t)J_0(\beta_n r_e)}{J_1^2(\beta_n r_\infty)}\times \\ \sum_{i=1}^{m}\left(\frac{T_f(x,t)-T_{s0}}{\log\left(\frac{r_\delta(x,t)}{r_e}\right)}\left[\exp(\alpha_s\beta_n^2\tau)\right]_{t-1}^{t}\right)\end{array}\right)+T_{s0}$	Mehdid et al. (2018)

Developing models that predict outlet air temperature with low relative error is helpful in developing the parametric study, that we can depend on it in the EAHE system installation.

I.3.3. Parametric studies of EAHE system

The parametric study of EAHE system that touch several parameters such as material, length, diameter, burial depth, air flow and different types of soil on the thermal efficiency

performance of EAHE systems is very important in selecting the optimum geometry and properties of EAHE system.

Darius et al. (2017) prepared a review article with previous models used to analyse the EAHE system and the operating parameters that affect the thermal performance of the Earth to Air Heat Exchanger (EAHE) as of February 2017. Recent results on the parameters that affect the EAHE performance have been presented and discussed. They conclude their work with the advent of CFD methods, the investigative work has been oriented towards modelling and simulation work because it saves time and money. Understanding of EAHE's operating parameters and their impact on system performance is largely determined. They declare that the future studies should focus on the influence of soil properties such as moisture content, soil density and soil type on the thermal performance of EAHE system.

Menhoudj et al. (2018) check the material performance of EAHE system. The study has been realized in two adjoining rooms at university of campus IGCMO-USTOMB (Oran, Algeria). They use Zinc sheet metal and PVC in pipes material for comparison study, where the two separate systems have the same geometric condition. Their cooling performance results were 35.41 (%) and 58.42 (%) for Zinc pipe and PVC pipe, respectively. They have compared the experimental records with simulation results that found by Trnsys, where it gives satisfied agreements. Later, they use the numerical simulation in varying parameters as climate, burial depth, length and pipe diameter to observe their performances. Simulations show that energy supplied by EAHE system is more significant in the south cities (Adrar and Bechar) than in the north cities (Oran) (Figure I.24).

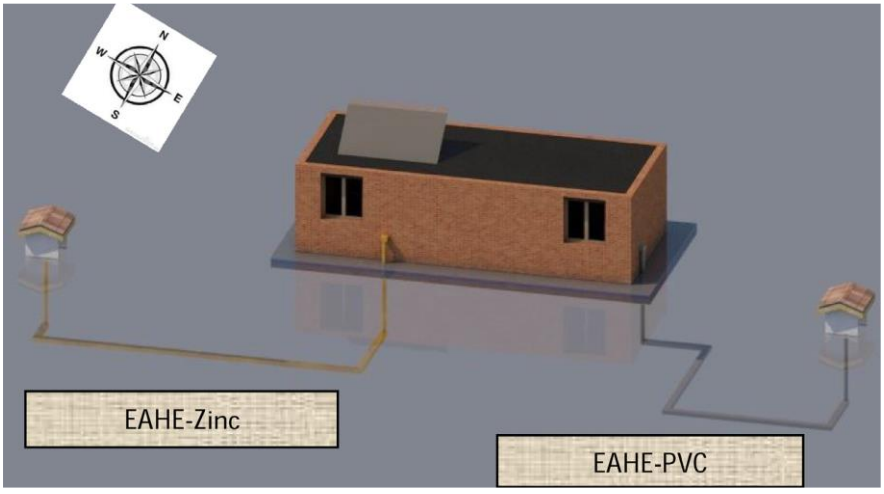

Fig. I.24 Comparison of using different material in EAHE system. (Menhoudj et al. 2018)

I.4. Conclusion

Bibliographic studies touched most important points that are main in this thesis, which are predicting outlet air temperature of EAHE system and predicting soil temperature in shallow depths.

For predicting air temperature of EAHE system, we note that the studies were concerned the most with providing simplified models by neglecting the axial conduction through the soil in comparison with the radial conduction, so that analytical or semi-analytical solutions of these models can be easily obtained. We are, on the other hand, concerned in the present study with providing a more detailed mathematical representation of the system in question so an accurate simulation can be obtained.

For the soil temperature prediction, many authors have used reference year of air temperature in certain site to calculate the average air temperature and its amplitude, where it has been mentioned that these values are available for ground too, as it simulates the yearly undisturbed soil temperature and yearly soil surface thermal wave amplitude, respectively. The authors of the present work propose a research that include comparison about using air data and soil data in predicting soil temperature and create reference year describe soil thermal behaviour in Covilhã-Portugal. To develop this research, it has been used records of ground temperature for 3 years (16/05/2016 until 13/05/2019) in 3 different places (Covilhã-Portugal), from 1 to 5 m of depths. Also, they use the known 1D heat conduction model to predict the soil thermal distribution with changing input parameters (air data and soil data).

Reference

BANSAL, V., MISHRA, R., AGARWAL, G. D. & MATHUR, J. 2012a. Performance analysis of integrated earth–air-tunnel-evaporative cooling system in hot and dry climate. *Energy and Buildings,* 47**,** 525-532.

BANSAL, V., MISRA, R., AGRAWAL, G. D. & MATHUR, J. 2010. Performance analysis of earth–pipe–air heat exchanger for summer cooling. *Energy and Buildings,* 42**,** 645-648.

BANSAL, V., MISRA, R., AGRAWAL, G. D. & MATHUR, J. 2012b. Performance evaluation and economic analysis of integrated earth–air–tunnel heat exchanger–evaporative cooling system. *Energy and Buildings,* 55**,** 102-108.

BELAHYA, H., BOUBEKRI, A. & KRIKER, A. 2017. A comparative study about the energetic impact of dryland

residential buildings with the integration of photovoltaic system *ScienceDirect,* 139**,** 738-743.

BELATRACHE, D., BENTOUBA, S. & BOUROUIS, M. 2016. Numerical analysis of earth air heat exchangers at operating conditions in arid climates. *International Journal of Hydrogen Energy,* 42**,** 8898-8904.

BELLOUFI, Y., BRIMA, A., ZEROUALI, S., ATMANI, R., AISSAOUI, F., ROUAG, A. & MOUMMI, N. 2017. Numerical and experimental investigation on the transient behavior of an earth air heat exchanger in continuous operation mode. *International Journal of Heat and Technology,* 35**,** 279-288.

BEN JMAA DERBEL, H. & KANOUN, O. 2010. Investigation of the ground thermal potential in tunisia focused towards heating and cooling applications. *Applied Thermal Engineering,* 30**,** 1091-1100.

BENFATAH, H., MOUMMI, N., HATRAF, N., MOUMMI, A. & ALI, S. Y. 2010. Etude Theorique Et Experimentale Du Rafraichissement Par La Geothermie, Application A L'habitat. *Séminaire International sur le Génie Climatique et l'Énergétique, SIGCLE'2010.*

BENHAMMOU, M., DRAOUI, B. & HAMOUDA, M. 2017. Improvement of the summer cooling induced by an earth-to-air heat exchanger integrated in a residential building under hot and arid climate. *Applied Energy,* 208**,** 428-445.

BISONIYA, T. S., KUMAR, A. & BAREDAR, P. 2013. Experimental and analytical studies of earth–air heat exchanger (EAHE) systems in India: A review. *Renewable and Sustainable Energy Reviews,* 19**,** 238-246.

BRUM, R. S., RAMALHO, J. V. A., RODRIGUES, M. K., ROCHA, L. A. O., ISOLDI, L. A. & DOS SANTOS, E. D. 2019. Design evaluation of Earth-Air Heat Exchangers with multiple ducts. *Renewable Energy,* 135**,** 1371-1385.

CHO, S.-W. & IHM, P. 2018. Development of a Simplified Regression Equation for Predicting Underground Temperature Distributions in Korea. *Energies,* 11**,** 2894.

DARIUS, D., MISARAN, M. S., RAHMAN, M. M., ISMAIL, M. A. & AMALUDIN, A. 2017. Working parameters affecting earth-air heat exchanger (EAHE) system performance for passive cooling: A review. *IOP Conference Series: Materials Science and Engineering,* 217**,** 012021.

GAUR, M. K. & SQUIRES, V. R. 2018. Geographic Extent and Characteristics of the World's Arid Zones and Their Peoples. 3-20.

GINTING , M., PANJAITAN, M. & SITORUS, T. 2018. Simulation of fluid flow in an earth-air heat exchanger with the open loop system. *IOP Conference Series: Materials Science and Engineering,* 420**,** 012026.

GOSWAMI, D. Y. & DHALIWAL, A. S. 1985. Heat Transfer Analysis in Environmental Control Using an Underground Air Tunnel. *Journal of Solar Energy Engineering,* 107**,** 141-145.

HAMDI, O., BRIMA, A., MOUMMI, N. & NEBBAR, H. 2018. Experimental study of the performance of an earth to air heat exchanger located in arid zone during the summer period. *International Journal of Heat and Technology,* 36**,** 1323-1329.

HATRAF, N., CHABANE, F., BRIMA, A., MOUMMI, N. & MOUMMI, A. 2014. Parametric Study of to Design an Earth to Air Heat Exchanger with Experimental Validation. *Engineering Journal,* 18**,** 41-54.

HOLLMULLER, P. 2003. Analytical characterisation of amplitude-dampening and phase-shifting in air/soil heat-exchangers. *Heat and Mass Transfer,* 46**,** 4303–4317.

HSU, C.-Y., CHIANG, Y.-C., CHIEN, Z.-J. & CHEN, S.-L. 2018. Investigation on performance of building-integrated earth-air heat exchanger. *Energy and Buildings,* 169**,** 444-452.

KAYACI, N. & DEMIR, H. 2018. Numerical modelling of transient soil temperature distribution for horizontal ground heat exchanger of ground source heat pump. *Geothermics,* 73**,** 33-47.

LARWA, B. 2018. Heat Transfer Model to Predict Temperature Distribution in the Ground. *Energies,* 12**,** 25.

LARWA, B. & KRZYSZTOF, K. 2019. Study of temperature distribution in the ground. *Chemical and Process Engineering,* 40**,** 123-137.

MA, X. & HUETE, A. 2016. *Semi-arid ecosystems particularly sensitive to mega-droughts* [Online]. University of Technology Sydney: OzEWEX. Available: http://ozewex.org/semi-arid-ecosystems-particularly-sensitive-to-mega-droughts/.

MEHDID, C.-E., BENCHABANE, A., ROUAG, A., MOUMMI, N., MELHEGUEG, M.-A., MOUMMI, A., BENABDI, M.-L. & BRIMA, A. 2018. Thermal design of Earth-to-air heat exchanger. Part II a new transient semi-analytical model and experimental validation for estimating air temperature. *Journal of Cleaner Production,* 198**,** 1536-1544.

MENHOUDJ, S., MOKHTARI, A. M., BENZAAMA, M.-H., MAALOUF, C., LACHI, M. & MAKHLOUF, M. 2018. Study of the energy performance of an earth—Air heat exchanger for refreshing buildings in Algeria. *Energy and Buildings,* 158**,** 1602-1612.

MISRA, R., BANSAL, V., AGARWAL, G. D., MATHUR, J. & ASERI, T. 2012. Thermal performance investigation of hybrid earth air tunnel heat exchanger. *Energy and Buildings,* 49**,** 531-535.

OZGENER, O. & OZGENER, L. 2013. Three Cooling Seasons Monitoring of Exergetic Performance Analysis of an EAHE Assisted Solar Greenhouse Building. *Journal of Solar Energy Engineering,* 135.

OZGENER, O., OZGENER, L. & GOSWAMI, D. Y. 2017. Seven years energetic and exergetic monitoring for vertical and horizontal EAHE assisted agricultural building heating. *Renewable and Sustainable Energy Reviews,* 80**,** 175-179.

OZGENER, O., OZGENER, L. & TESTER, J. W. 2013. A practical approach to predict soil temperature variations for geothermal (ground) heat exchangers applications. *International Journal of Heat and Mass Transfer,* 62**,** 473-480.

PERETTI, C., ZARRELLA, A., DE CARLI, M. & ZECCHIN, R. 2013. The design and environmental evaluation of earth-to-air heat exchangers (EAHE). A literature review. *Renewable and Sustainable Energy Reviews,* 28**,** 107-116.

ROUAG, A., BENCHABANE, A. & MEHDID, C.-E. 2018. Thermal design of Earth-to-Air Heat Exchanger. Part I a new transient semi-analytical model for determining soil temperature. *Journal of Cleaner Production,* 182**,** 538-544.

SALEM., M. B. B. 1992. Foresterie en zones arides - Guide à l'intention des techniciens de terrain.

SAMUEL, D. G. L., NAGENDRA, S. M. S. & MAIYA, M. P. 2013. Passive alternatives to mechanical air conditioning of building: A review. *Building and Environment,* 66**,** 54-64.

SINGH, B., KUMAR, R. & ASATI, A. K. 2018. Influence of parameters on performance of earth air heat exchanger in hot-dry climate. *Journal of Mechanical Science and Technology,* 32**,** 5457-5463.

Chapter II

Theoretical Study

II.1. Introduction

Simulation of the EAHE system depends on different parameters. We would like to mention three of those parameters in this chapter. First parameter is inlet air temperature, where it could be constant or variable (in this work we will present it as the variable ambient temperature). Second parameter is soil temperature, where we will introduce the parameters that control its value. Third parameter is outlet air temperature of EAHE system, where in this part of thesis we will present the simple analytical model of outlet air temperature.

II.2. Mathematical models

II.2.1. Inlet air temperature

To monitor the evolution of the outlet air temperature from EAHE system, it is important to know the variation of the ambient temperature (where system's inlet air is the outdoor air).

The outdoor (ambient) temperature, also known as the outside dry temperature, is affected by several factors, such as incident solar radiation in the earth, the duration of the day, the latitude and the altitude of the site under consideration, the surrounding weather conditions, wind, close proximity to the sea and lakes as well as mountains and vegetation.

The outside ambient temperature prediction model during a year is developed by Chabane et al. (2016). It is based essentially on the minimum temperature data T_{min} and the maximum temperature data T_{max}, where these parameters are generally based on experimental surveys carried out over several years by meteorological stations in certain geographical site.

$$T_{inlet} = Y_0 + \left(97.275 / \left(w(X_c)\sqrt{\frac{\pi}{2}} \right) \right) \exp\left(-2\left(\frac{AST - X_c}{w(X_c)} \right)^2 \right) \quad \text{II.1}$$

Where

$$Y_0 = -0.369 + 0.854\left(\frac{T_{\max} - T_{\min}}{2} \right) \quad \text{II.2}$$

$$X_c = 12.34 + 0.328\left(T_{\max} - T_{\min} \right) \quad \text{II.3}$$

$$w(X_c) = 97334.6 - 23517.399 X_c + 2127.83 X_c^2 - 85.438 X_c^3 + 1.2845 X_c^4 \quad \text{II.4}$$

II.2.2. Soil Temperature

The assessment of the potential of the use of surface geothermal energy using buried air-to-soil exchanger technology requires the determination of changes over the year from soil temperature in different depths. These variations are obtained by simple modelling, which considers the properties of the soil and the ambient temperatures.

The evolution of the ambient outside temperature is also a function of the time (day), described by a semi-empirical relation as shown in the preceding paragraph.

The soil temperature model adopted in this work considers that the heat transfer to the soil is one-dimensional, taking place solely by a dominant conduction, while considering that it is a homogeneous medium. The governing equation of the variation of the temperature in the soil is given by the following expression (Ben Jmaa Derbel and Kanoun, 2010).

$$T_{soil}(z,t) = T_{Undis} + T_{Amp}.e^{-Z\sqrt{\frac{\pi}{365a}}}\left[\cos\left(\frac{2.\pi}{365}.(t-t_0) - \frac{z}{2}.\sqrt{\frac{365}{\pi.a}}\right)\right] \quad \text{II.5}$$

With: t_0: the day that has maximum temperature in the year (days)

Z: the depth of burial from the surface of the air/soil heat exchanger (m)

α: the thermal diffusivity (m^2. $days^{-1}$)

A soil is characterized by three main parameters that directly influence its annual thermal behavior. So, these parameters affect the outlet air temperature of the EAHE system, mainly the evolution of the temperature of the injected air along the pipe depends, the soil thermal diffusivity, depth and the hottest period in year.

In this simulation study we considered several soil thermal diffusivities (Figure II.1), which allowed to follow the variation of the soil temperature for several types of soil as function of time along the year (for more information observe the Annex 1). Also, in Figure II.2 we show the affection of soil depth. The other relevant parameters that have been used took the same values in Figure II.1 and Figure II.2 are presented in Table II.1

Table II.1

Input parameters

Parameter	Value	Unit
Undisturbed soil temperature	23	(ºC)
Amplitude soil temperature	11.75	(ºC)
Hottest day in year	213	(Day)

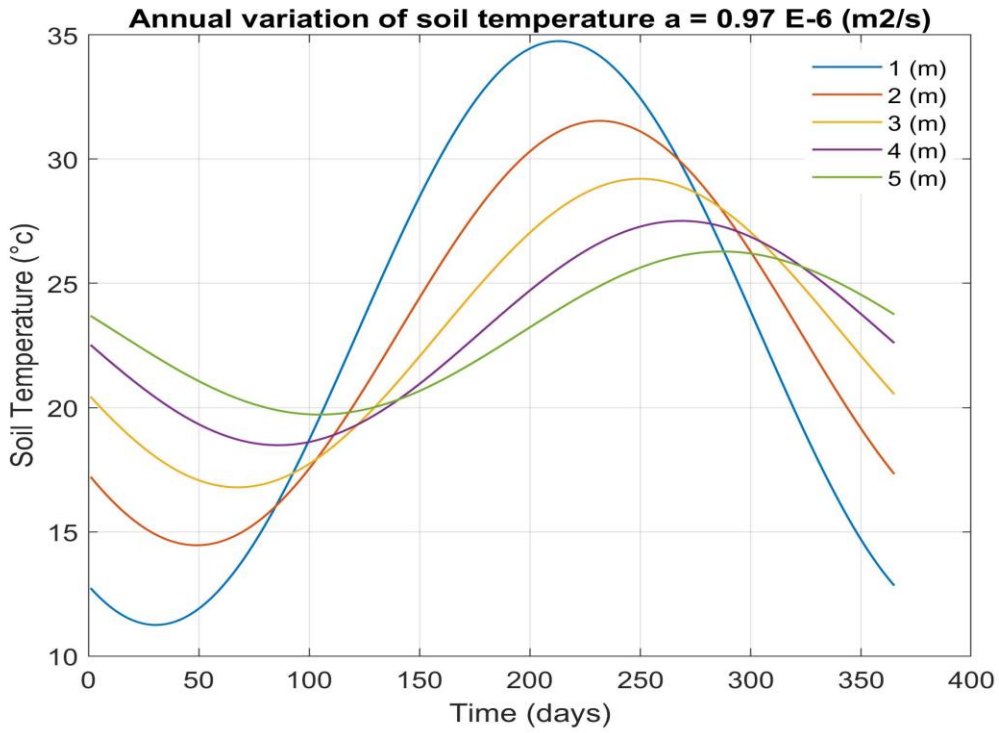

Fig. II.1 Annual variation of soil temperature in different depth,

where $\alpha = 0.97 \times 10^{-6}$ ($m^2.s^{-1}$)

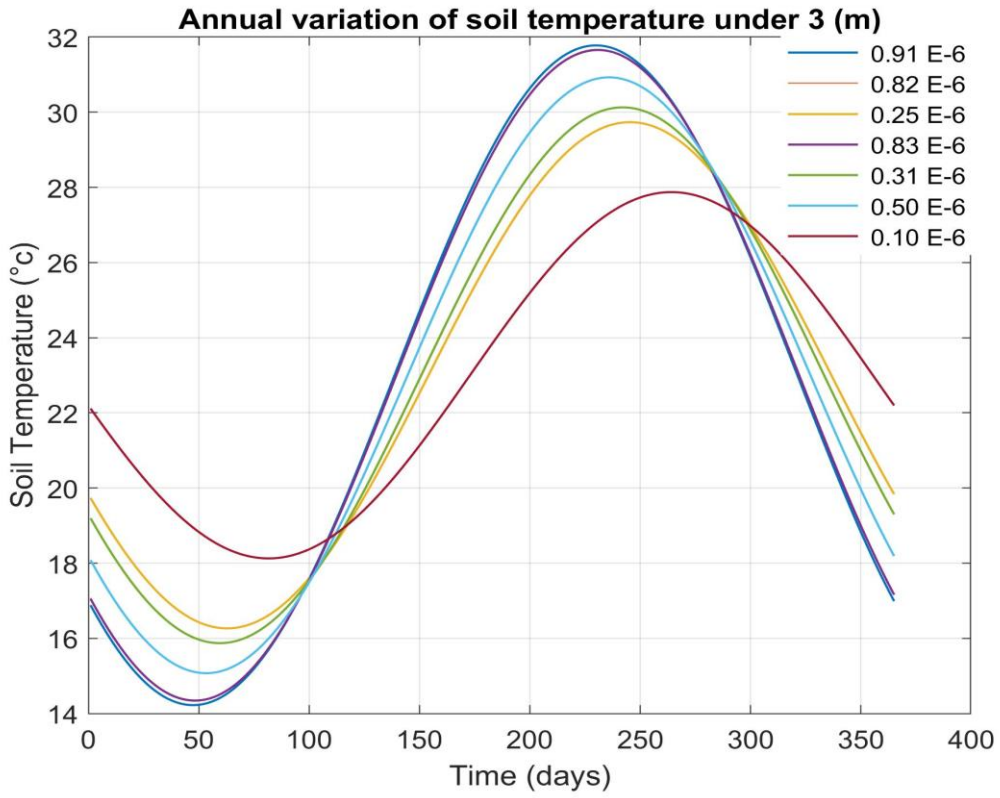

Fig. II.2 Annual variation of soil temperature for different soil types, where the depth is 3 (m)

From both Figure II.1 and Figure II.2, we can see that low thermal diffusivity and shallow depth are affected in reaching stable soil temperature during the year. The soil types are named in the Table II.2.

Table II.2

Soil type of thermal diffusivity that are showed in Figure II.4, (Andujar Marquez et al., 2016)

Type of soil	Peat	Dry gravel, dry sand	Dry clay / silt	Water saturated clay / silt	Water saturated sand	Loam
Thermal diffusivity 10^{-6} ($m^2.s^{-1}$)	0.10	0.25	0.31	0.50	0.83	0.91

II.2.3. Outlet air temperature

The evolution of the temperature at the exit of the air conveyed inside the buried air/soil exchanger is obtained from the elementary thermal balance through a section of length dx of the exchanger tube.

Integration from input to output gives the expression of the theoretical air temperature at a certain distance travelled by the fluid, which is described by the following steady analytical model (Mehdid et al., 2018).

$$T_{outlet}(L) = T_{soil} + \left(T_{inlet} - T_{soil}\right) \cdot e^{\frac{-U}{\dot{m} \cdot C_{pair}} L} \qquad \text{II.6}$$

With T_{inlet}: Corresponds to the outside ambient temperature (°C), we use the curves in figures II.5 and II.6 as examples to describe the variation of air temperature in the 15th day of December month and the 15th day of July month.

m : Mass flow of air in the pipe ($m^3.s^{-1}$)

Cp_{air} : Specific heat at constant pressure of the air ($J.kg^{-1}.K^{-1}$)

U: Overall heat transfer coefficient between air and soil ($W.m^{-1}.K^{-1}$), calculated accordingly to the next relation:

$$U = \frac{1}{R_{soil} + R_{tub} + R_{conv}} \qquad \text{II-7}$$

With R_{soil} : Thermal resistance between tube and soil ($m.K.W^{-1}$), expressed by :

$$R_{soil} = \frac{1}{2.k_{soil}.\pi} \ln\left(\frac{r_{soil}}{r_{tub-ext}}\right) \qquad \text{II-8}$$

R_{tub} : Thermal resistance of buried tube ($m.K.W^{-1}$) calculate with the next expression :

$$R_{tub} = \frac{1}{2.k_{tub}.\pi} \ln\left(\frac{r_{tub-ext}}{r_{tub-int}}\right) \qquad \text{II-9}$$

R_{conv} : Thermal resistance convection between air and tube ($m.K.W^{-1}$), is expressed by the equation next :

$$R_{conv} = \frac{1}{2.h_{conv}.\pi.r_{tub-\text{int}}} \qquad \text{II-10}$$

With,

r_{soil} : Radius of the adiabatic soil layer (m)

k_{tub} : Thermal conductivity of the buried tube ($W.m^{-1}.K^{-1}$)

k_{soil} : Thermal conductivity of soil ($W.m^{-1}.K^{-1}$)

h_{conv} : Convection coefficient of air ($W.m^{-2}.K^{-1}$) is calculated from the Nusselt number, for a turbulent flow within a circular duct cross-section, expressed by :

$$h_{conv} = \frac{Nu.\lambda_{air}}{2.r_{tub-int}} \qquad \text{II-11}$$

Where the number of Nusselt is given by the following relation:

$$Nu = 0{,}026 \cdot \mathrm{Re}^{0,8}\ \mathrm{Pr}^{0,33} \qquad \text{II-12}$$

With, Re : is the Reynolds number :

$$\mathrm{Re} = \frac{\rho_{air} V_{air} D_{inner-tube}}{\mu_{air}} \qquad \text{II-13}$$

Pr : is the Prandtl number :

$$\mathrm{Pr} = \frac{\mu_{air}.Cp_{air}}{k_{air}} \qquad \text{II-14}$$

With V_{air} : Average air velocity in the system pipe ($m.s^{-1}$).

$D_{inner\text{-}tube}$: Inside diameter of pipe (m)

μ_{air} : Dynamic viscosity of the air ($kg.m^{-1}.s^{-1}$).

k_{air} : Thermal conductivity of the air ($W.m^{-1}.K^{-1}$).

We will highlight the EAHE system function in 15th December and its function in 15th July. Also, we will highlight velocity, pipe length and pipe material affections on the outlet air temperature of EAHE system. These comparisons can be observed in Figure II.5 to Figure II.9 for $x = L$, where we suppose that daily soil temperature is constant.

As input, we have used the mentioned parameters in Table II.3

Table II.3

Shared input parameter in Equation II.6

Parameter	Value	Unit
Undisturbed air temperature	27.8 (July) 18.8 (December)	(ºC)
Amplitude air temperature	13.2	(ºC)
Soil thermal conductivity	1.5	($W.m^{-1}K^{-1}$)
Pipe thermal conductivity	0.17	($W.m^{-1}K^{-1}$)
Pipe length and system depth	55 & 3	(m)

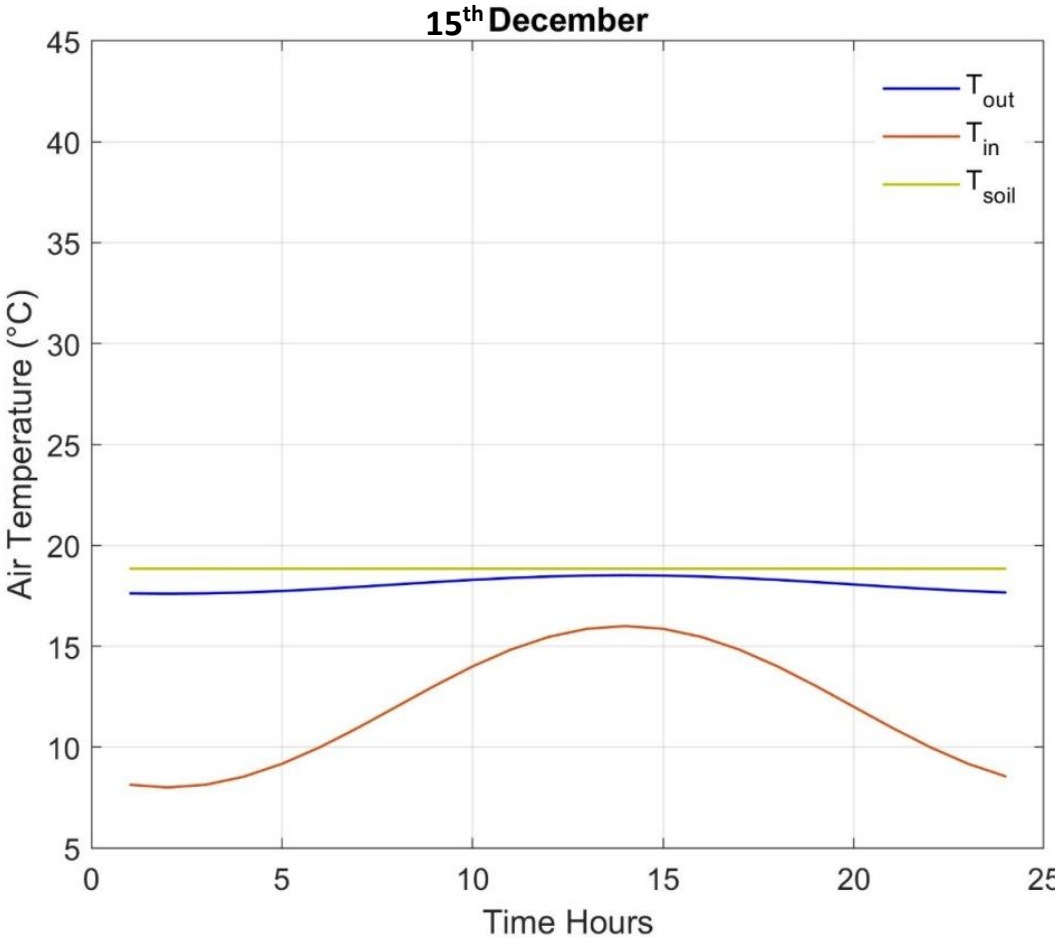

Fig. II.3 EAHE system function as pre-heater; V=3.5 ($m.s^{-1}$)

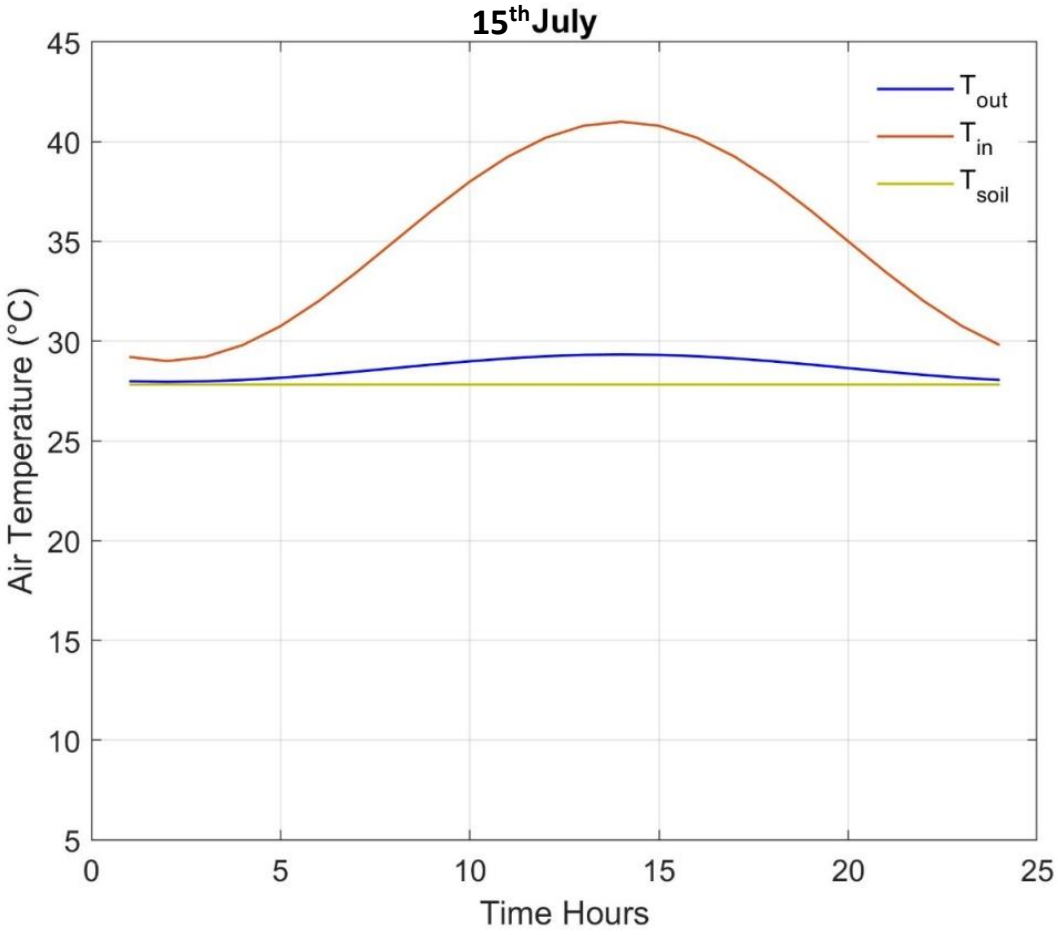

Fig. II.4 EAHE system function as pre-cooler; V=3.5 (m.s-1)

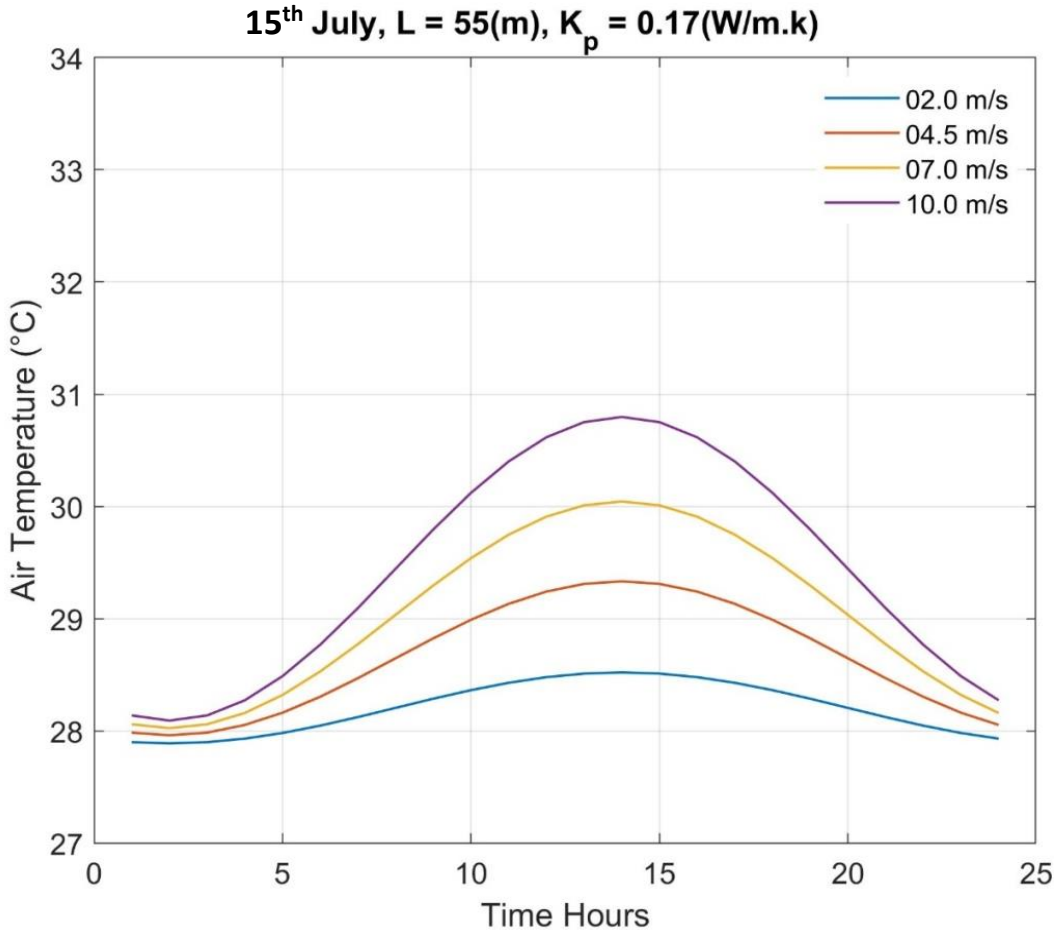

Fig. **II.5** Affection of velocity value on the outlet air temperature

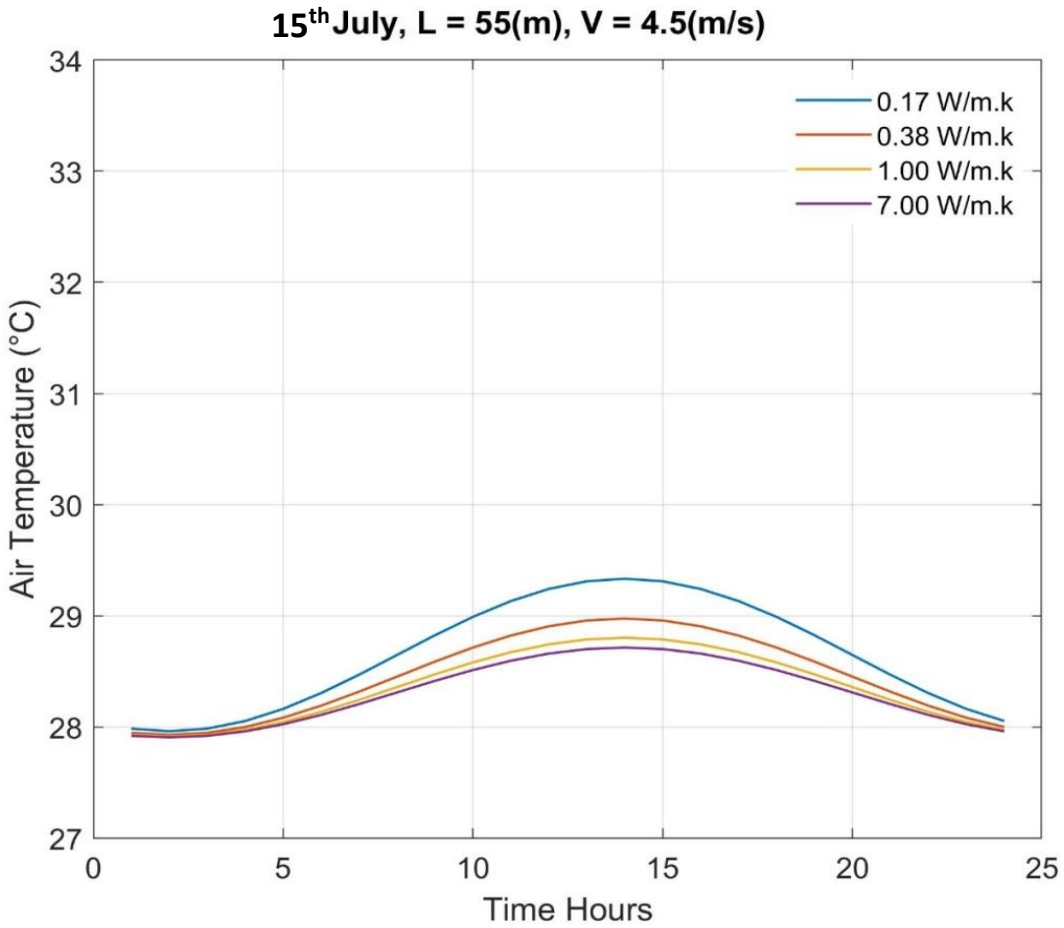

Fig. II.6 Affection of pipe thermal conductivity value on the outlet air temperature

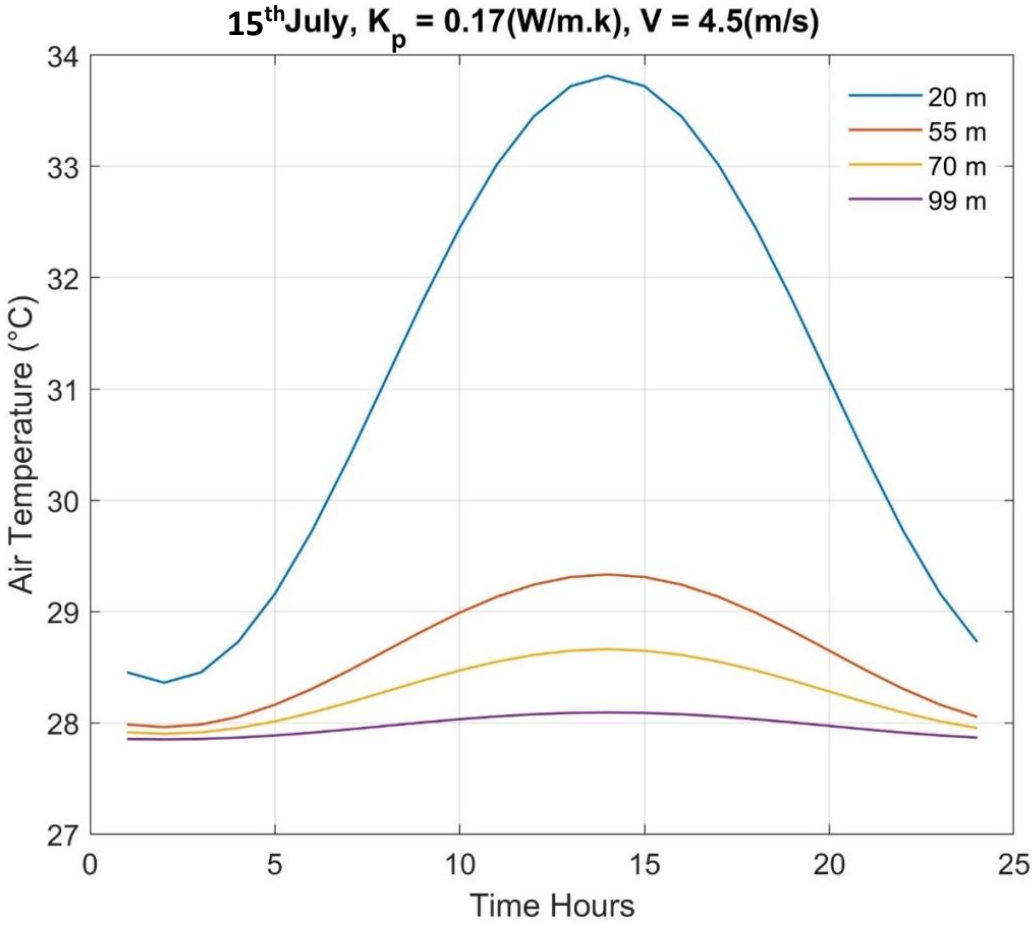

Fig. II.7 Affection of pipe length on the outlet air temperature

Figures II.3 and II.4 showed the variation of EAHE functions during the hot period and cold period. Figure II.5, Figure II.6 and Figure II.7 show the affection of velocity, pipe thermal conductivity and pipe length variation. During EAHE system function, we can see that low air velocity; higher pipe thermal conductivity and longer pipe give close temperature value to the soil one. Also, we can see that these parameters have limitations, otherwise their value will be extra useless materials.

II.3. Conclusion

1. Maximum and minimum air temperatures are parameters that could be used in predicting outdoor air temperature for a continue period.
2. Low thermal diffusivity and shallow depth do affect in reaching stable soil temperature during the year.
3. EAHE system can be used as pre-heater in cold period of year (winter). Also, it could be used as pre-cooler in hot period of the year (summer).

4. Low velocity value produce air temperature in outlet closer to the soil temperature, while it gives less quantity of cooled air.
5. The use of thermal conductivity that is higher than 0 ($W.m^{-1}K^{-1}$) and lower than 1 ($W.m^{-1}K^{-1}$) produce observable air temperature differences. While the use of thermal conductivity that is higher than 1 ($W.m^{-1}K^{-1}$) produce less observable differences.
6. Longer pipe produce air temperature closer to the soil temperature and the opposite is correct.

Reference

ANDUJAR MARQUEZ, J. M., MARTINEZ BOHORQUEZ, M. A. & GOMEZ MELGAR, S. 2016. Ground Thermal Diffusivity Calculation by Direct Soil Temperature Measurement. Application to very Low Enthalpy Geothermal Energy Systems. *Sensors (Basel),* 16**,** 306.

BEN JMAA DERBEL, H. & KANOUN, O. 2010. Investigation of the ground thermal potential in tunisia focused towards heating and cooling applications. *Applied Thermal Engineering,* 30**,** 1091-1100.

CHABANE, F., MOUMMI, N., BRIMA, A. & MOUMMI, A. 2016. Prediction of the theoretical and semi-empirical model of ambient temperature. *Frontiers in Energy,* 10**,** 268-276.

MEHDID, C.-E., BENCHABANE, A., ROUAG, A., MOUMMI, N., MELHEGUEG, M.-A., MOUMMI, A., BENABDI, M.-L. & BRIMA, A. 2018. Thermal design of Earth-to-air heat exchanger. Part II a new transient semi-analytical model and experimental validation for estimating air temperature. *Journal of Cleaner Production,* 198**,** 1536-1544.

Chapter III

Experimental Study

III.1. Introduction

In this chapter, we were interested to collect and realize two experiences. The first series of experiences were about soil temperature records that carried out in University of Beira Interior (UBI), Covilhã-Portugal between 16/05/2016 and 13/05/2019, where the shared work comes after the collaboration that have been realized in parallel when I was in Portugal for ERASMUS+ program. The purpose of these experiences was to record soil temperature and compare the use of soil data and the use of air data in predicting soil temperature in shallow depths. Later, we create references years of soil temperature.

The second experimental work were about analysing the density and texture of soil from different sites included in Algeria's arid and semi-arid regions, where the samples took from Elkantara, Biskra, Tolga and Ouargla. The experimental protocols were realized in the physico-chemical analysis laboratory of the agronomy department, Mohamed Khider University, Biskra-Algeria.

III.2. First experience : Soil Temperature

III.2.1. Introduction

We have used the known analytical model developed using the one-dimensional heat conduction equation to predict the soil thermal distribution in shallow depth during year. As input, we use the annual average air temperature (air data) and soil temperature records (soil data) to compare the output. Later, we have validated the obtained results by using the records of ground temperature for the 03 years $(16/05/2016 \text{ until } 13/05/2019)$ in 3 different places in Covilhã-Portugal (Table III. 2), under 1 to 5 (m) of depth.

III.2.2. Analytical model

We suppose that each site is homogeneous. Then, we have changed the thermal diffusivity values in literature ranges, (Márquez et al., 2016), according to soil texture in Table III. 1, to reach better agreement in model results with experimental data. This proceeding is applied only in 1st(m) depth, where the thermal diffusivities that obtained are used in the other depths.

Warmest week in year is defined as t_0. Its values according to soil temperature records are 15, 17 and 16 (weeks) after 16 May in the 3 years of experiences, for A, B and C sites, respectively.

The mathematical model is developed using transient 1D heat conduction equation for homogenous solid (Ben Jmaa Derbel and Kanoun, 2010).

$$\frac{1}{\alpha}\frac{\partial T}{\partial t} = \frac{\partial^2 T}{\partial z^2} \quad \text{III.1}$$

Boundary condition

$$z = 0 \quad , \quad T(z,t) = T(0,t)$$
$$z \to +\infty \ , \quad T(z,t) = T_{undis}$$

Where

$$T(0,t) = T_{undis} + T_{amp}\left[\cos\left(\omega(t - t_0)\right)\right] \quad \text{III.2}$$

And

$$T(z,t) = T_{undis} + T_{amp}\left[\cos\left(\omega(t - t_0) - \frac{z}{d}\right)\right] e^{-\frac{z}{d}} \quad \text{III.3}$$

where $d = \sqrt{2\frac{\alpha}{\omega}}$, and $\omega = 2\pi/52$ and 52 is the number of weeks during year, ($52 \approx 365/7$)

T_{amp} is the soil temperature wave amplitude $\left(T_{max} - T_{min}\right)/2$.

With :

T	Temperature (ºC)
t	Time (weeks)
ω	Annual angular frequency (rad.week^{-1})
α	Soil thermal diffusivity (m^2.week^{-1})
$undis$	Undisturbed soil

III.2.3. Experimental studies

III.2.3.1. Purpose and description

In the present work, the purposes of recording soil temperatures are:

- Calculate parameters needed in the previous mathematical model (soil thermal wave amplitude and average soil temperature).
- Show the preciseness of model results in predicting soil temperature for different sites, using soil data and air data.
- Create reference year for soil temperature in each site.

Experimental setup was prepared and implemented in 2016 in Covilha-Portugal. Drillings were made in the soil to a depth of 5 meters in 3 different locations. Temperature probes, each one with 5 type-T thermocouples, were inserted in each hole for soil temperature measurements at different depths: 1 (m), 2 (m), 3 (m), 4 (m) and 5 (m).

Ground surface in site A is covered by trees. It is located between buildings and stream, where the distance between stream and site is about 4 (m), while that stream depth is about 5 (m). Ground surfaces in sites B and C are bare. Those last exist in hill, where site B exhibit in front solar in part of day (morning period) and site C exhibit in front solar in all daytime.

III.2.3.2. Soil analysis

Samples have been taken from the sites A, B and C to be analysed. Protocol used in analysing those samples is soil sifting after drying it, (Figures III.1 & III.2), where it has been found 3 soil textures with different percent in each sample of the three sites, (Table III. 1). Soil thermal diffusivities α of principle compositions in each soil type are defined according to literature (Márquez et al., 2016).

- Dry sand $[0.19 \div 0.34] \times 10^{-6} (m^2.s^{-1})$
- Water saturated sand $[0.59 \div 1.72] \times 10^{-6} (m^2.s^{-1})$
- Dry silt and clay $[0.25 \div 0.62] \times 10^{-6} (m^2.s^{-1})$
- Water saturated silt and clay $[0.26 \div 0.68] \times 10^{-6} (m^2.s^{-1})$.

Fig. **III.1** Soil Samples, A, B and C respectively

Fig. III.2 Soil sifting equipment

Table III. 1

Soil texture in sites A, B and C.

Texture		Sand	Clay	Pebbles	Thermal Diffusivity $10^{-6}(m^2.s^{-1})$
Site	A	45 (%)	19 (%)	36 (%)	0.9921
	B	46 (%)	42 (%)	12 (%)	1.5708
	C	47 (%)	34 (%)	19 (%)	0.8267

III.2.3.3. Soil temperature records (Equipment details)

Thermocouples used in the experiences are type T, where this type has larger range of temperature measurement. Datalogger acquisition used has 12 canals. Canals accept all thermocouple types. The accuracy of datalogger with thermocouple is $\Delta T = \pm 0.5$ (℃).

Fig. III.3 Drilling machine

Fig. III.4 Thermocouple type T

Fig. III.5 Probe inserted in perforated hole

Fig. III.6 Datalogger acquisition

III.2.4. Result and discussion

III.2.4.1. Soil data

Table III. 2

Weekly noon soil temperature records according to depth (16/05/2016 until 13/05/2019) Covilhã-Portugal

	Depth (m)	**Soil Temperature** (℃)						
	1	11.7	14.5	15.1	-	-	12.2	13.3
	2	12.8	13.6	14.6	-	-	11.8	14.1
A	3	13.3	14	14.7	-	-	13.5	14.6
	4	13.9	14.6	15.2	-	-	14.3	15.2
	5	14.8	15.4	15.9	-	-	15.5	15.4
	1	11.9	13.2	14.2	-	-	10.3	13
	2	11	10.6	12.1	-	-	12.2	12.1
B	3	11.2	11.1	11.7	-	-	12.9	9.9
	4	10.6	10	10.9	-	-	13.5	10.6
	5	10.2	10.3	11.2	-	-	14.8	14.5
	1	12.3	14.8	15.9	-	-	11.1	12.2
	2	11.5	11.4	13.9	-	-	12.3	11.3
C	3	11.9	11.8	12.9	-	-	13.1	10.2
	4	10.7	10.1	11.7	-	-	13.5	10
	5	11.3	11.4	12	-	-	13.2	9.7

Ground control volume is the soil from 1 to 5 (m) of depths. It has been used the records of 1 (m) depth to calculate the ground thermal wave amplitude (Table III.3). Also, it has been calculated the average ground temperature records in 5 (m) to be used as undisturbed temperature for each site (Table III.4).

Table III. 3

Ground thermal wave amplitude.

Time (year)		**2016/2017**	**2017/2018**	**2018/2019**	**Average**
	A	7.4	7.8	9.0	8.1
Temperature (℃)	**B**	7.7	6.2	5.7	6.5
	C	9.8	9.1	7.7	9.0

Table III. 4

Undisturbed ground temperature.

Time (year)		2016/2017	2017/2018	2018/2019	Average
	A	16.4	16.7	17.3	16.8
Temperature (℃)	**B**	13.3	13.2	13.3	13.3
	C	13.9	13.9	13.4	13.7

The different value of undisturbed soil temperature between A versus B and A versus C location is because: the large distance between locations and the different condition around those location, while the similar thermal behaviors between B and C locations are because of less distance and both are in the same hill (Tables III.4).

Damping depth

Ground thermal wave amplitude is important information. Using Equation III.3 minus T_{undis} allows the user to calculate the depth of undisturbed temperature in soil, which calls also damping depth. The present model shows damping depth in 10 (m) for A and C sites and in 11 (m) for B site (Figure III.7) with ± 0.5 (ºC) of yearly soil temperature variation.

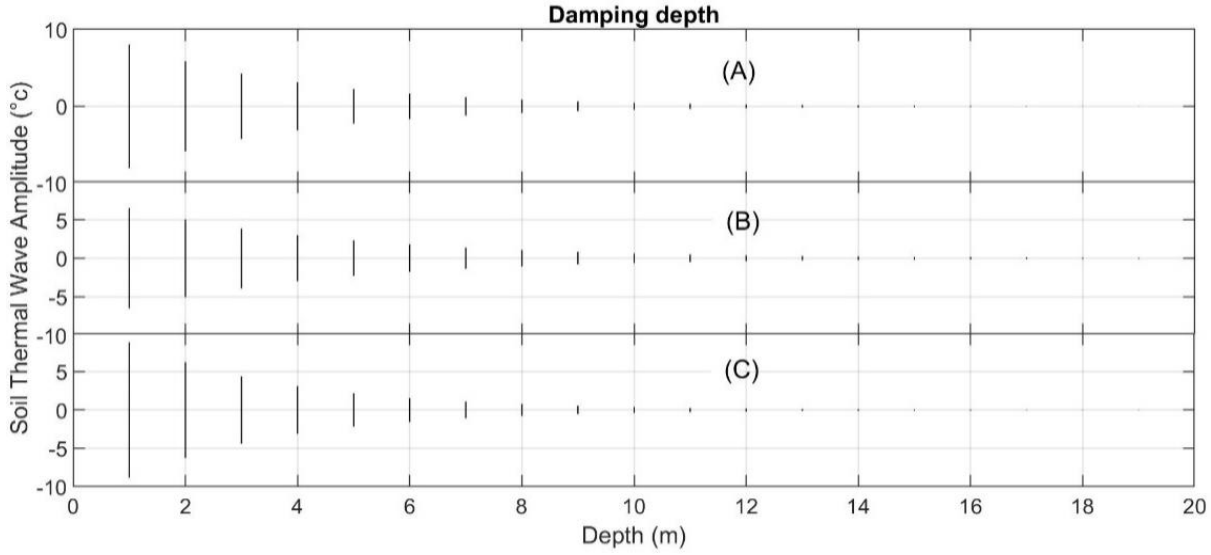

Fig. III.7 Damping depth for sites A, B and C

III.2.4.2. Air data

Typical reference year for air temperature in Covilhã from meteorological data bases of SolTerm software (Aguiar and Carvalho, 2012) is used to calculate the air thermal wave amplitude and the average air temperature, where those values were 7.7 (℃) and 12.1 (℃) respectively.

III.2.4.3. Comparison between air data and soil data

In this part, we show the differences between the average values of ground thermal wave amplitude and the average values of undisturbed ground temperature that took from Tables III.3 and III.4 as compared with Air data (Table III.5).

Table III.5

Air data versus soil data.

Site	Soil Data			Air Data
	A	B	C	A, B & C
Undisturbed Soil Temperature (ºC)	16.8	13.3	13.7	12.1
Amplitude Soil Temperature (ºC)	8.1	6.5	9.0	7.7

III.2.4.4. Validation and verification

To predict the soil temperature, we use the values of ground thermal wave amplitude and the values of undisturbed ground temperature of each year as input for Equation III.3 (Tables III.3 and III.4), where the inputs are named soil data. Also, we use air thermal wave amplitude and average air temperature as input for Equation III.3, where the inputs are named air data.

To validate the model results, we use the experimental records of soil temperatures in each year of A, B and C sites. Also, the model results are verified together (Figure III.8 until Figure III.22).

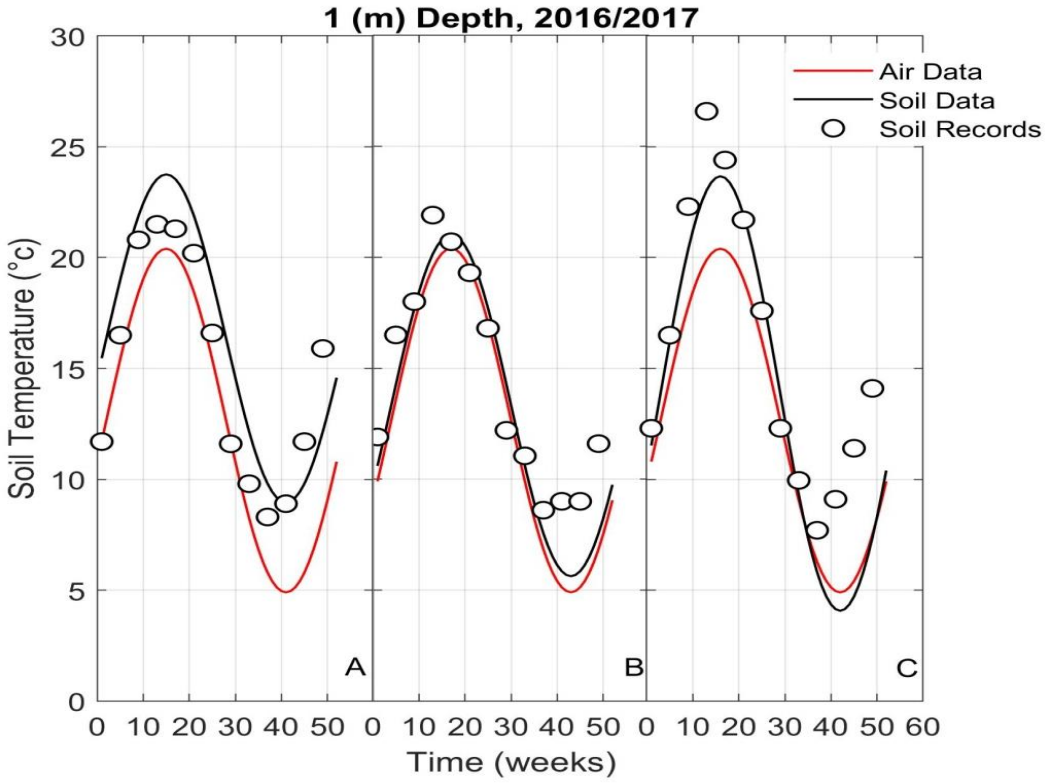

Fig. III.8 Validation and verification of model results with ground temperature records for 2016/2017 in A, B and C sites, under 1 (m) depth

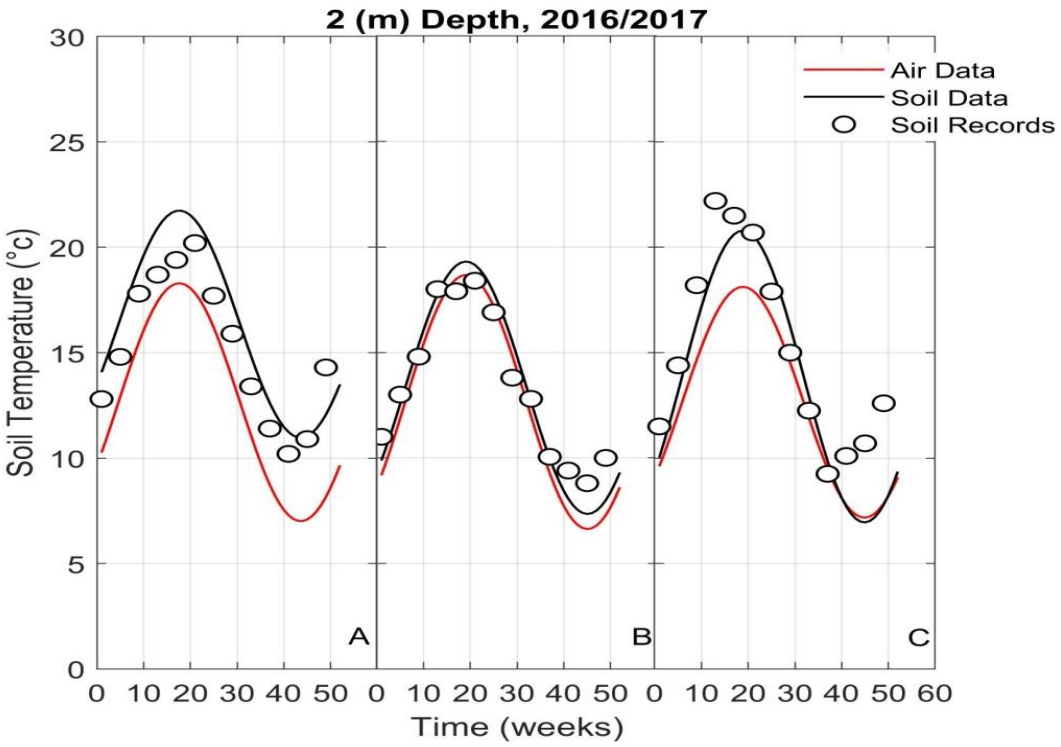

Fig. III.9 Validation and verification of model results with ground temperature records for 2016/2017 in A, B and C sites, under 2 (m) depth

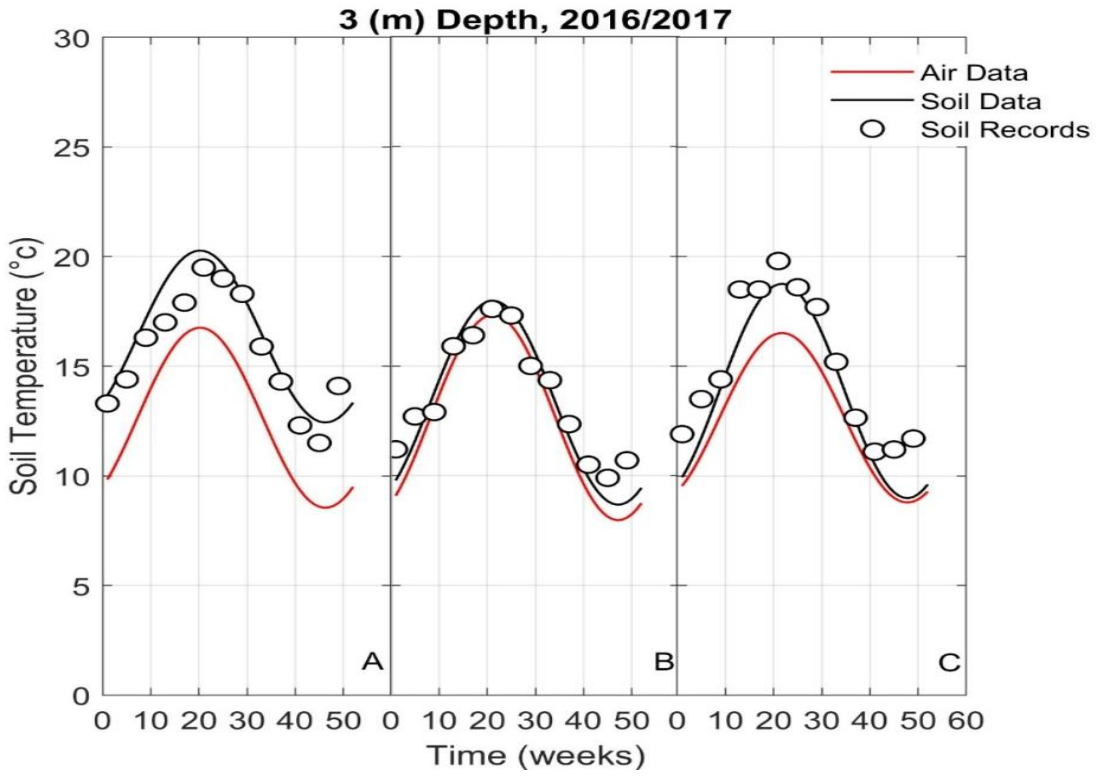

Fig. III.10 Validation and verification of model results with ground temperature records for 2016/2017 in A, B and C sites, under 3 (m) depth

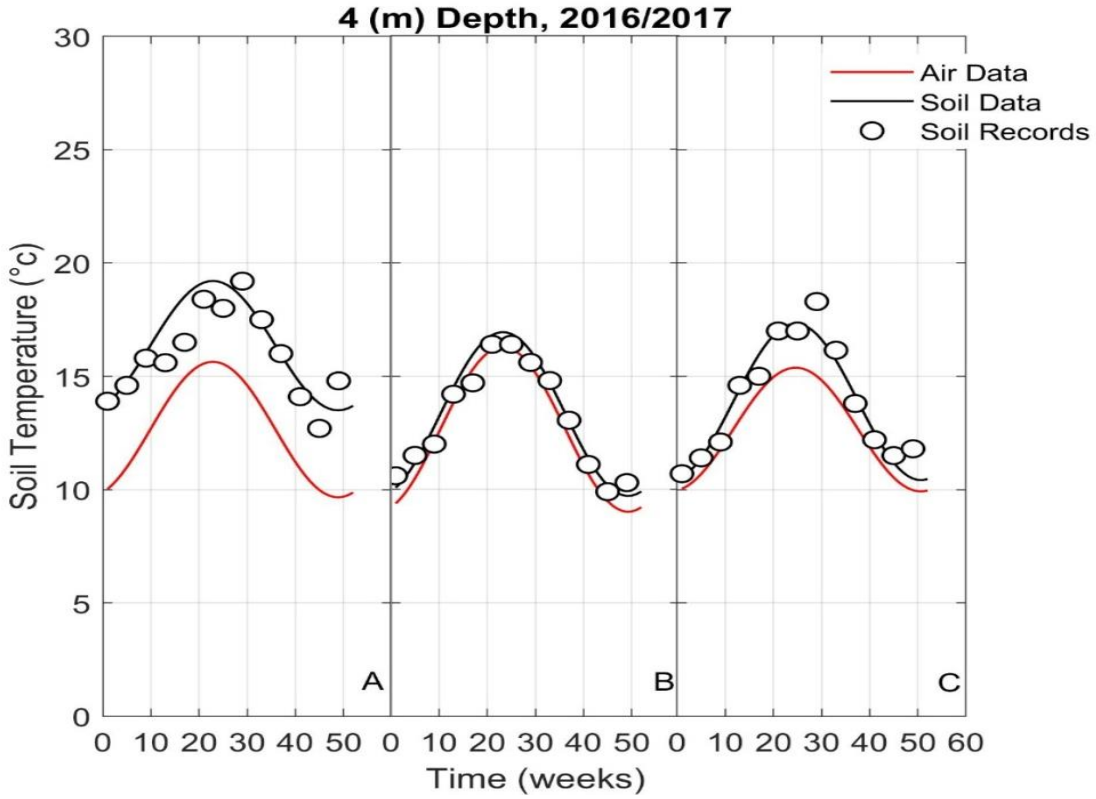

Fig. III.11 Validation and verification of model results with ground temperature records for 2016/2017 in A, B and C sites, under 4 (m) depth

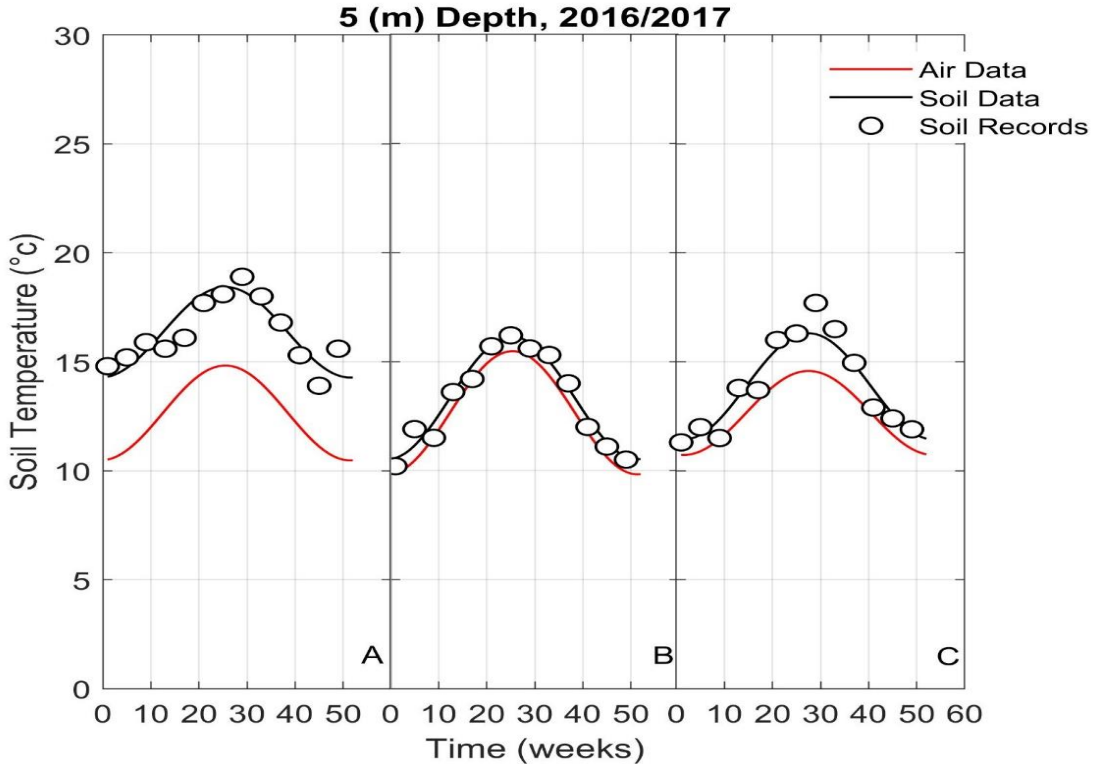

Fig. III.12 Validation and verification of model results with ground temperature records for 2016/2017 in A, B and C sites, under 5 (m) depth

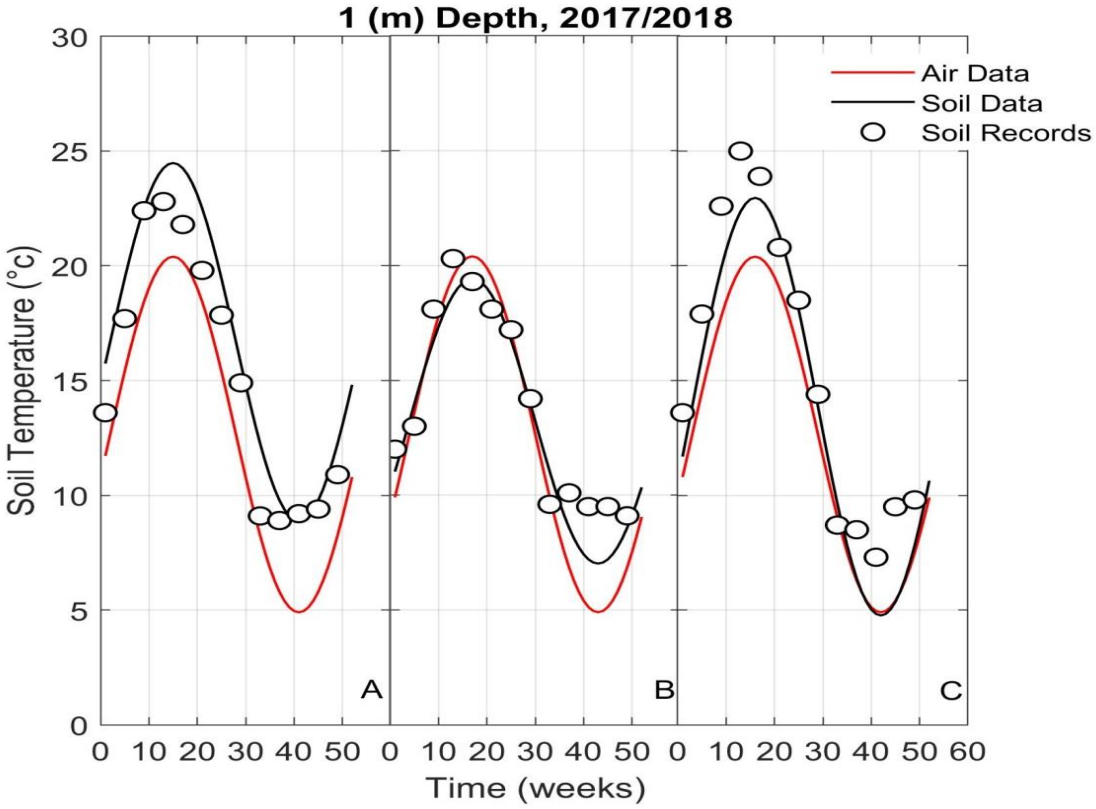

Fig. III.13 Validation and verification of model results with ground temperature records for 2017/2018 in A, B and C sites, under 1 (m) depth

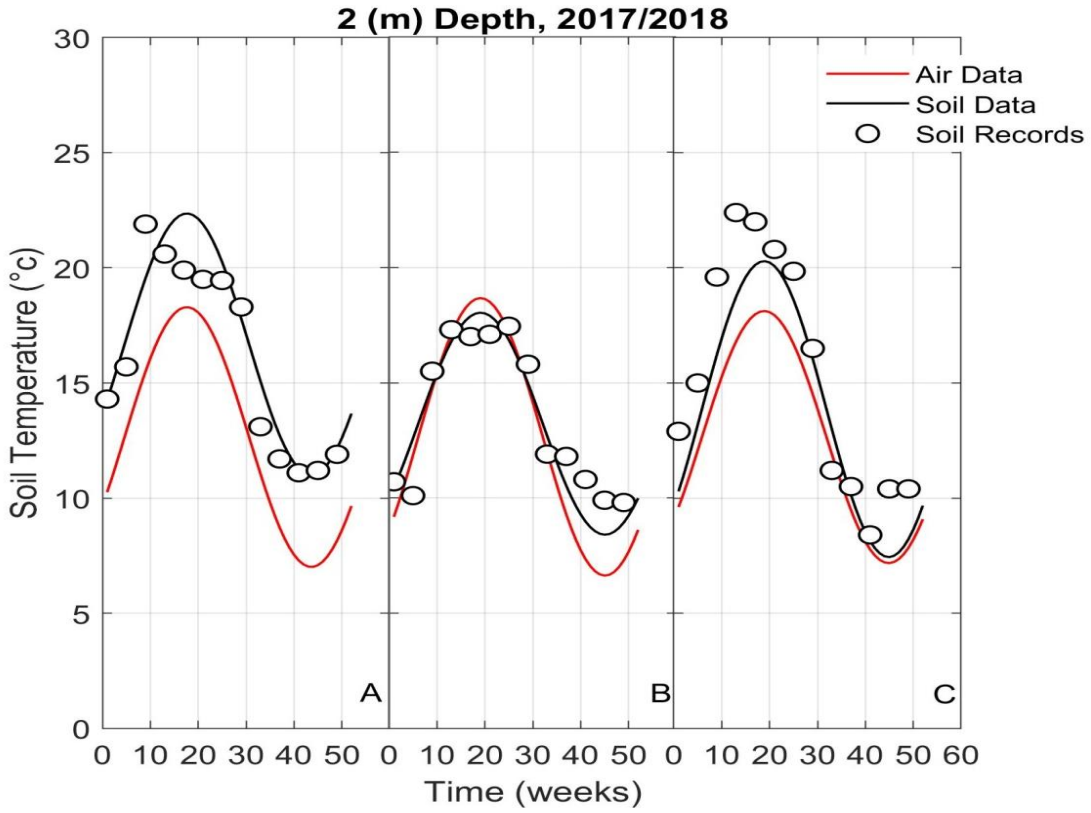

Fig. III.14 Validation and verification of model results with ground temperature records for 2017/2018 in A, B and C sites, under 2 (m) depth

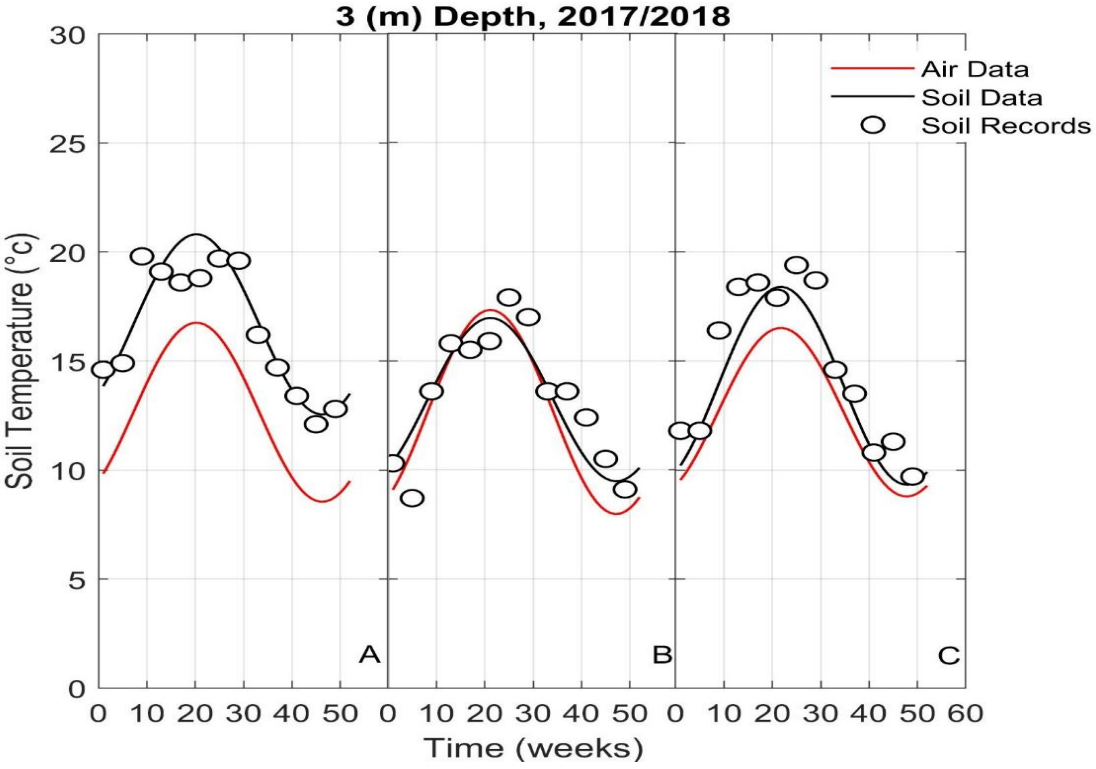

Fig. III.15 Validation and verification of model results with ground temperature records for 2017/2018 in A, B and C sites, under 3 (m) depth

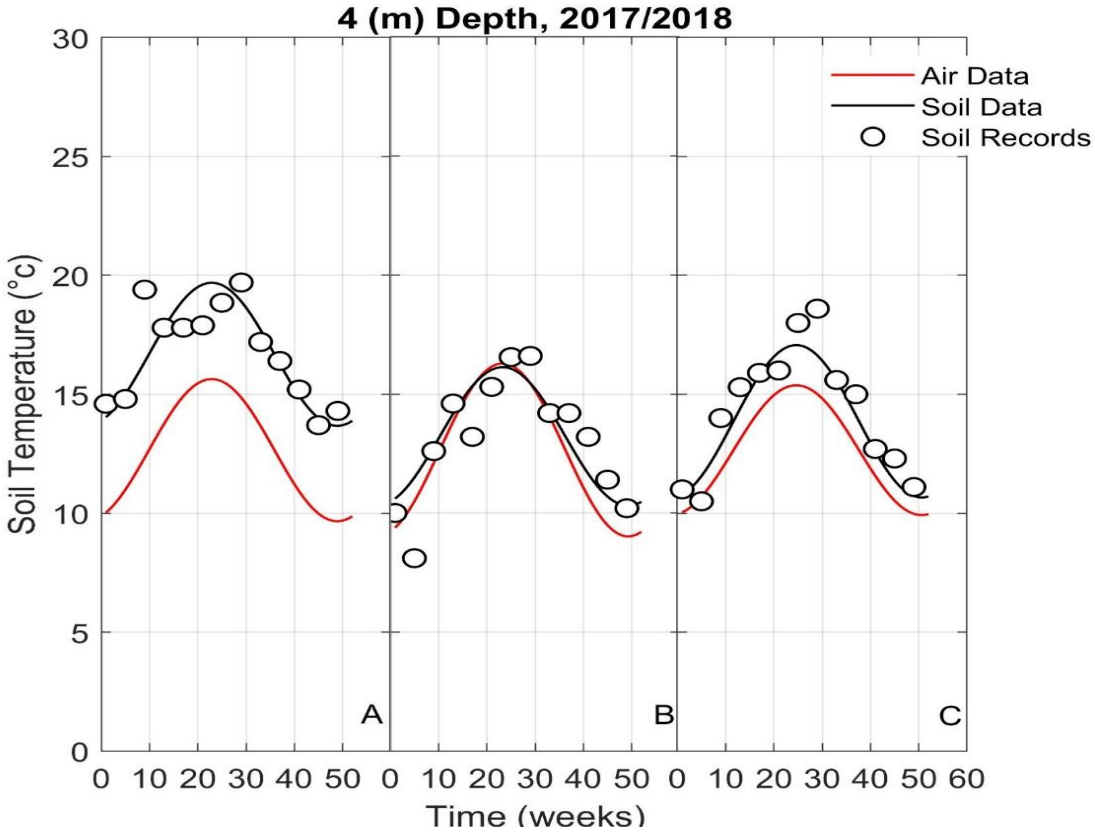

Fig. III.16 Validation and verification of model results with ground temperature records for 2017/2018 in A, B and C sites, under 4 (m) depth

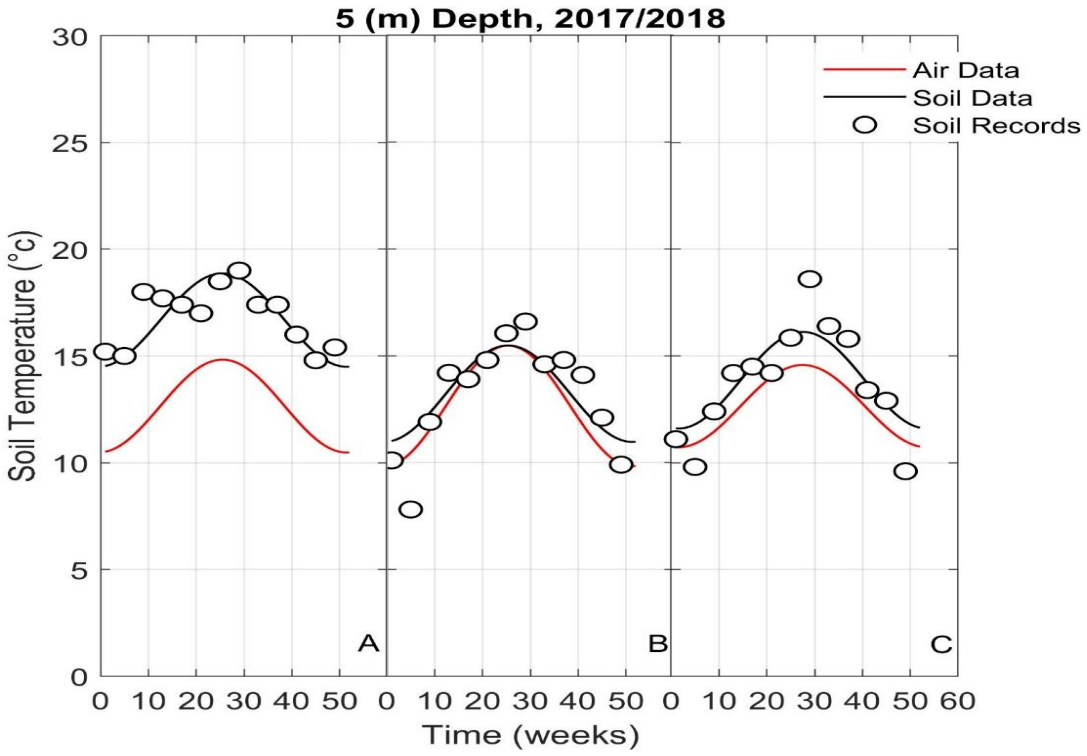

Fig. III.17 Validation and verification of model results with ground temperature records for 2017/2018 in A, B and C sites, under 5 (m) depth

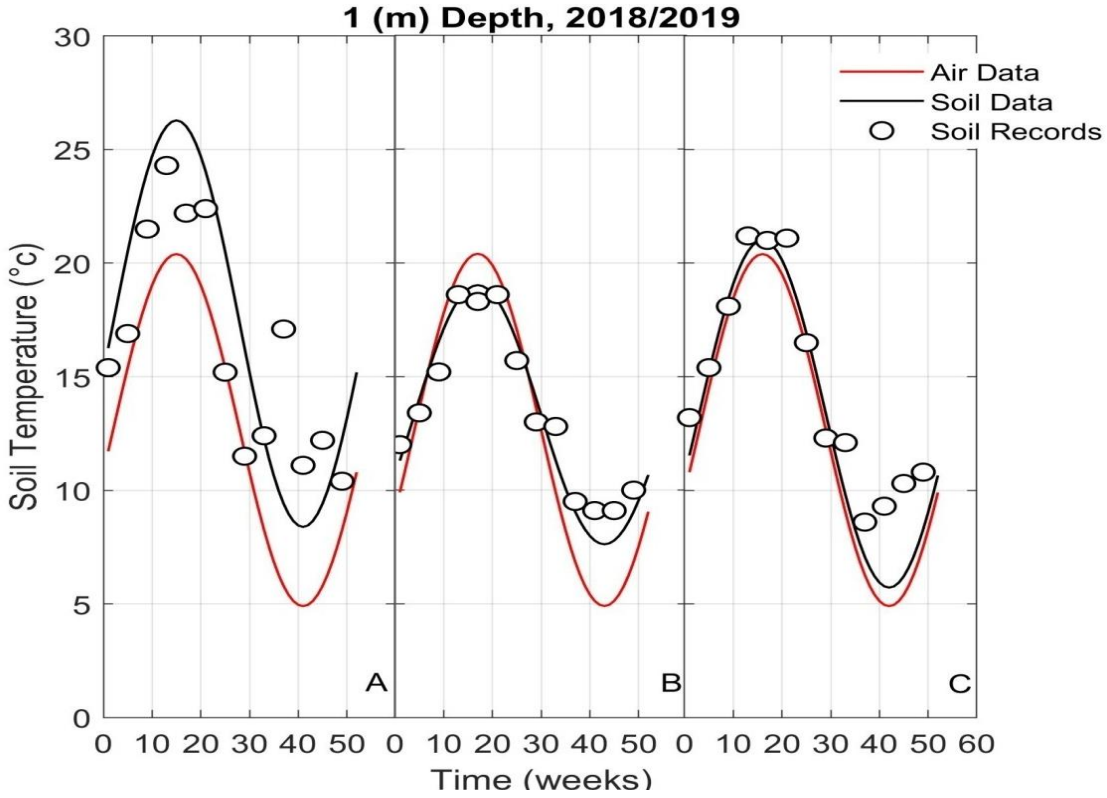

Fig. III.18 Validation and verification of model results with ground temperature records for 2018/2019in A, B and C sites, under 1 (m) depth

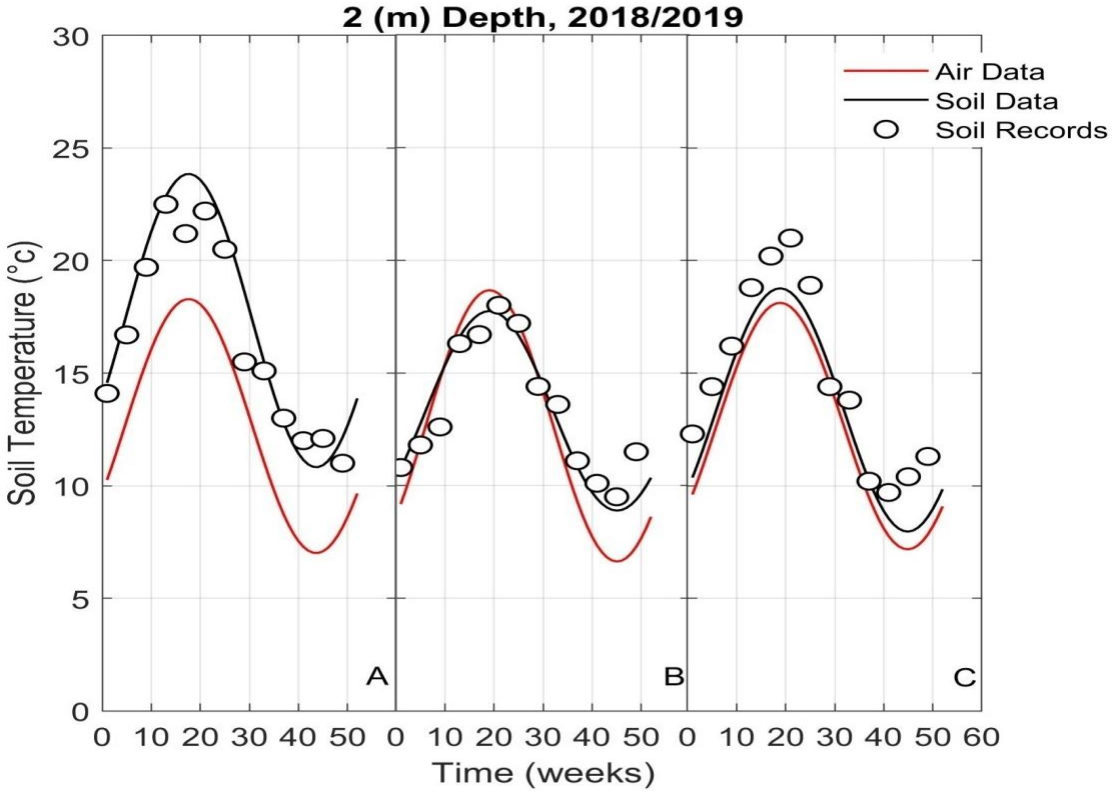

Fig. III.19 Validation and verification of model results with ground temperature records for 2018/2019 in A, B and C sites, under 2 (m) depth

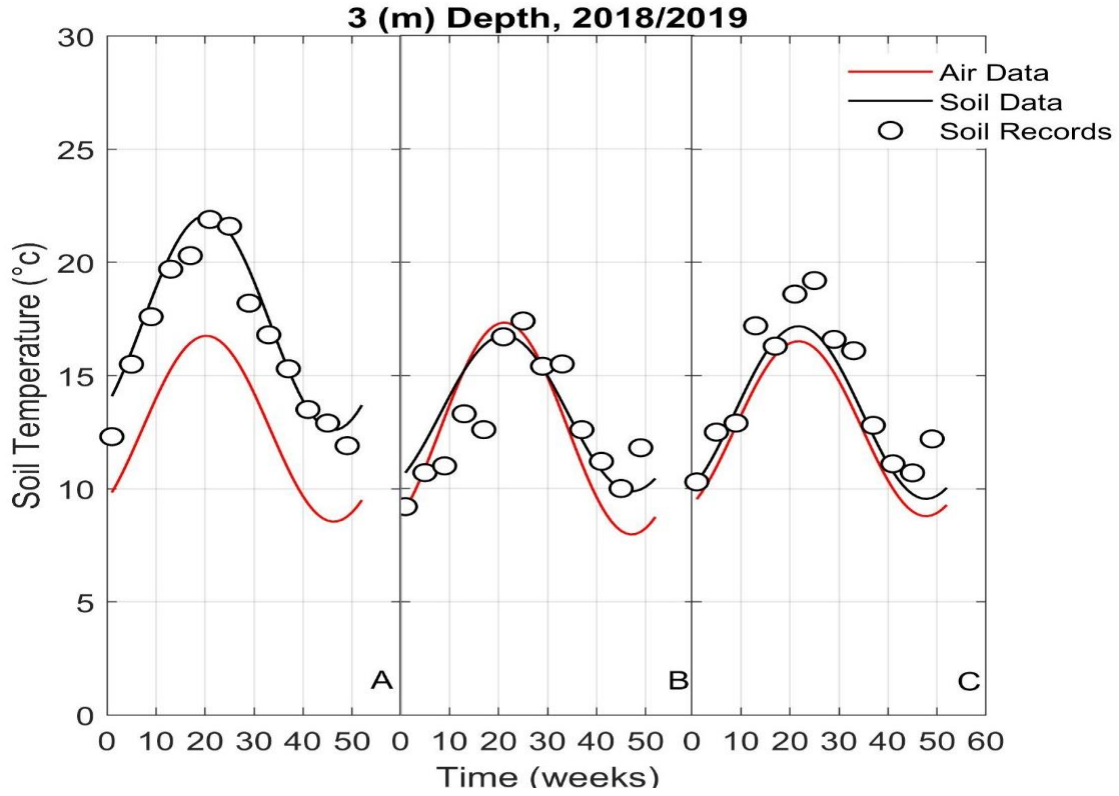

Fig. III.20 Validation and verification of model results with ground temperature records for 2018/2019 in A, B and C sites, under 3 (m) depth

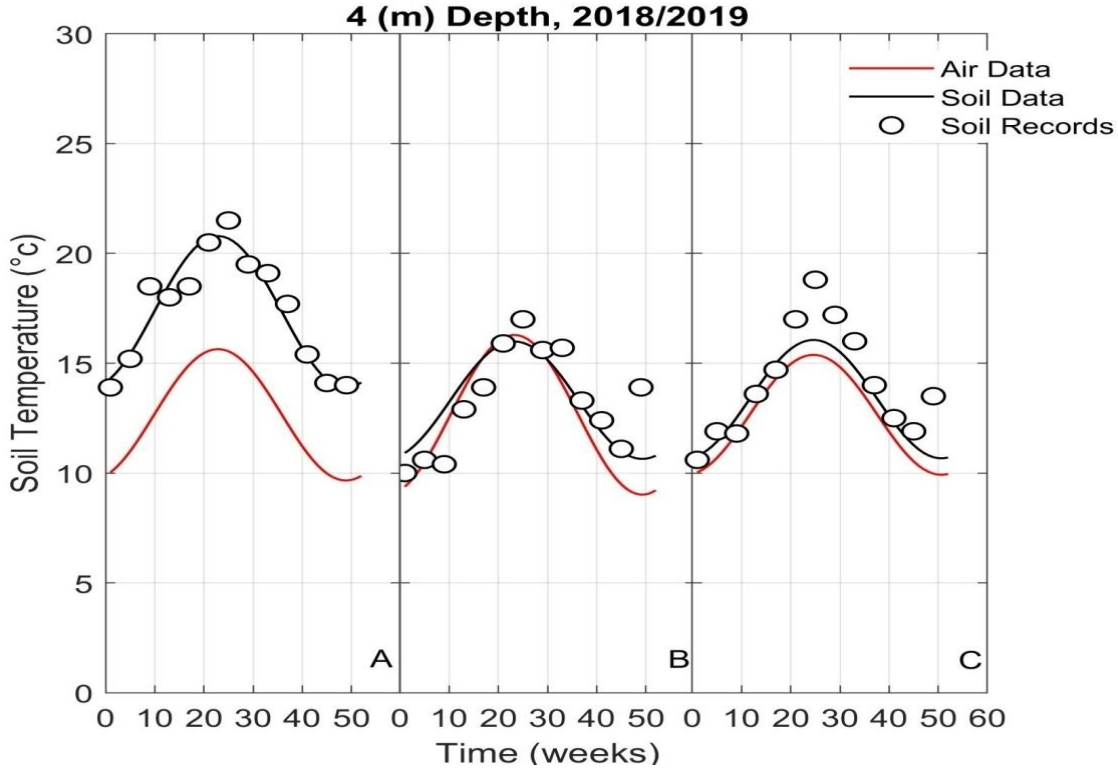

Fig. III.21 Validation and verification of model results with ground temperature records for 2018/2019 in A, B and C sites, under 4 (m) depth

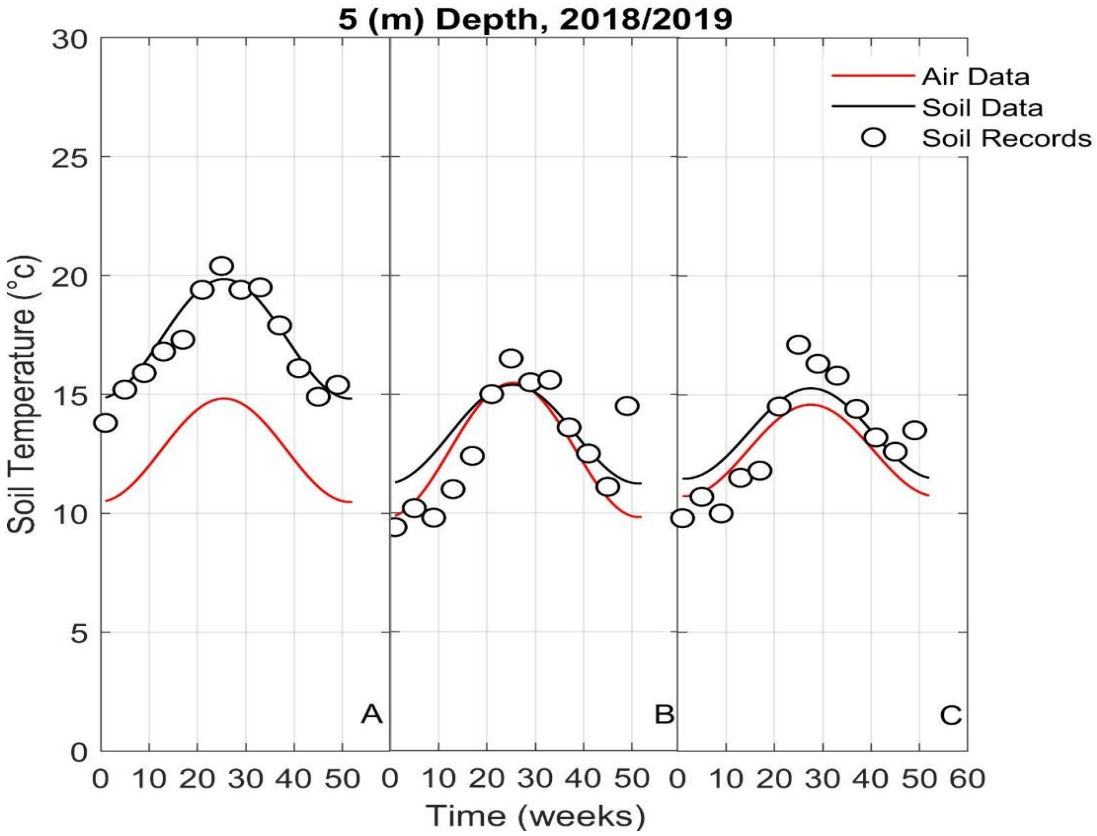

Fig. III.22 Validation and verification of model results with ground temperature records for 2018/2019 in A, B and C sites, under 5 (m) depth

Using the soil data gives better agreements in predicting soil temperature with experimental records in all depths and in all sites. The difference between air data and soil data in the undisturbed soil temperature is 4.7 (ºC) according to Table III.5 in site A. This affects the soil temperature prediction, where the errors increase by depth (Figures III.8 until III.22).

III.2.4.5. Create soil temperature reference year

The soil data that are mentioned in Table III.5 are distinguishing parameters to create the reference years for each site. To show the validity of the created reference years, we compare it with the calculated soil temperature differences from the 3 years records (16/05/ 2016 until 13/05/2019), where the differences values are used as weekly bars. The average difference was 2 (°C) in A, B and C sites for all depths (Figure III.23 until III.27).

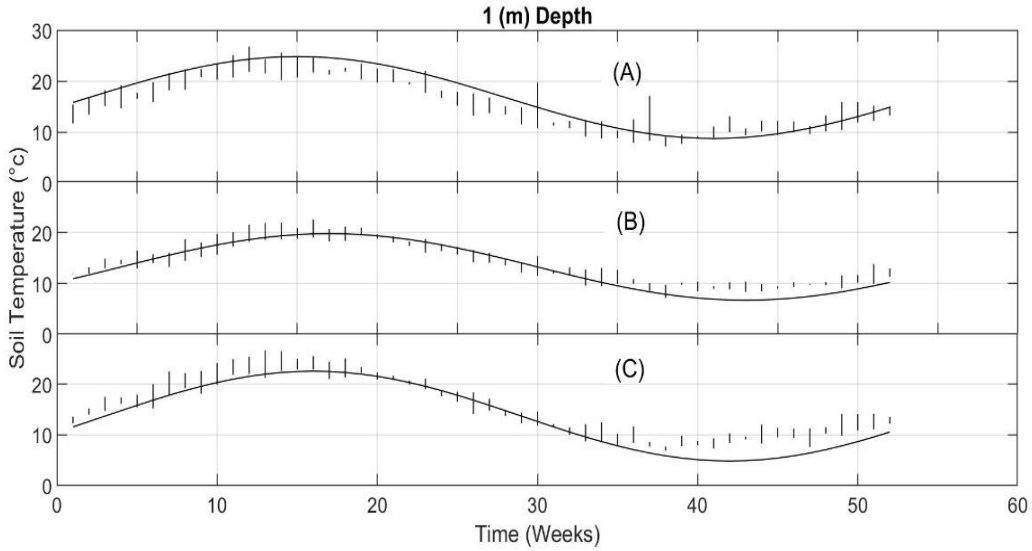

Fig. III.23 Validation of soil temperature reference years in A, B and C sites, under 1 (m) depth

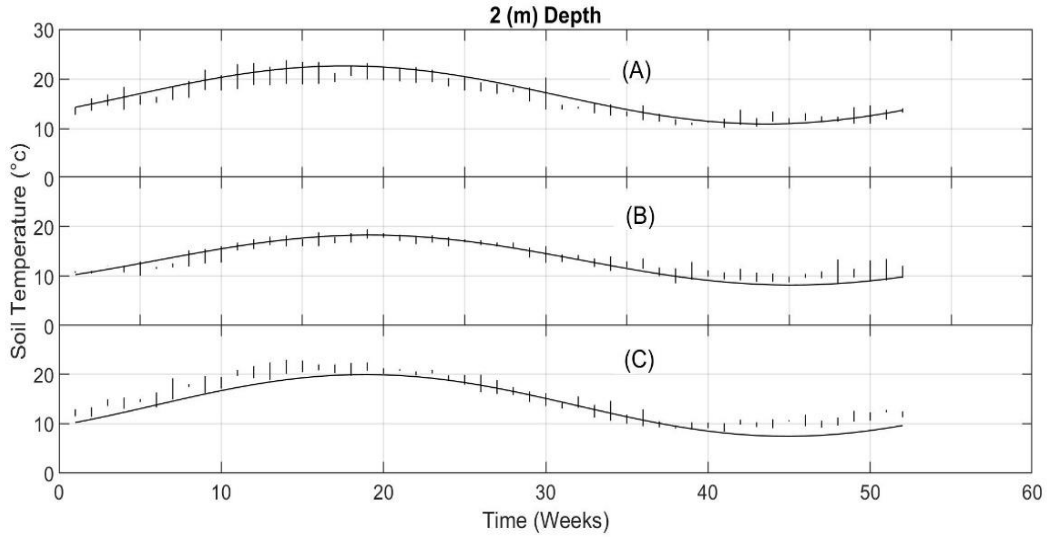

Fig. III.24 Validation of soil temperature reference years in A, B and C sites, under 2 (m) depth

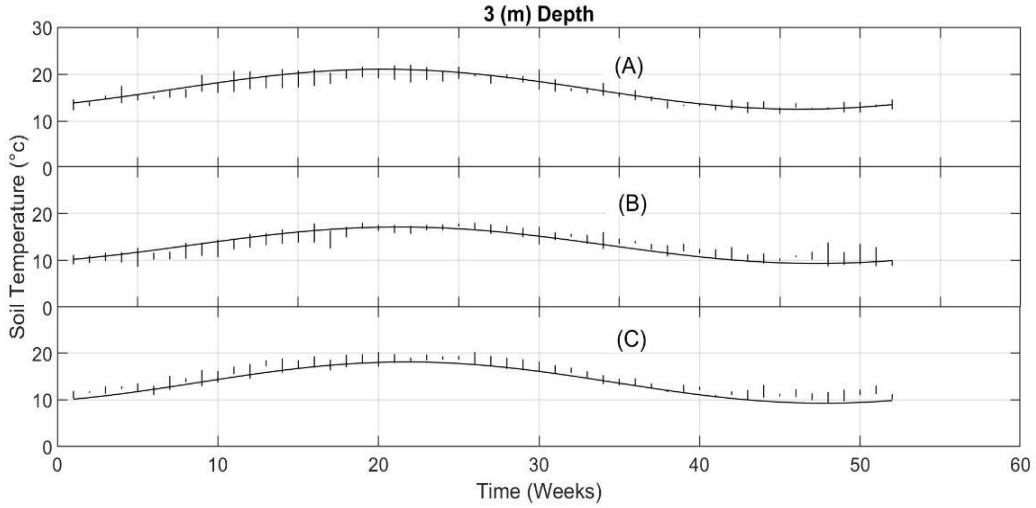

Fig. III.25 Validation of soil temperature reference years in A, B and C sites, under 3 (m) depth

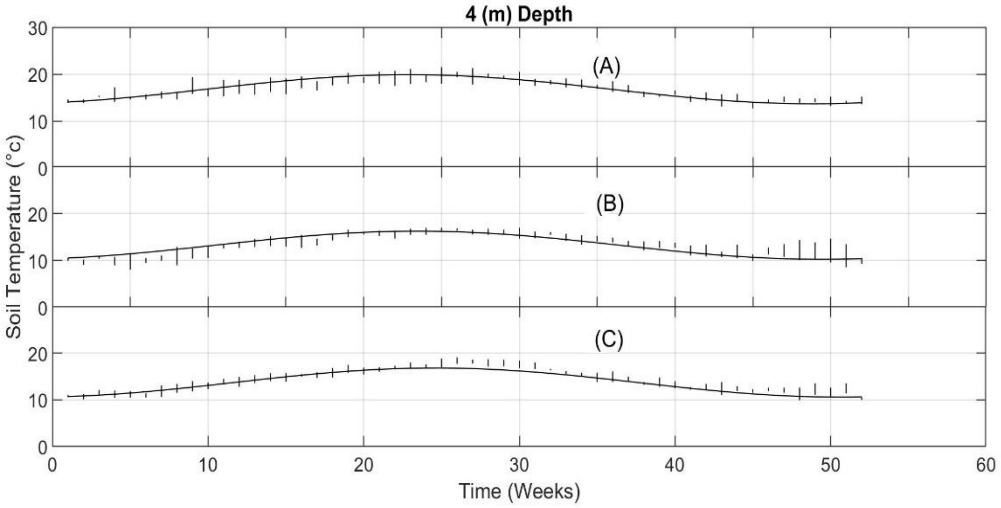

Fig. III.26 Validation of soil temperature reference years in A, B and C sites, under 4 (m) depth

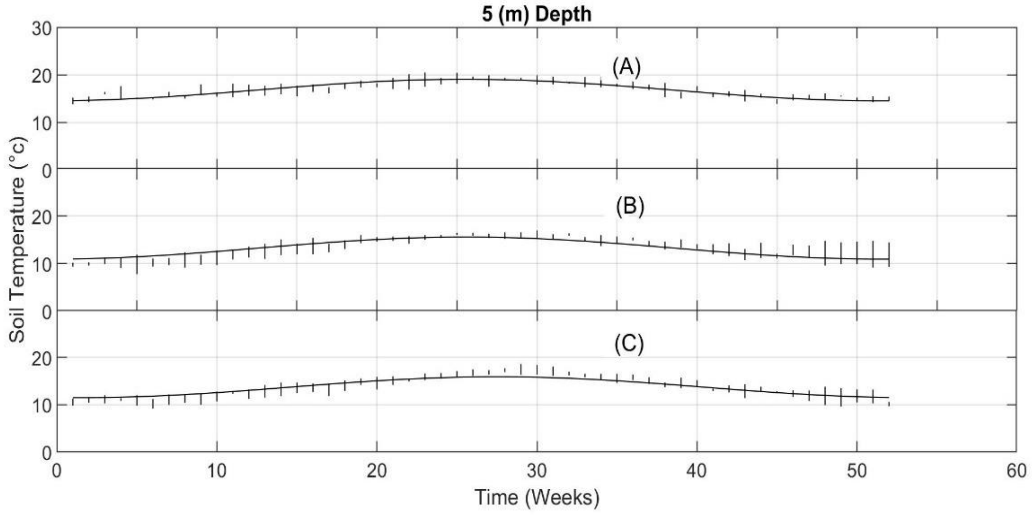

Fig. III.27 Validation of soil temperature reference years in A, B and C sites, under 5 (m) depth

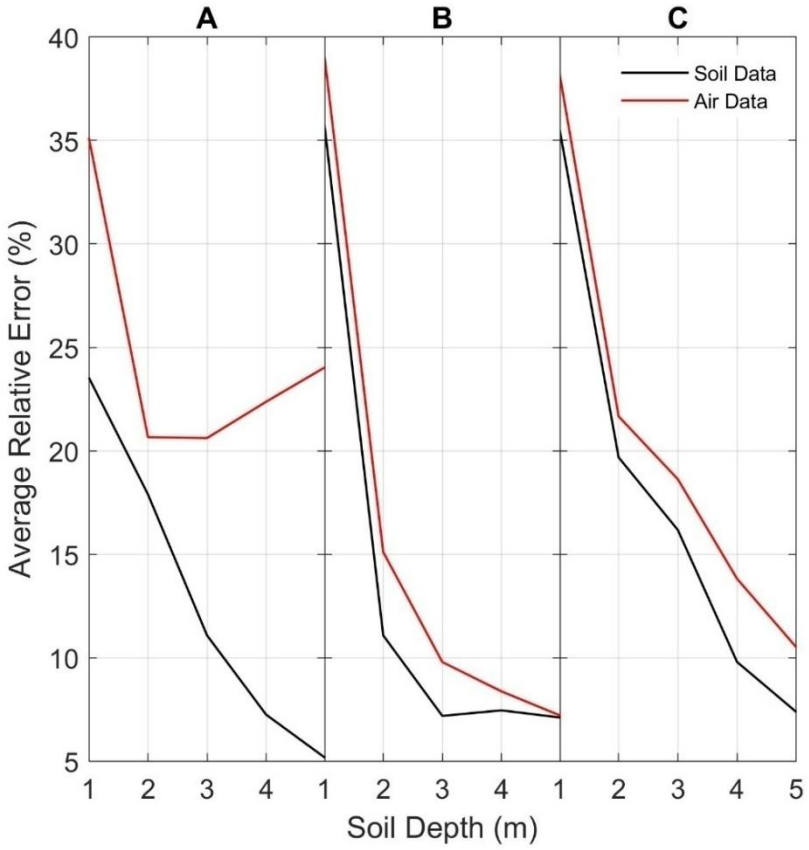

Fig. III.28 Average relative errors of using air data / soil data in predicting soil temperature of 3 years as function by depth.

We have used the soil temperature records of each year to validate and to compare the use of soil data and air data in predicting the soil temperature in shallow depths (results are showed in the Figure III.28). The use of air data in predicting soil temperature in cases B and C gives better agreements as compared with case A. Also, the use of soil data in predicting the soil temperature gives better agreements as compared with the results of using air data.

III.2.5. Conclusion

1. In practical terms the average annual air temperature can be used to define the air data used in predicting the soil temperature in shallow depths. This procedure avoids having to measure the soil temperature at greater depths, however the error is higher.
2. Using air data in some cases (A for example) gives high relative error that increase by depth, where the difference between air data and soil data is relatively high.
3. Reference years of soil temperatures are useful to select the available sites for the wanted function (pre-heating or pre-cooling).
4. The sites B and C have low undisturbed ground temperature. They are good sites to install EAHE as pre-cooler system.
5. Site A has higher undisturbed temperature. It gives better results as pre-heater with EAHE system.

III.3. Second experience: Soil Analysis

III.3.1. Introduction

In order to take an idea about textures and densities of soil in Algeria's arid and semi-arid regions, we used ten samples of soil from El Kantara, Tolga, Biskra and Ouargla cities. Samples were taken from different depths from 0 (m) to 8 (m). We prepared the samples for analysis protocol in the physico-chemical analysis laboratory of the agronomy department, Mohamed Khider University (Figures III.29 to III.31).

Fig. III.29 Procedure of taking samples with drilling tool.

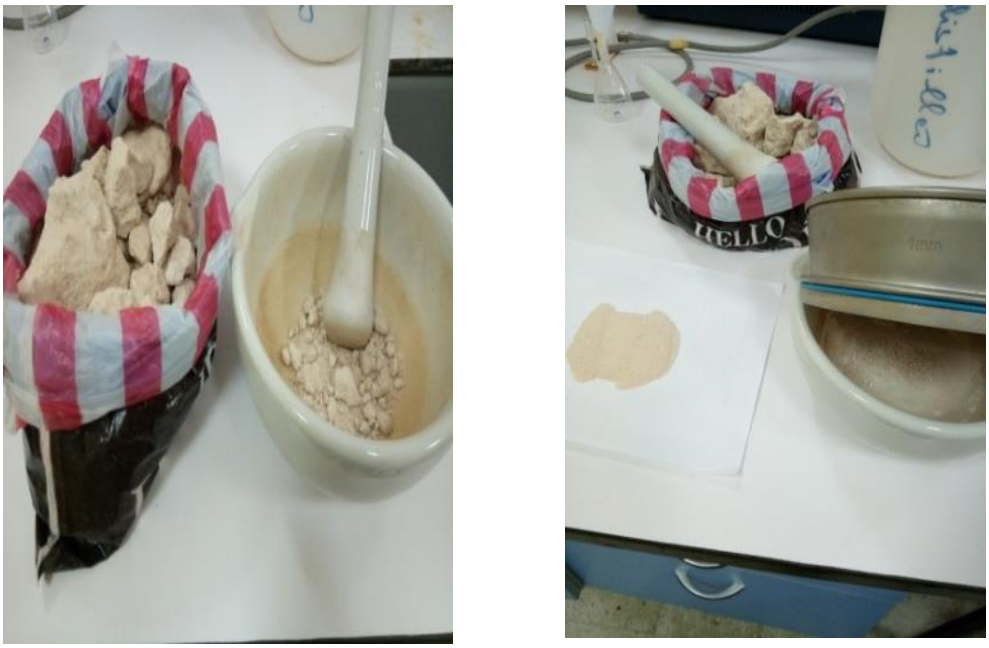

Fig. III.30 Preparing samples for analysis.

Fig. III.31 Samples for analysing the density and soil chemical composition.

III.3.2. Soil texture

Protocol in soil texture depends on the diameter of grain (Kaszubkiewicz et al., 2017). For that, we prepared 50 (g) of each sample in separate graduated cylinder. We soaked the samples with water and shake it well. After four days at rest the samples were divided into layers (Figure III.32). The height of the layers for each cylinder are registered in Table III. 6 (From down to up, layers are sand, silt and clay).

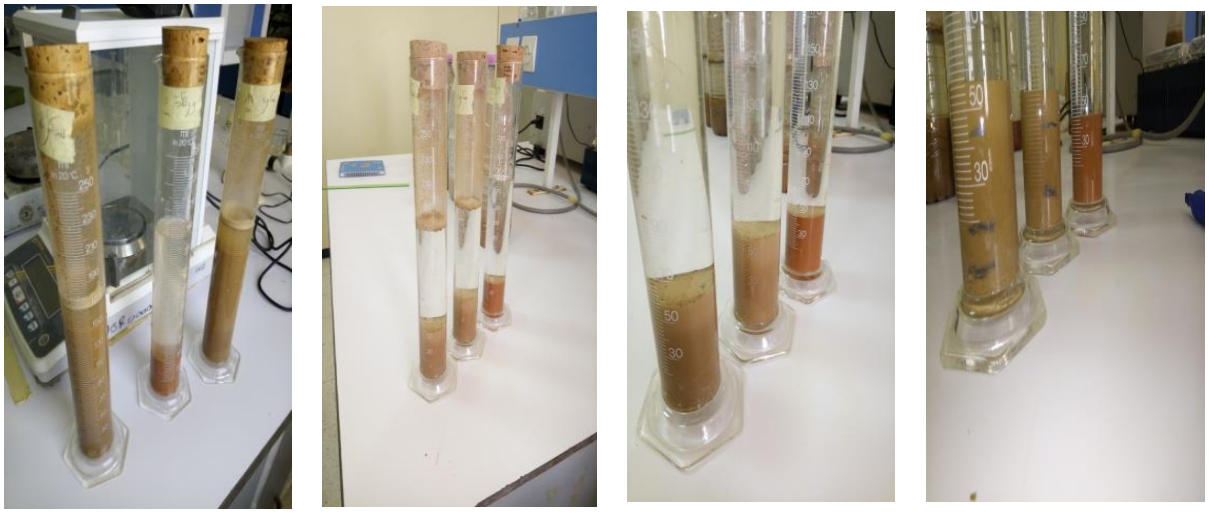

Fig. III.32 Graduated cylinders containing different samples of soil grains analyzed after several days in stable position.

Texture Triangle Excel Version (XLSM; 6.11 MB) is used to indicate in which soil type zone correspond the samples (George, 2010). Also, Table III. 6 shows the link between city, depth and type of soil (Figures III.32 and Figure III.33).

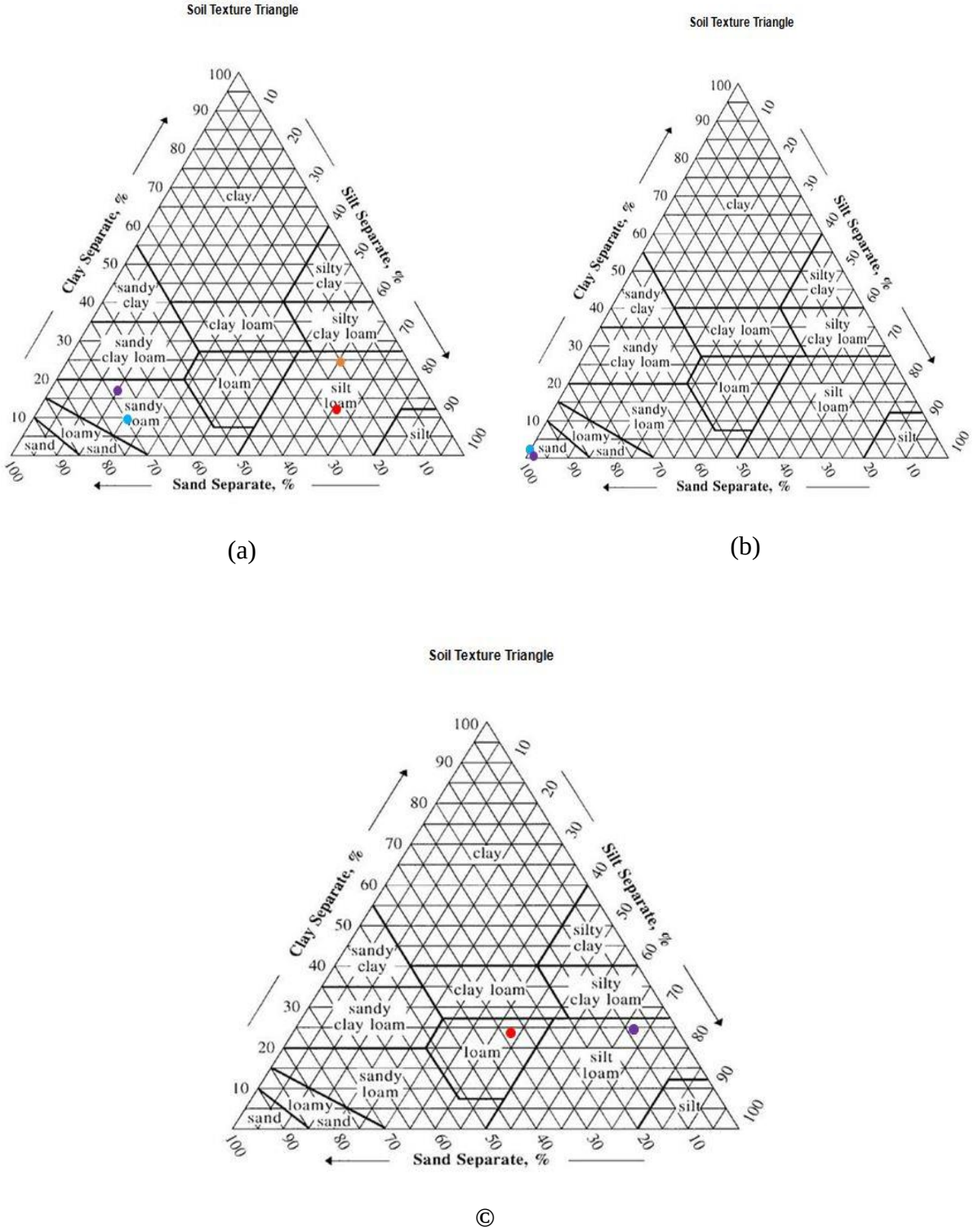

Fig. III.33 Soil texture triangles of El kantara (a), Ouargla (b) and Biskra (c)

Table III. 6

Table of soils textures.

Area name	Depth (m)	Height (cm)			Total Height (cm)	Height (%)			Soil types
		Sand	Silt	Clay		Sand	Silt	Clay	
El Kantara	1	1.5	4.5	0.8	6.8	22.1	66.18	11.76	Silt loam
	1.5÷2	1	4	1.6	6.6	15.2	60.61	24.24	
	6	4.5	1	1.1	6.6	68.2	15.15	16.67	sandy loam
	8	4.6	1.4	0.6	6.6	69.7	21.21	9.091	
Ouargla	0	5.3	0	0.1	5.4	98.1	0	1.852	Sand
	3	5.2	0	0.1	5.3	98.1	0	1.887	
Tolga	0.3	0	0	0	5.5	0	0	0	Gypsum
	2	0	0	0	6	0	0	0	
Biskra	0.2	2	2.6	1.4	6	33.3	43.33	23.33	Loam
	0.4	0.5	3.9	1.4	5.8	8.62	67.24	24.14	Silt loam

III.3.3. Density

Density depends on the weight of sample in natural condition as compared with its weight soaked in distilled water.

- First, we measure 15 (g) of each sample.
- Second, we measure the pycnometer empty and full of distilled water.
- Third, the weighted samples are put in the pycnometer.

Then, it has been filled with distilled water and take its weight again (Figure III.34). The obtained values are utilized in calculating the samples densities using the equation below. Results are mentioned in Table III. 7.

$$D = \frac{15}{(\alpha + b) - (c + d)} \qquad \text{III.4}$$

With

α: weight of pycnometer + 15(g) of the sample.
b: pycnometer filled with distilled water weight (g)
c: weight of pycnometer empty (g)
d: pycnometer weight that carries the sample immersed in distilled water (g)

Laboratory analytical precision electronic scales balances

Powdered soil sample

Empty pycnometer

Filling pycnometer by soil sample and distilled water

Fig. III.34 Operation of determining the sample density for different soil types (from the density experience)

Table III. 7

Table of soils densities.

Area Name	Depth(m)	Weight of pycnometer empty (g)	Weight of pycnometer+ 15 (g) of the sample	Pycnometer filled with distilled water weight (g)	Pycnometer weight that carries the sample immersed in distilled water (g)	Density ($cm^3.g^{-1}$)	Density ($m^3.kg^{-1}$)
El Kantara	1	42.54	57.54	145.64	153.42	2.07756	2077.56
	1.5÷2				154.09	2.29008	2290.08
	6				154.13	2.30415	2304.15
	8				154.14	2.30769	2307.69
Ouargla	0				154.72	2.53378	2533.78
	3				154.52	2.45098	2450.98
Tolga	0.3				153.65	2.14592	2145.92
	2				153.42	2.07756	2077.56
Biskra	0.2				153.71	2.1645	2164.5
	0.4				154.03	2.26929	2269.29

III.3.4. Conclusion

The ten samples that we have analyzed show five types of soil, which are Silt loam, Sandy loam, Sand, Gypsum and Loam. Samples densities values change between $2077.56\ (m^3.kg^{-1})$ and $2533.78\ (m^3.kg^{-1})$, where the lowest value belong to Gypsum soil in Tolga and Silt loam soil in El Kantara. Silt loam soil does also exist in Biskra but with higher density. The highest density value belongs to Sand soil in Ouargla.

References

AGUIAR, R. & CARVALHO, M. J. 2012. Performance analysis of solar thermal and photovoltaic systems,. Lisbon, Portugal,: Solterm software, National Laboratory of Energy and Geology

BEN JMAA DERBEL, H. & KANOUN, O. 2010. Investigation of the ground thermal potential in tunisia focused towards heating and cooling applications. *Applied Thermal Engineering,* 30**,** 1091-1100.

GEORGE, D. 2010. *Soil Texture Calculator* [Online]. New England. Available : https://www.nrcs.usda.gov/wps/portal/nrcs/detail/soils/survey/?cid=nrcs142p2_054167.

KASZUBKIEWICZ, J., WILCZEWSKI, W., NOVÁK, T. J., WOŹNICZKA, P., FALIŃSKI, K., BELOWSKI, J. & KAWAŁKO, D. 2017. Determination of soil grain size composition by measuring apparent weight of float submerged in suspension. *International Agrophysics,* 31**,** 61-72.

MÁRQUEZ, J. M. A., BOHÓRQUEZ, M. Á. M. & MELGAR, S. G. 2016. Ground Thermal Diffusivity Calculation by Direct Soil Temperature Measurement. Application to very Low Enthalpy Geothermal Energy Systems. *Sensors*.

Chapter IV

Numerical Study

IV.1. Introduction

In this chapter, a mathematical approach is developed to predict outlet air temperature of EAHE system in the horizontal portion. We used the energy balance equation in the air part and the heat conduction equation in the soil around pipe to describe the heat exchange phenomena. A simple numerical solution is used as it will be shown next. The significant of this model is to show whether or not the soil axial heat flux could be neglect as it is mentioned widely in literature. The developed approach is verified with models from literature. Also, it has been validated using experiences from literature. Later, we show the heat conduction ratio radially and axially around the control volume (soil).

IV.2. Theoretical analysis

The problem encountered here concerns the conjugate heat transfer that takes place between the air flowing inside horizontal pipe (we ignored the effects of elbows / bends), buried underground, and the surrounding soil initially at uniform temperature. The heat conduction and energy equations can be simplified for the present problem by assuming the following hypotheses:

The soil is homogeneous, and all its properties are constant;

1. The heat conduction in the soil is unsteady ax-symmetric with no heat source;
2. The air flow is one-dimensional along the x-axis and all its properties are constant;
3. The air thermal inertia is neglected (yet the air temperature can vary with time instantaneously due to the variation of the boundary conditions, as it will be seen later);
4. The pipe thermal inertia is neglected (i.e. the heat transfer through which is instantaneous), while its thermal resistance is taken into account;
5. The thermal contact between the pipe and the soil is perfect (i.e. there are no air gaps in the pipe-soil interface).

By taking into account the above hypotheses, the heat conduction equation can be written as:

$$\frac{1}{\alpha_s}\frac{\partial T_s}{\partial t} = \frac{1}{r}\frac{\partial T_s}{\partial r} + \frac{\partial^2 T_s}{\partial r^2} + \frac{\partial^2 T_s}{\partial x^2} \qquad \text{IV.1}$$

This equation has to be solved subjected to the following initial and boundary conditions:

$$T_s(0, x, r) = T_\infty \qquad \text{IV.2}$$

$$T_s(t,x,\infty)=T_\infty \quad \text{IV.3}$$

$$T_s(t,\pm\infty,r)=T_\infty \quad \text{IV.4}$$

and from the heat balance between the soil and the pipe interface, we have:

$$2\pi R_{ext}k_s\frac{\partial T_s}{\partial r}(t,x,R_o)=U\left(T_s(t,x,R_o)-T_f\right) \quad \text{IV.5}$$

Where U is the equivalent heat transfer coefficient given by:

$$\frac{1}{U}=\frac{1}{2\pi R_{int}h}+\frac{1}{2\pi k_p}\ln\left(\frac{R_o}{R_i}\right) \quad \text{IV.6}$$

With the convection heat coefficient $h=\mathrm{Nu}\,k_f/D_i$ being calculated from:

$$\mathrm{Nu}=0.023\mathrm{Re}^{0.8}\,\mathrm{Pr}^{0.33} \quad \text{IV.7}$$

For turbulent flow, whereas $\mathrm{Nu}=3.66$ is taken when the flow is laminar (BERGMAN et al., 2011). The boundary condition Equation IV.5 is applied at the soil-pipe interface from the inlet (at $x=0$) to the outlet (at $x=L$), otherwise the pipe is considered to be insulated (see Figure IV.1). The one-dimensional energy equation in the air region is written as:

$$\dot{m}c_p\frac{\partial T_f}{\partial x}=U\left(T_s(t,x,R_o)-T_f\right) \quad \text{IV.8}$$

With:

$$T_f(t,0)=T_{in}(t) \quad \text{IV.9}$$

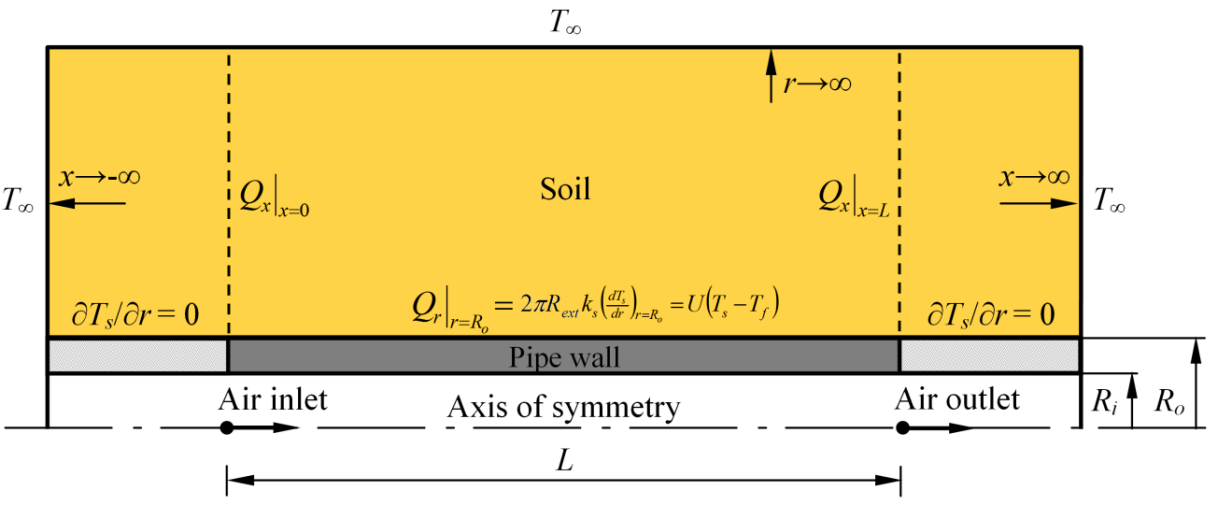

Fig. IV.1 The physical domain and the boundary conditions

IV.3. Solution method

The previous set of equations are solved using the finite difference method. A uniform mesh is generated for the soil region with N×M grid points, in which the following implicit finite difference formula has to be solved:

$$\left(1+2\frac{\alpha_s\Delta t}{\Delta r^2}+2\frac{\alpha_s\Delta t}{\Delta x^2}\right)T_{si,j}^{\,k}=\frac{\alpha_s\Delta t}{\Delta x^2}\left(T_{si+1,j}^{\,k}+T_{si-1,j}^{\,k}\right)+\left(\frac{\alpha_s\Delta t}{\Delta r^2}+\frac{\alpha_s\Delta t}{2r_j\Delta r}\right)T_{si,j+1}^{\,k}+\left(\frac{\alpha_s\Delta t}{\Delta r^2}-\frac{\alpha_s\Delta t}{2r_j\Delta r}\right)T_{si,j-1}^{\,k}+T_{si,j}^{\,k-1} \quad \text{IV.10}$$

With the corresponding boundary conditions:

$$T_{si,j}^{\,0}=T_\infty \quad \text{IV.11}$$

$$T_{si,M}^{\,k}=T_\infty \quad \text{IV.12}$$

$$T_{s1,j}^{\,k}=T_{sN,j}^{\,k}=T_\infty \quad \text{IV.13}$$

at the soil-pipe interface:

$$T_{si,1}^{\,k}=\frac{T_{si,2}^{\,k}+\left(\frac{U\Delta r}{2\pi R_{ext}k_s}\right)T_{fi}^{\,k}}{1+\left(\frac{U\Delta r}{2\pi R_{ext}k_s}\right)} \quad \text{IV.14}$$

and along the adiabatic length:

$$T_{si,1}^{\,k}=T_{si,2}^{\,k} \quad \text{IV.15}$$

The scheme used to approximate the convective term in the Equation IV.8 leads to the formula:

$$T_{fi}^{\,k}=\frac{T_{fi-1}^{\,k}+\left(\frac{U\Delta x}{\dot{m}c_p}\right)T_{si,1}^{\,k}}{1+\left(\frac{U\Delta x}{\dot{m}c_p}\right)} \quad \text{IV.16}$$

with the following boundary condition at the pipe inlet:

$$T_{f1}^{\,k}=T_{in}^{\,k} \quad \text{IV.17}$$

As we have mentioned earlier the air temperature varies with time as a result of the time-dependent boundary conditions $T_{in}^{\,k}$ and $T_{si,1}^{k}$. The Equation IV.10, Equation IV.14 and Equation IV.16 are solved simultaneously according to the following algorithm:

1. Calculate the air temperature from Equation IV.16
2. Calculate the temperature at the soil-pipe interface from Equation IV.14
3. Guess the soil temperature field and solve Equation IV.10 to obtain a new soil temperature field, and use it as a new guess for the next iteration
4. Repeat the previous steps until a converged solution is obtained.

IV.4. Results and discussion

The results presented below were obtained for an EAHE system that consists of a PVC pipe buried under 3 (m) from the ground surface in homogeneous soil, and operates in cooling mode with constant air velocity. The geometry of the EAHE system, the thermo-physical properties, the operating conditions as well as the duration of the system operation were selected according to the experimental investigations (Mehdid et al., 2018, Benhammou et al., 2017, Belloufi et al., 2017) with which a comparison of the simulation results was performed (see the Table IV. 1).

A conductive heat flux ratio defined as the ratio between the axial conductive flux leaving the soil control volume at both boundaries $x = 0$ and $x = L$, and the radial conductive flux entering the soil control volume at the boundary $r = R_o$, is calculated to verify whether or not the assumption of dominant radial (one dimensional) heat conduction in the soil (Mehdid et al. (2018)) is supported.

Table IV. 1

The input parameters

	Parameter	Belloufi et al. (2017)	Benhammou et al. (2017)	Mehdid et al. (2018)
Air	ρ (kg.m^{-3})	1.2	1.1774	1.225
	Cp (J.kg^{-1}.K^{-1})	1000	1005.7	1005
	k (W.m^{-1}.K^{-1})	0.0242	0.02624	0.0242
	μ (kg.m^{-1}.s^{-1})	1.85x10^{-5}	1.983 x10^{-5}	1.85 x10^{-5}
Pipe	k (W.m^{-1}.K^{-1})	0.17	0.16	0.16
Soil	ρ (kg.m^{-3})	1450	2050	1340
	Cp (J.kg^{-1}.K^{-1})	880	1840	1800
	k (W.m^{-1}.K^{-1})	1.25	1.16	1.5
Geometry	R_{int} (m)	0.055	0.1	0.055
	R_{ext} (m)	0.057	0.102	0.057
	L (m)	47	60	47
Initial conditions	V (m.s^{-1})	3.5	0.6	3.5
	T_∞ (°C)	26	27.43	22
Timestep	dt (min)	15	60	15

IV.4.1. Air temperature

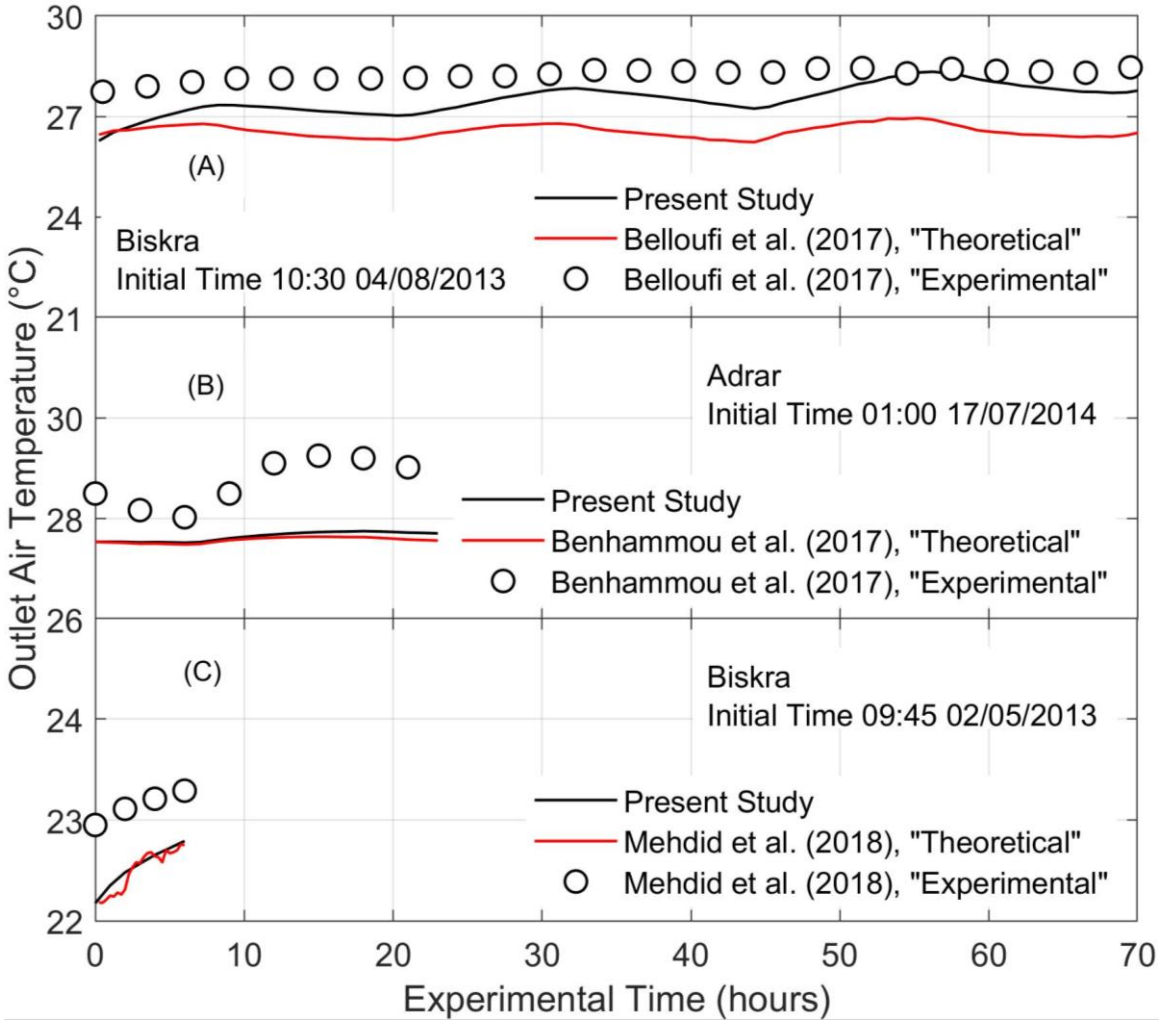

Fig. IV.2 Outlet air temperature according to time variations $x = L$.

The Figure IV.2 shows the variation of the outlet air temperature obtained from the numerical simulation and the data from experimental investigations (Belloufi et al. (2017); Mehdid et al. (2018); Benhammou et al. (2017)) carried out in the University of Biskra in August the 4th 2013 (Figure IV.2 A) and in May the 2nd 2013 (Figure IV.2 C), and in the University of Adrar in July the 17th 2014 (Figure IV.2 B).

It can be seen that when the EAHE operates in relatively short period of time (6 and 24 hours), the results from the present numerical simulation coincide with those predicted by the analytical and semi-analytical models proposed in the previous investigations; however for relatively long period of time (71 hours), the numerical results are more consistent with the experimental data as compared to the analytical model of Belloufi et al. (2017).

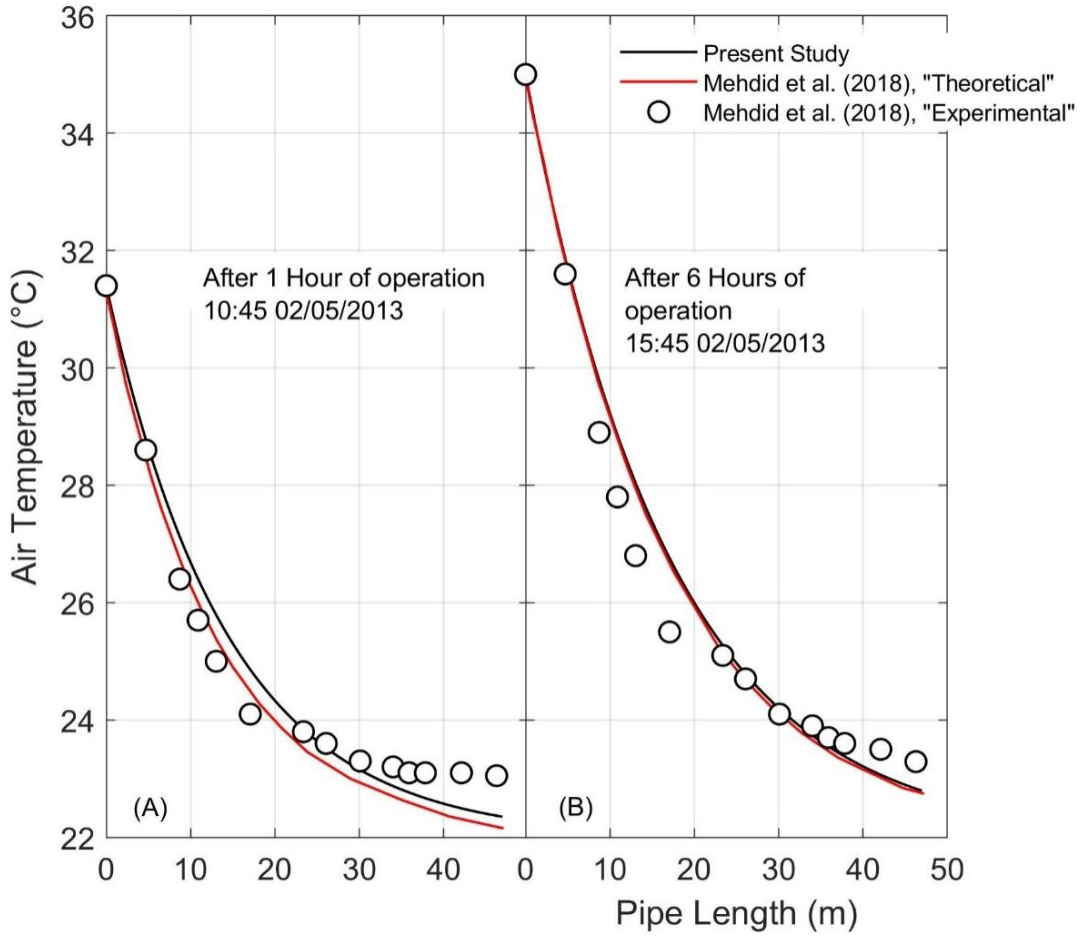

Fig. IV.3 Air temperature function by length after 1 and 6 (hours) of operation

Figure IV.3 shows the evolution of the air temperature along the pipe, (A) after 1 hour of operation and (B) after 6 hours of operation. The two models fit well the experimental data where the close agreement between these models is probably attributed to the time of the day in which the measurement have been taken, as well as to the short period of operation of the EAHE system, as it will be better demonstrated below.

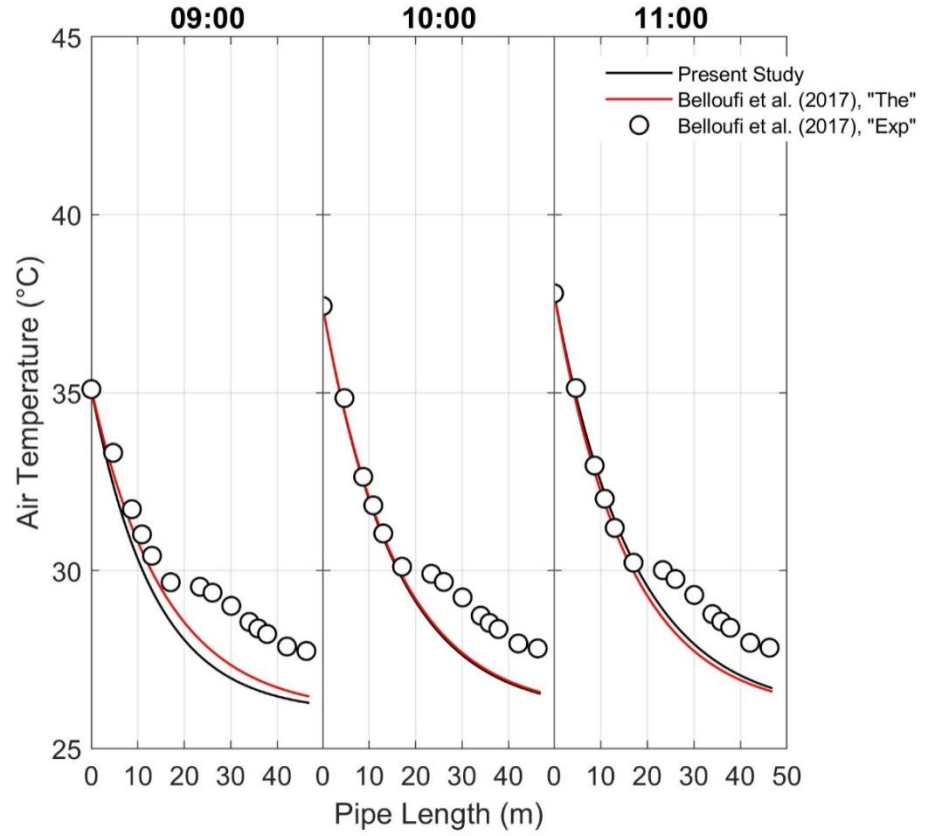

Fig. IV.4 Air temperature distribution by length at beginning of system operation 04/08/2013

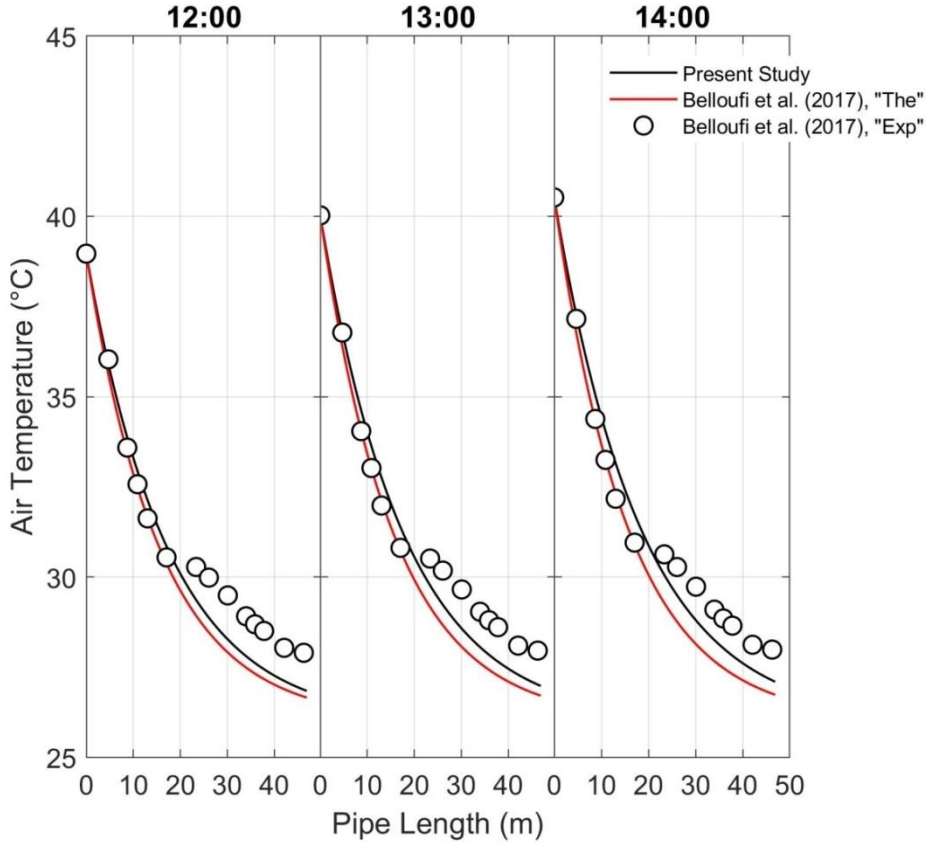

Fig. IV.5 Air temperature distribution by length after 3 hours of system operation 04/08/2013

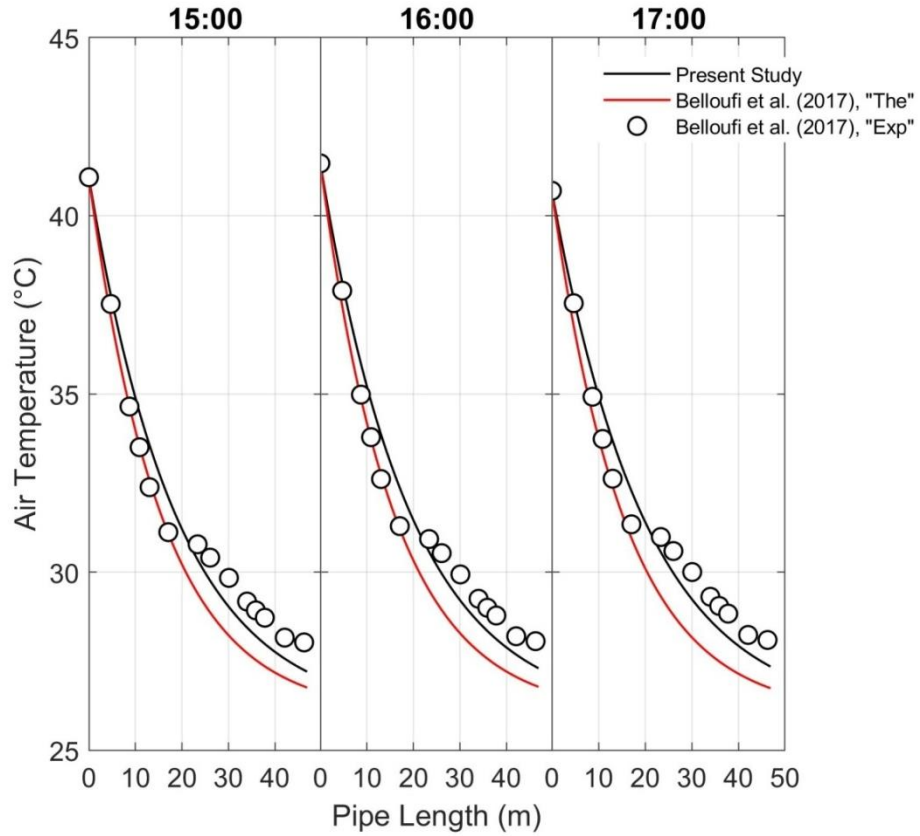

Fig. IV.6 Air temperature distribution by length after 6 hours of system operation 04/08/2013

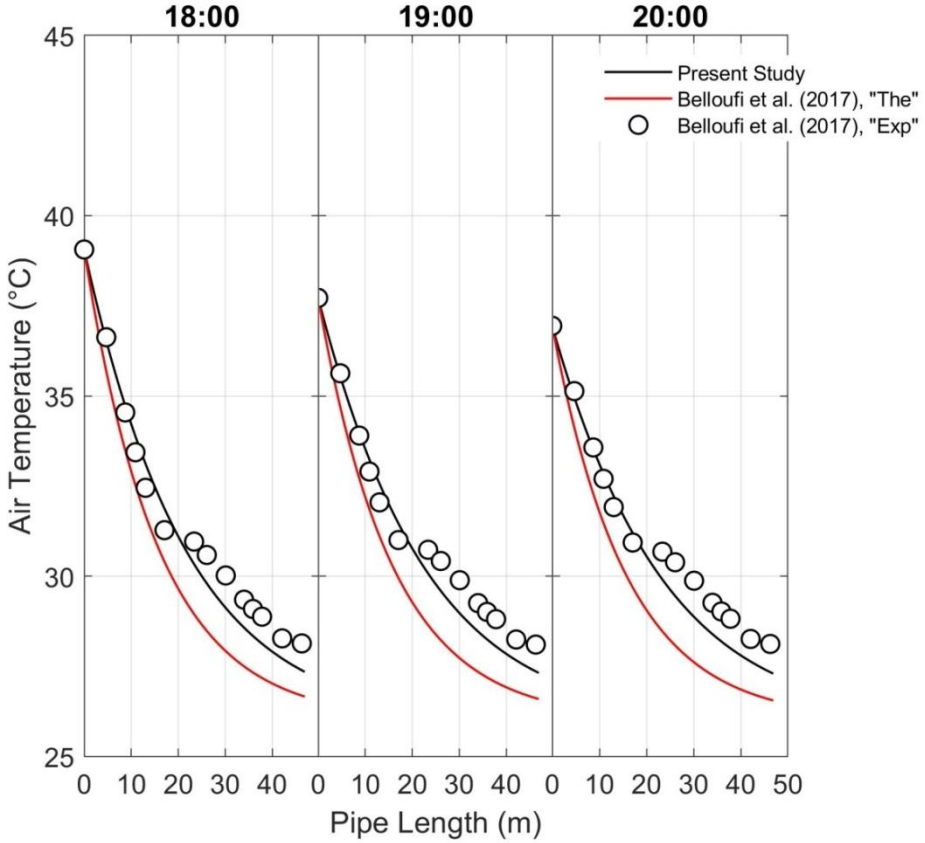

Fig. IV.7 Air temperature distribution by length after 9 hours of system operation 04/08/2013

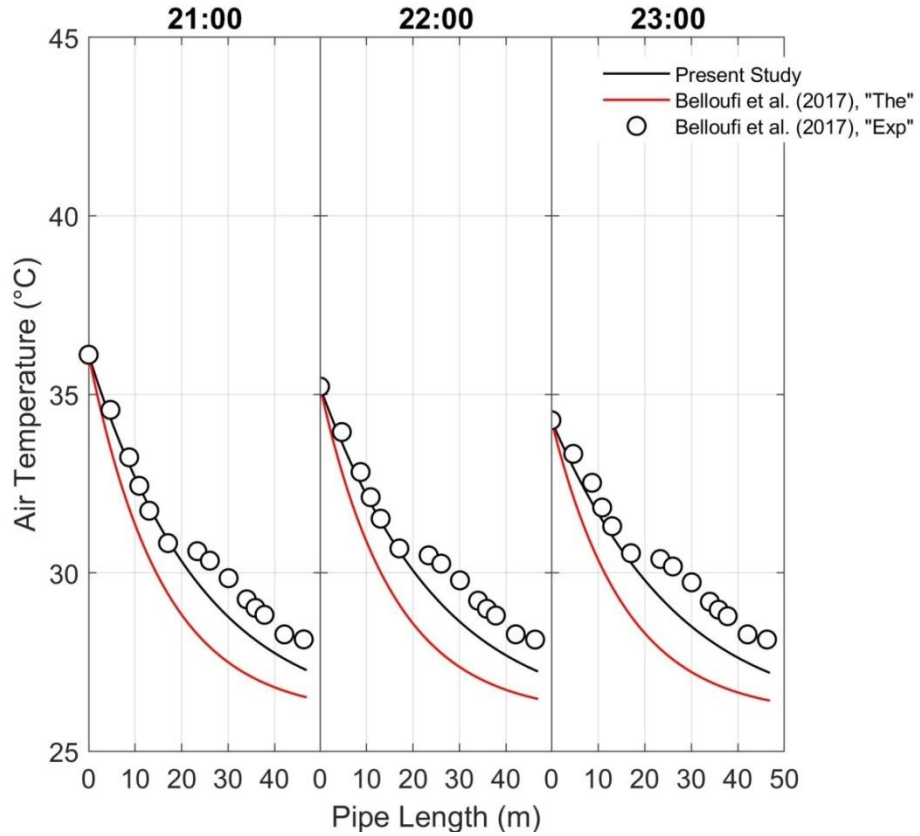

Fig. IV.8 Air temperature distribution by length after 12 hours of system operation 04/08/2013

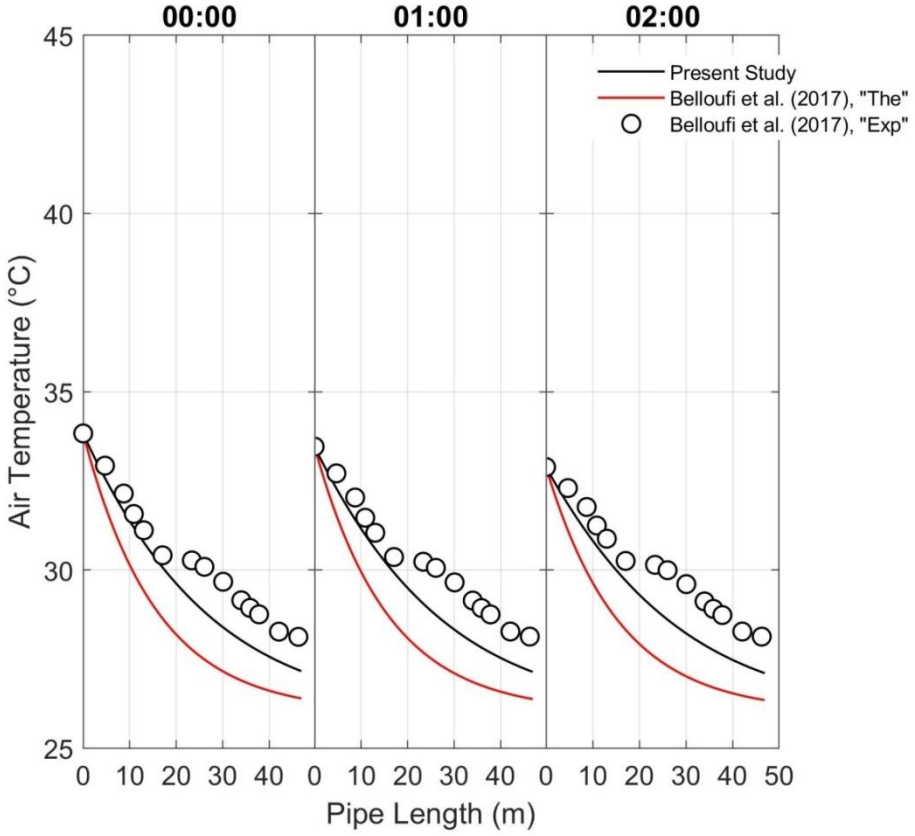

Fig. IV.9 Air temperature distribution by length after 15 hours of system operation 05/08/2013

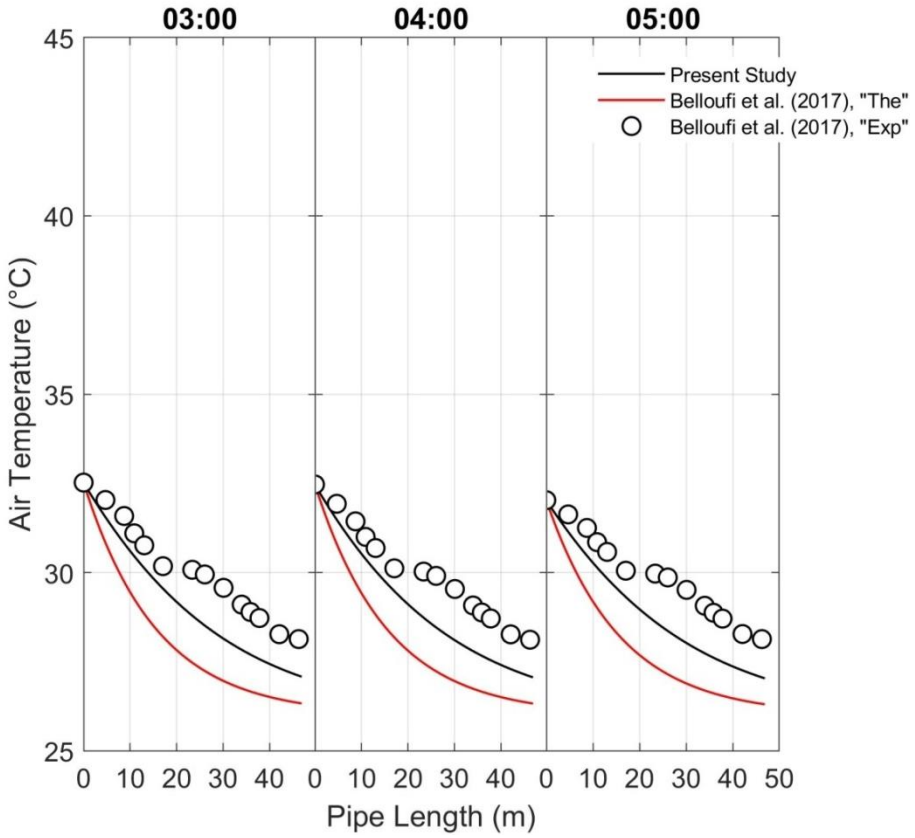

Fig. IV.10 Air temperature distribution by length after 18 hours of system operation 05/08/2013

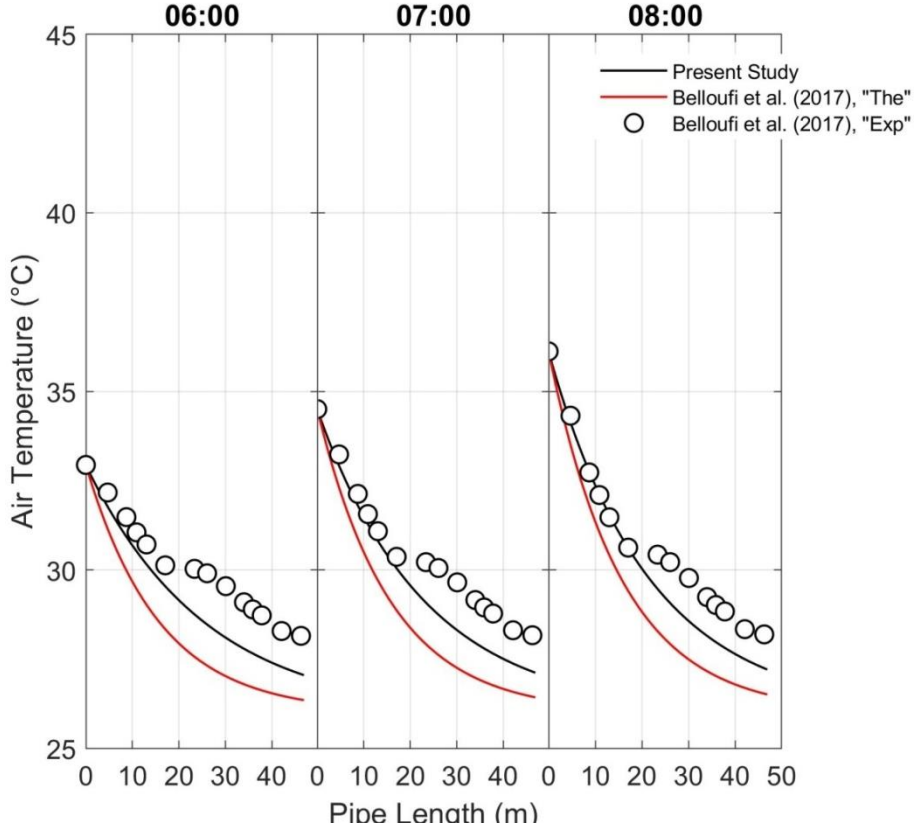

Fig. IV.11 Air temperature distribution by length after 21 hours of system operation 06/08/2013

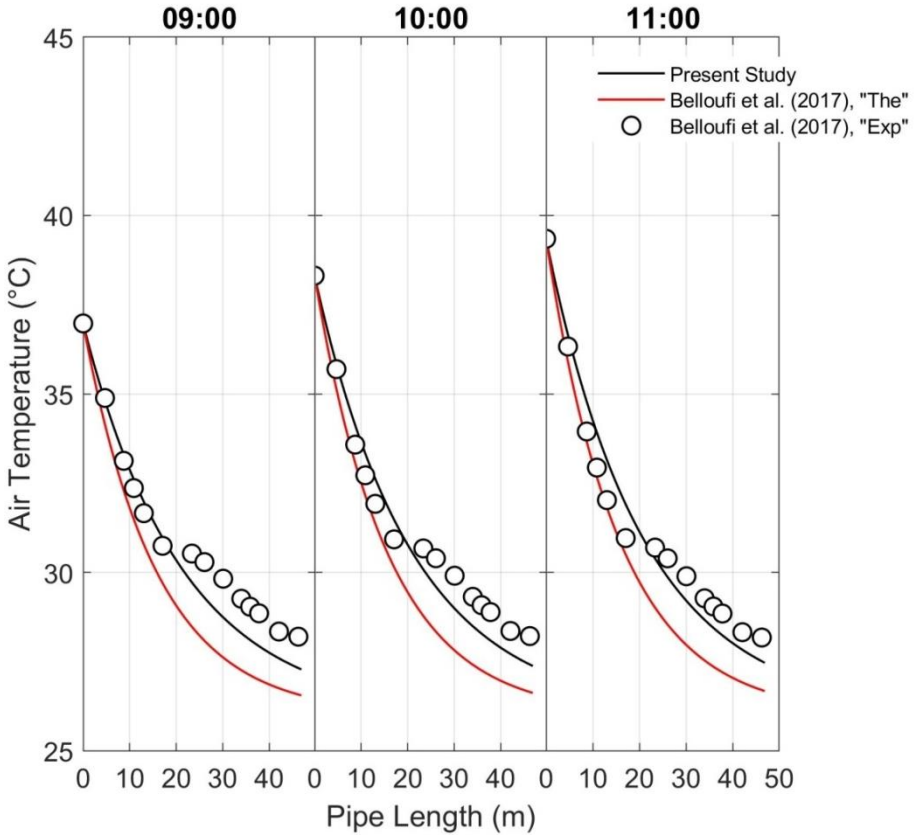

Fig. IV.12 Air temperature distribution by length after 24 hours of system operation 05/08/2013

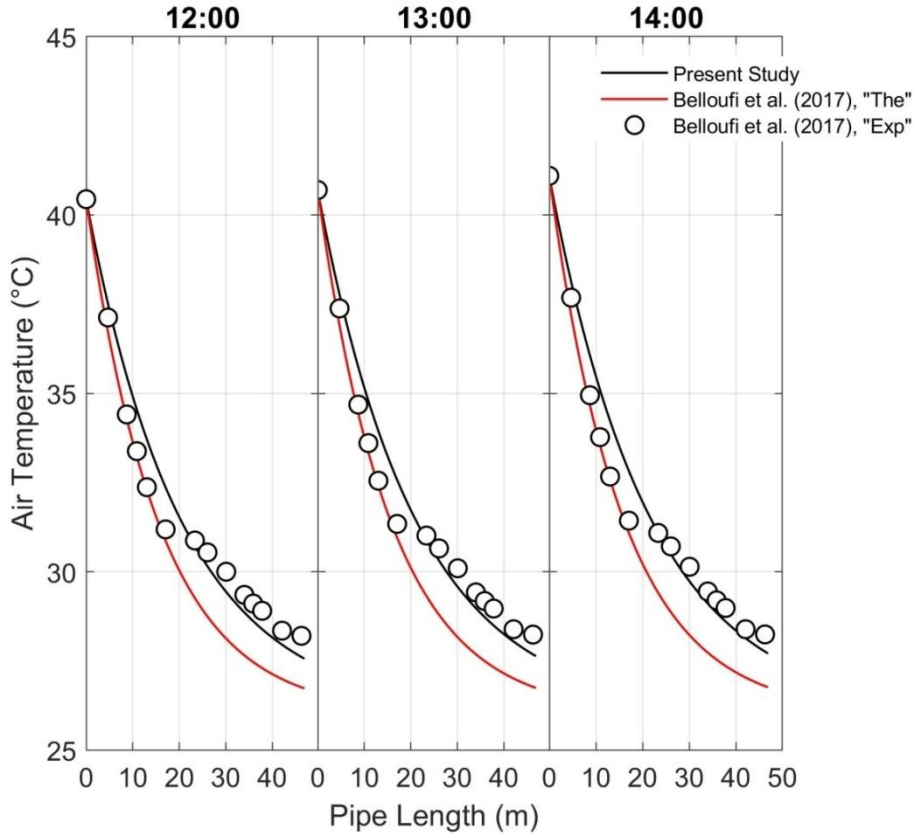

Fig. IV.13 Air temperature distribution by length after 27 hours of system operation 05/08/2013

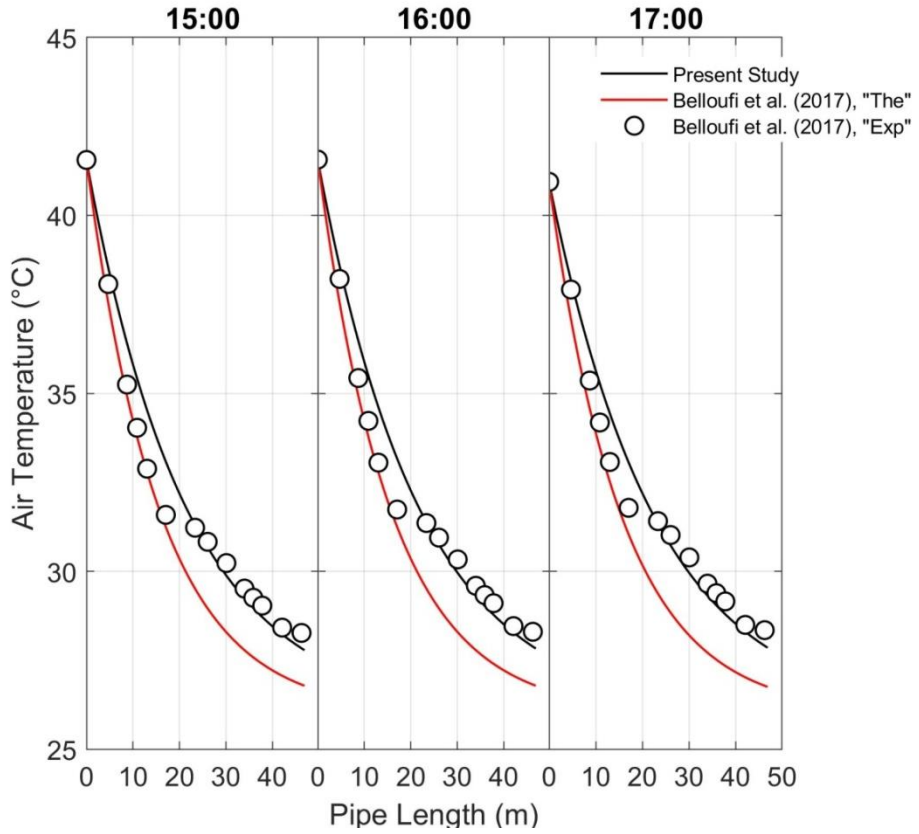

Fig. IV.14 Air temperature distribution by length after 30 hours of system operation 05/08/2013

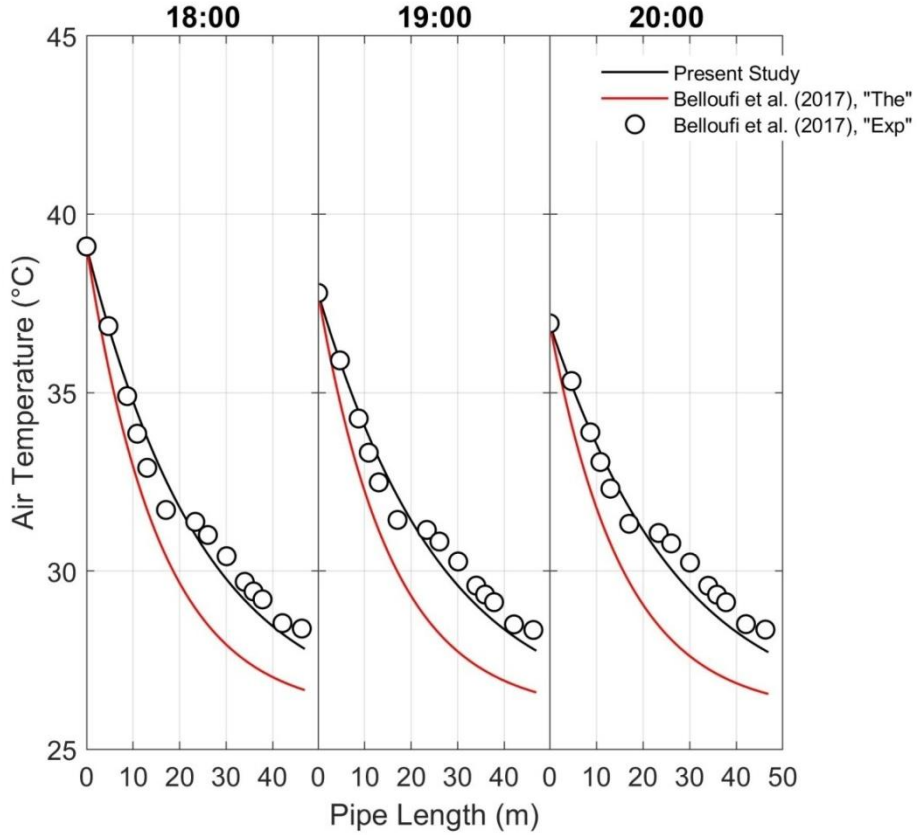

Fig. IV.15 Air temperature distribution by length after 33 hours of system operation 05/08/2013

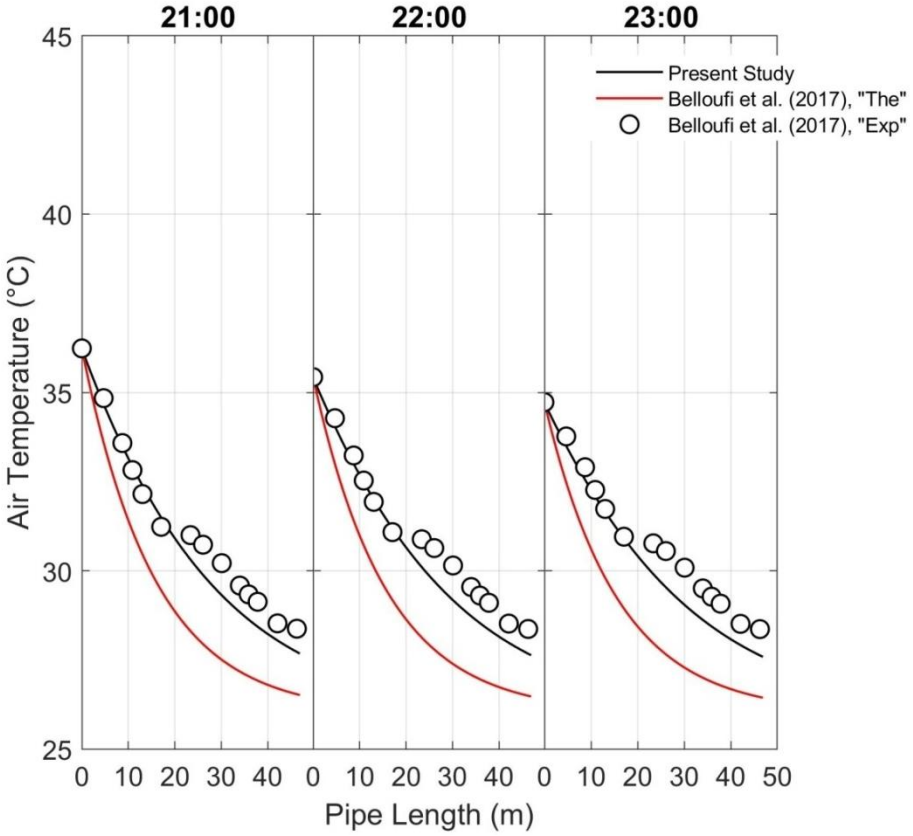

Fig. IV.16 Air temperature distribution by length after 36 hours of system operation 05/08/2013

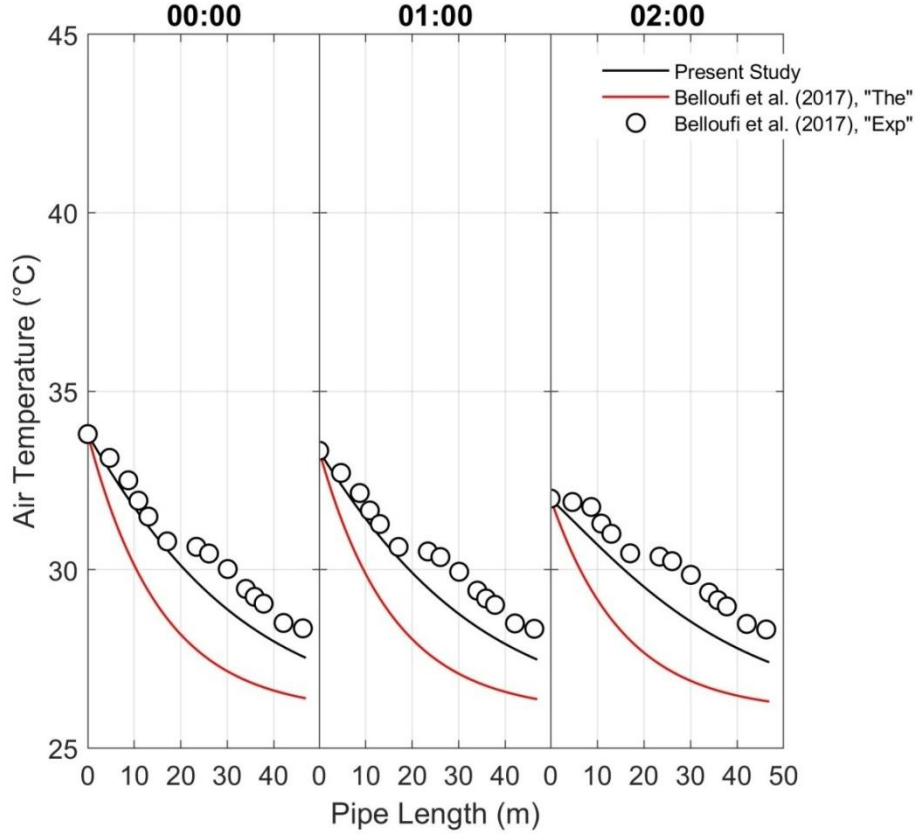

Fig. IV.17 Air temperature distribution by length after 39 hours of system operation 06/08/2013

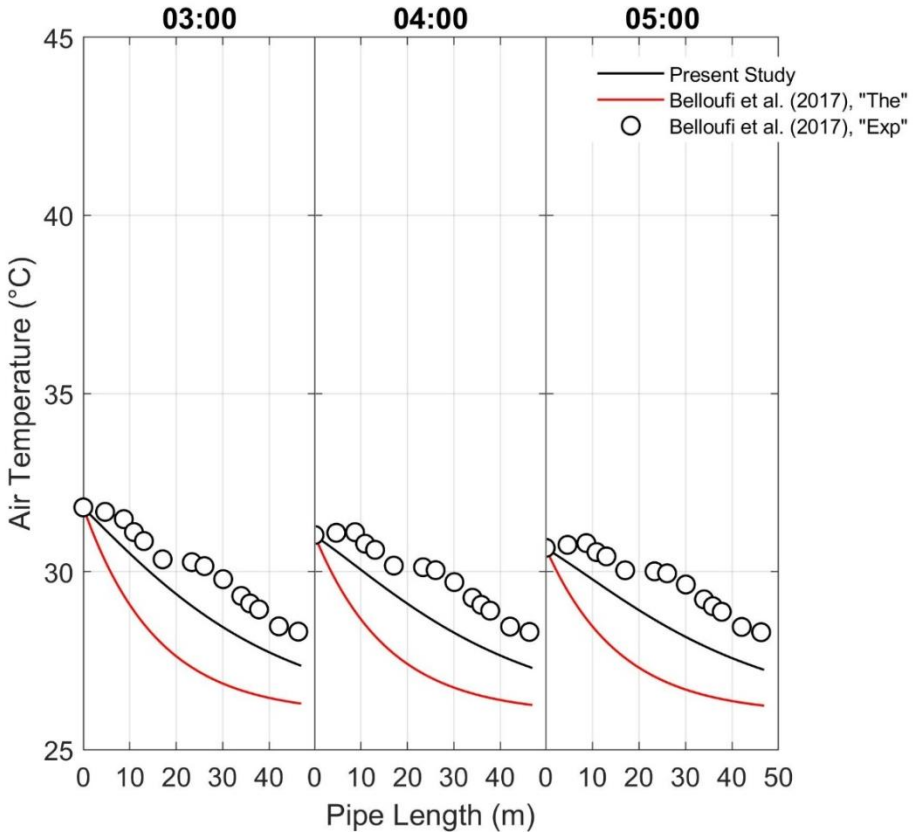

Fig. IV.18 Air temperature distribution by length after 42 hours of system operation 06/08/2013

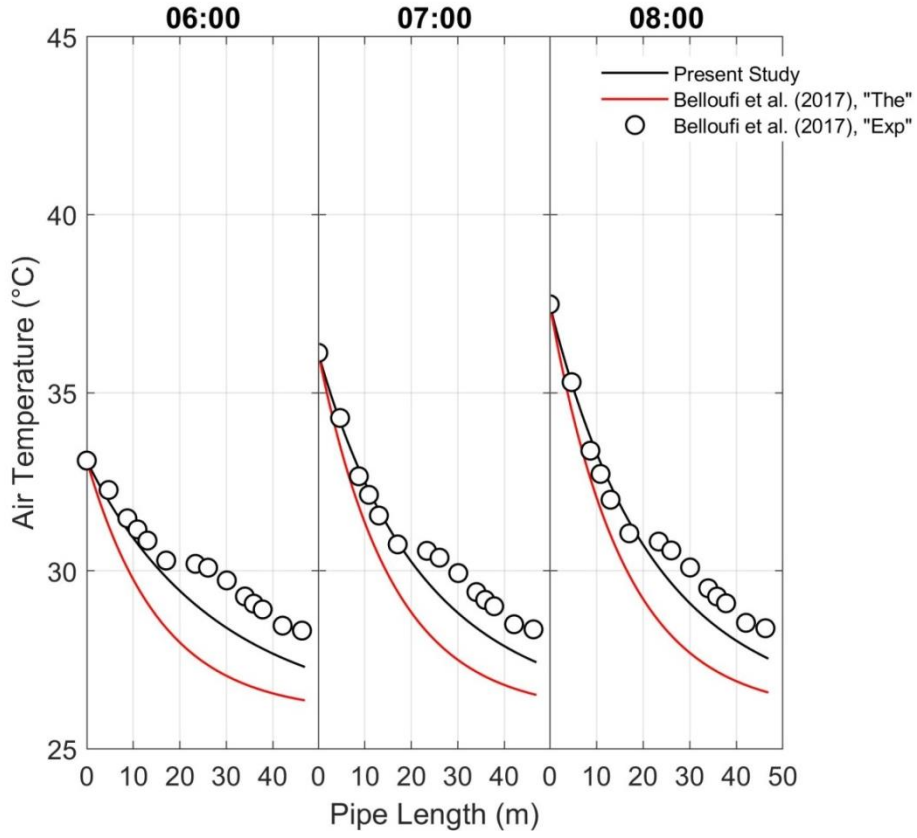

Fig. IV.19 Air temperature distribution by length after 45 hours of system operation 06/08/2013

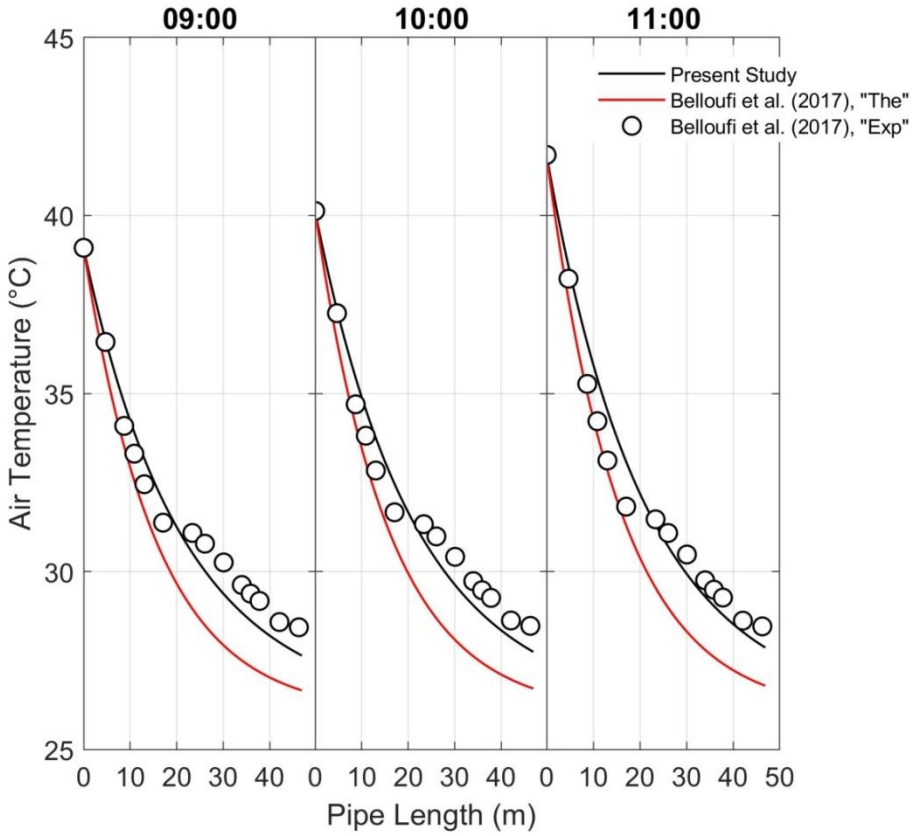

Fig. IV.20 Air temperature distribution by length after 48 hours of system operation 06/08/2013

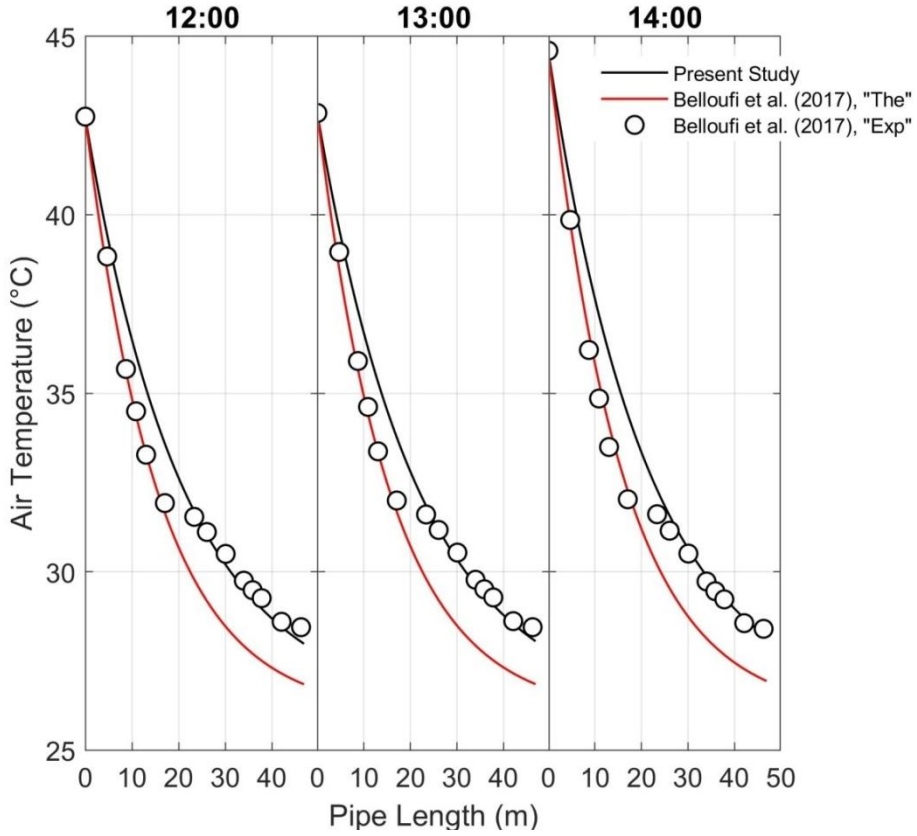

Fig. IV.21 Air temperature distribution by length after 51 hours of system operation 06/08/2013

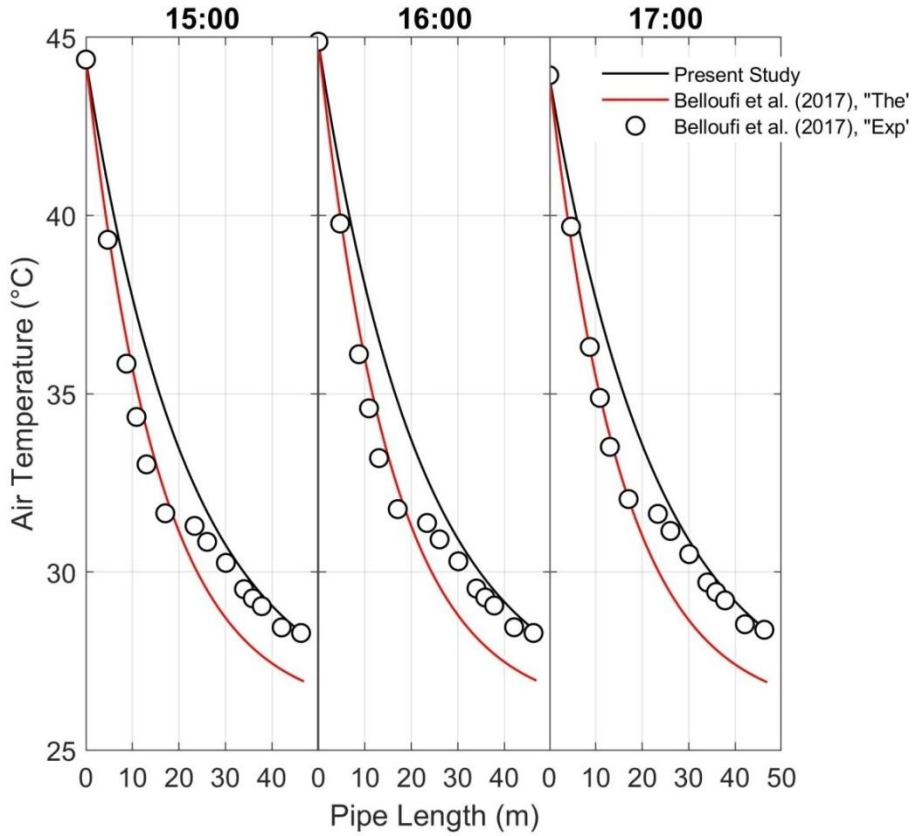

Fig. IV.22 Air temperature distribution by length after 54 hours of system operation 06/08/2013

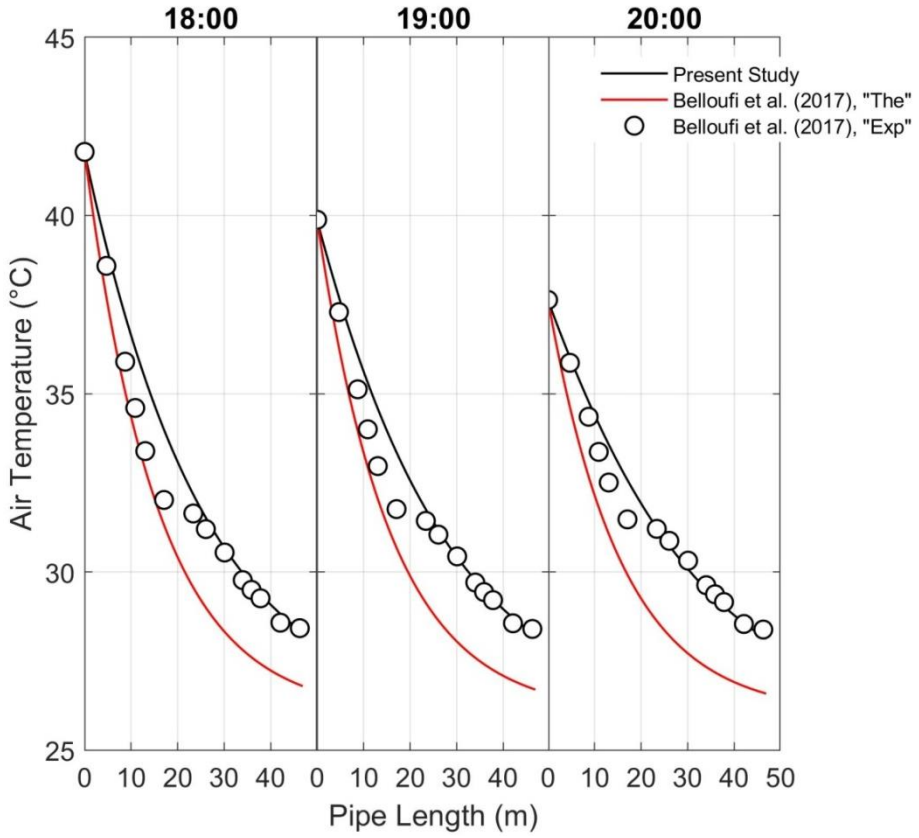

Fig. IV.23 Air temperature distribution by length after 57 hours of system operation 06/08/2013

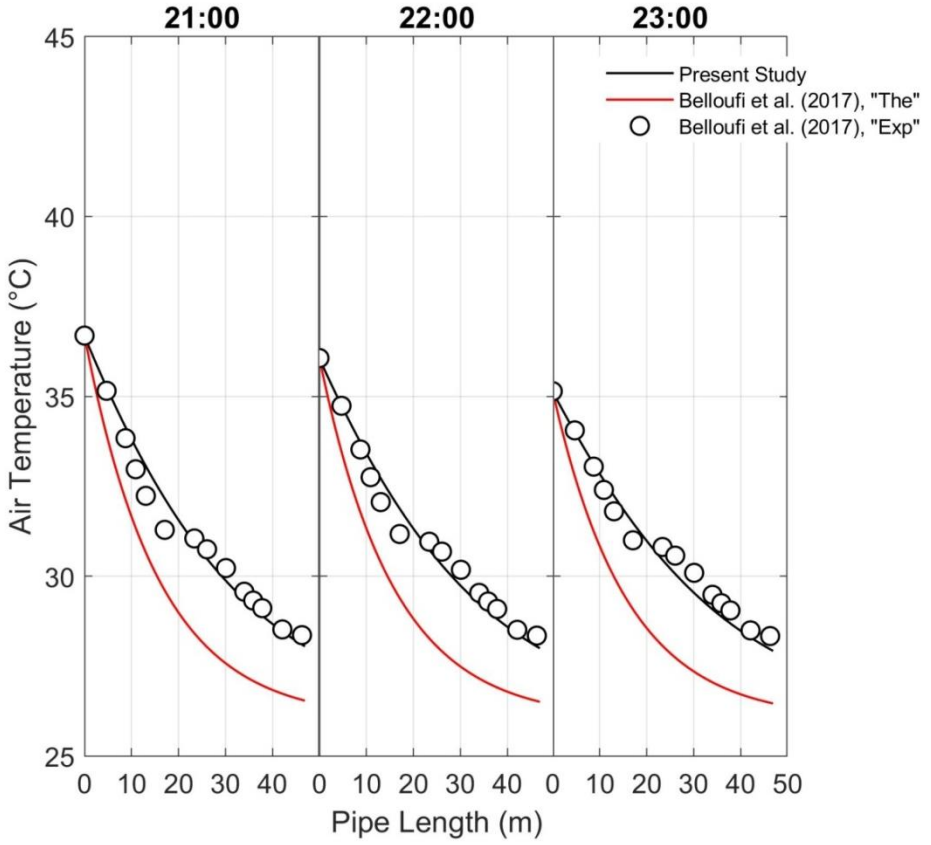

Fig. IV.24 Air temperature distribution by length after 60 hours of system operation 06/08/2013

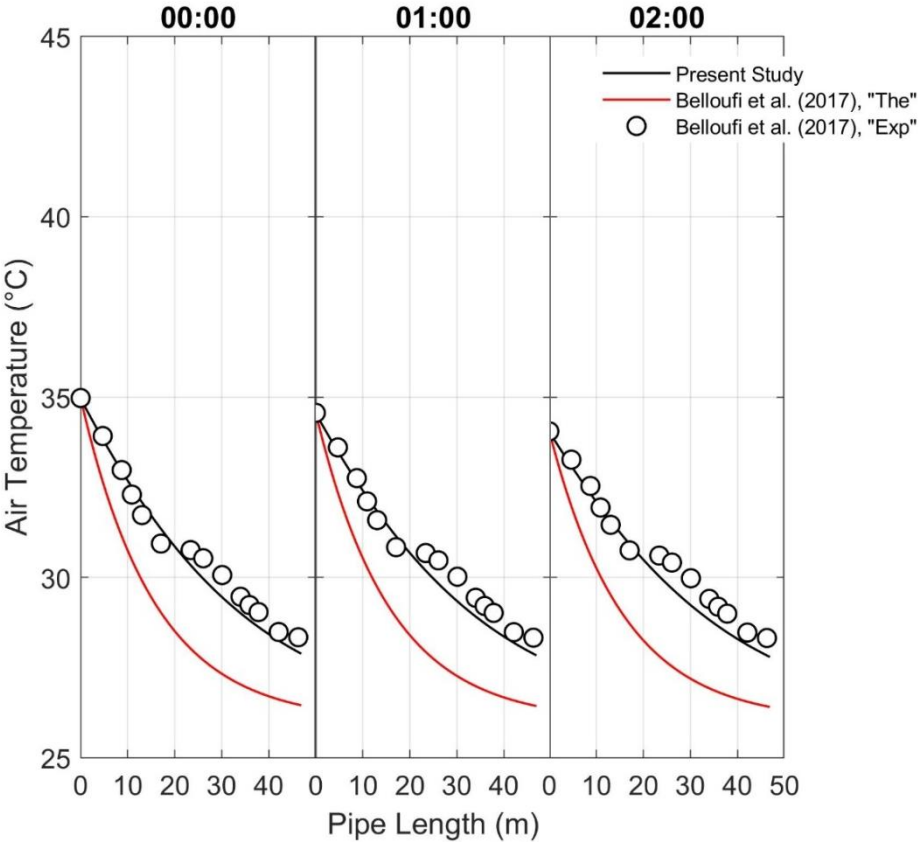

Fig. IV.25 Air temperature distribution by length after 63 hours of system operation 07/08/2013

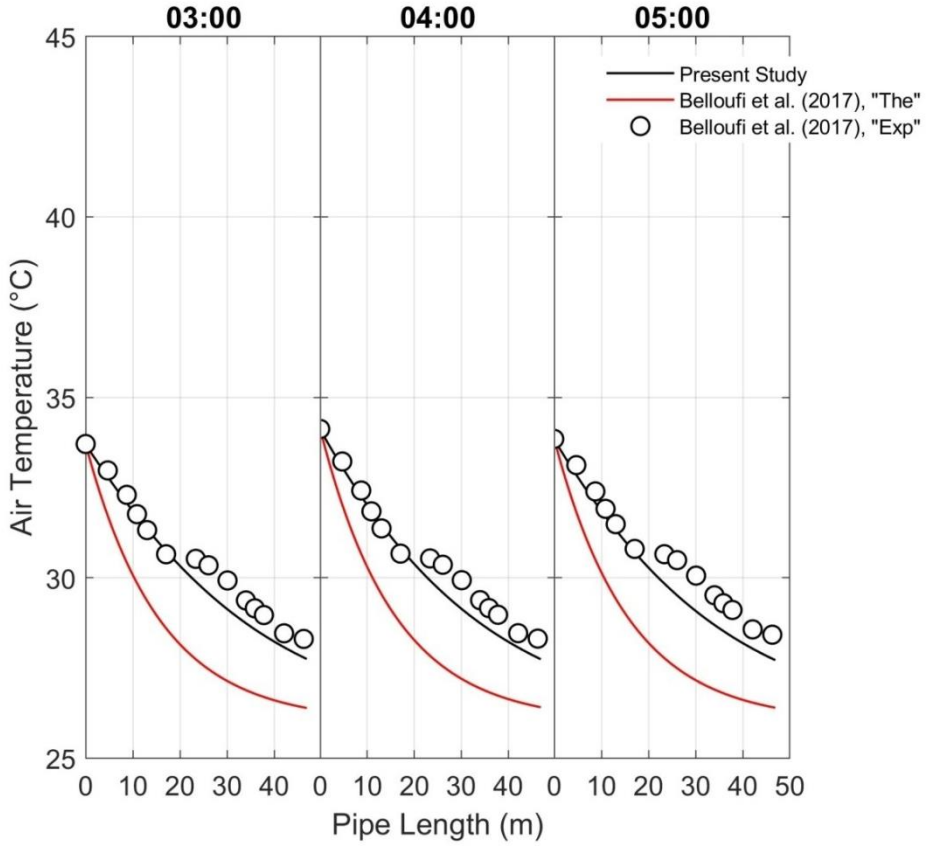

Fig. IV.26 Air temperature distribution by length after 66 hours of system operation 07/08/2013

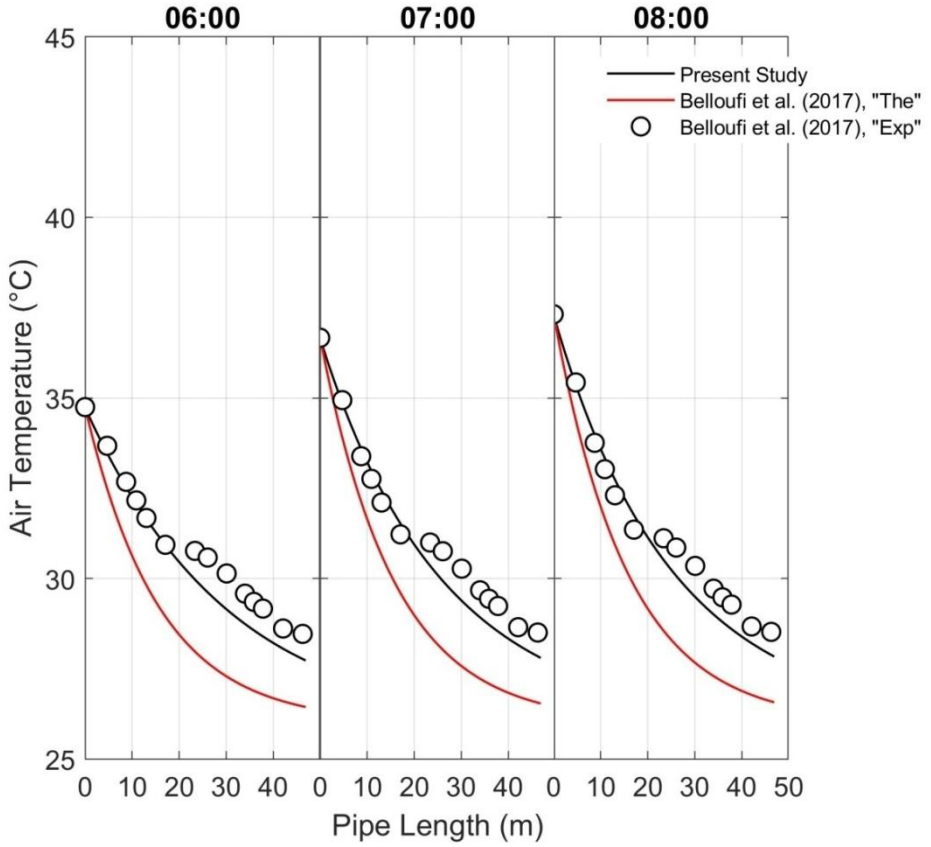

Fig. IV.27 Air temperature distribution by length after 69 hours of system operation 07/08/2013

Figure IV.4 to Figure IV.27 show the evolution of the air temperature along the pipe, at daytime and at night. As it was observed for the previous figures, the present model is overall more accurate as compared to the model proposed by Belloufi et al. (2017). At daytime, when the ambient temperature is relatively high, the two models give good results that fit well the experimental data. At night, when the ambient temperature is relatively low, the present model is still in very good agreement with the experimental data, while the model of Belloufi et al. (2017) tends to underestimate the air temperature.

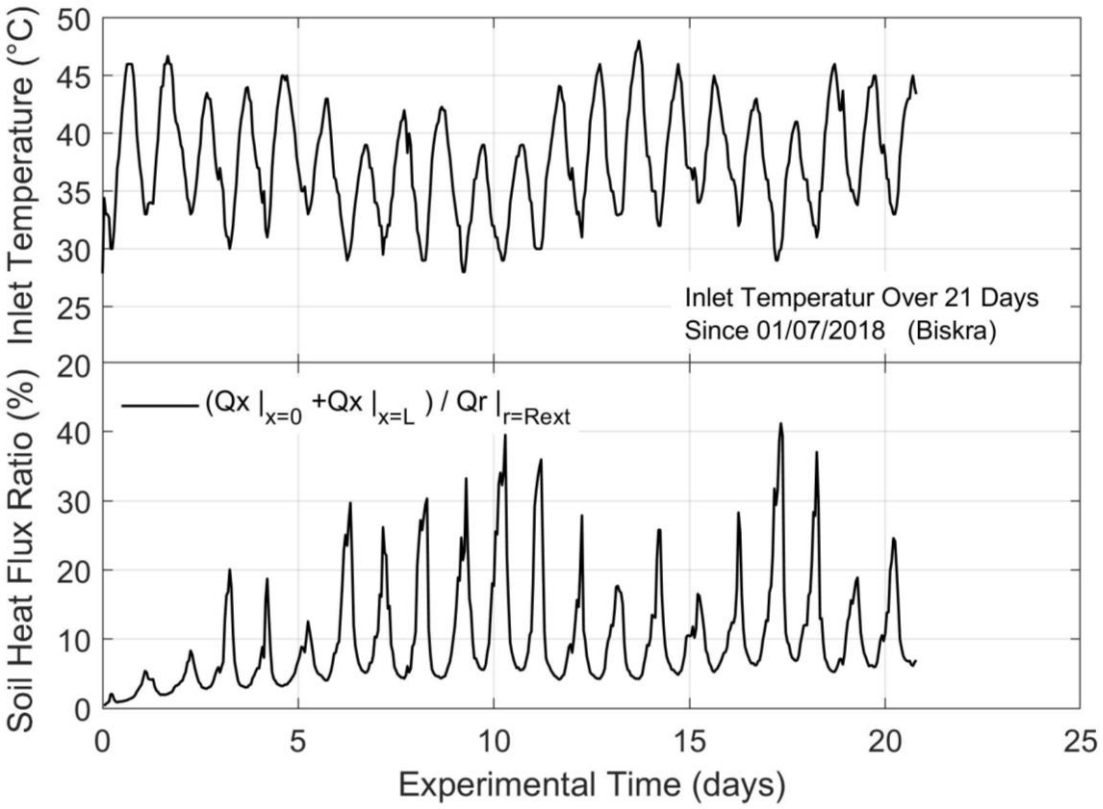

Fig. IV.28 The ambient air temperature variations for 21 (days) and the conduction heat flux ratio of EAHE operation in that period variations

Figure IV.28 shows the variation over time of the ambient (inlet) temperature from Laurent (2019) and the corresponding numerical results of the conduction heat flux ratio in the soil using the system's thermo-physical properties from Mehdid et al. (2018) and the undisturbed soil temperature from the semi-finite heat conduction model (Ben Jmaa Derbel and Kanoun, 2010). The evolution of the ambient temperature is an almost-periodic function, while the evolution of the conduction heat flux ratio resembles multi-peak distribution which has the same frequency as that of the ambient temperature. It can be seen that each peak corresponds to the lowest ambient temperature recorded each day, and the peak value increases as the

minimum ambient temperature decreases (the peak reaches a maximum value of approximately 40% for a minimum ambient temperature of about 28 °C between 01/07/2018 and 21/07/2018).

At daytime, temperature difference between air and undisturbed soil is maximum which leads to a maximum radial heat flux at the boundary $r = R_o$ where the greater portion is stored in the soil of initially low temperature, and the other portion is primarily diffused in the same (radial) direction, which allows neglecting the axial heat flux. At night, temperature difference between air and undisturbed soil decreases which leads to a minimum radial heat flux; on the other hand, the heat stored in the soil at daytime is diffused in all directions and evacuated from the soil control volume through the boundaries $x = 0$ and $x = L$ which reflects the contribution of axial conduction term in the soil heat conduction equation during night time.

IV.4.2. Soil around pipe temperature

In this part of research, we are going to show the predicted changes in soil around pipe temperature. We have used Belloufi et al. (2017) experience parameters as an example.

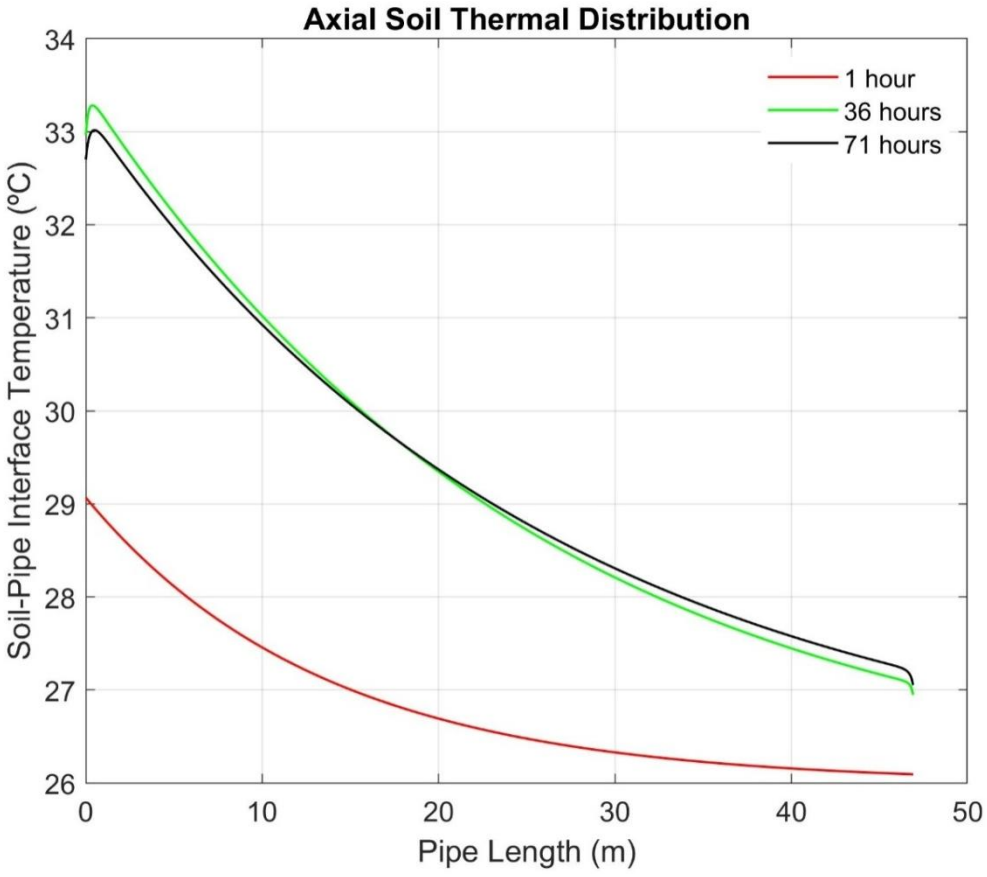

Fig. IV.29 Axial soil thermal distribution at different time during system operation in soil-pipe interface.

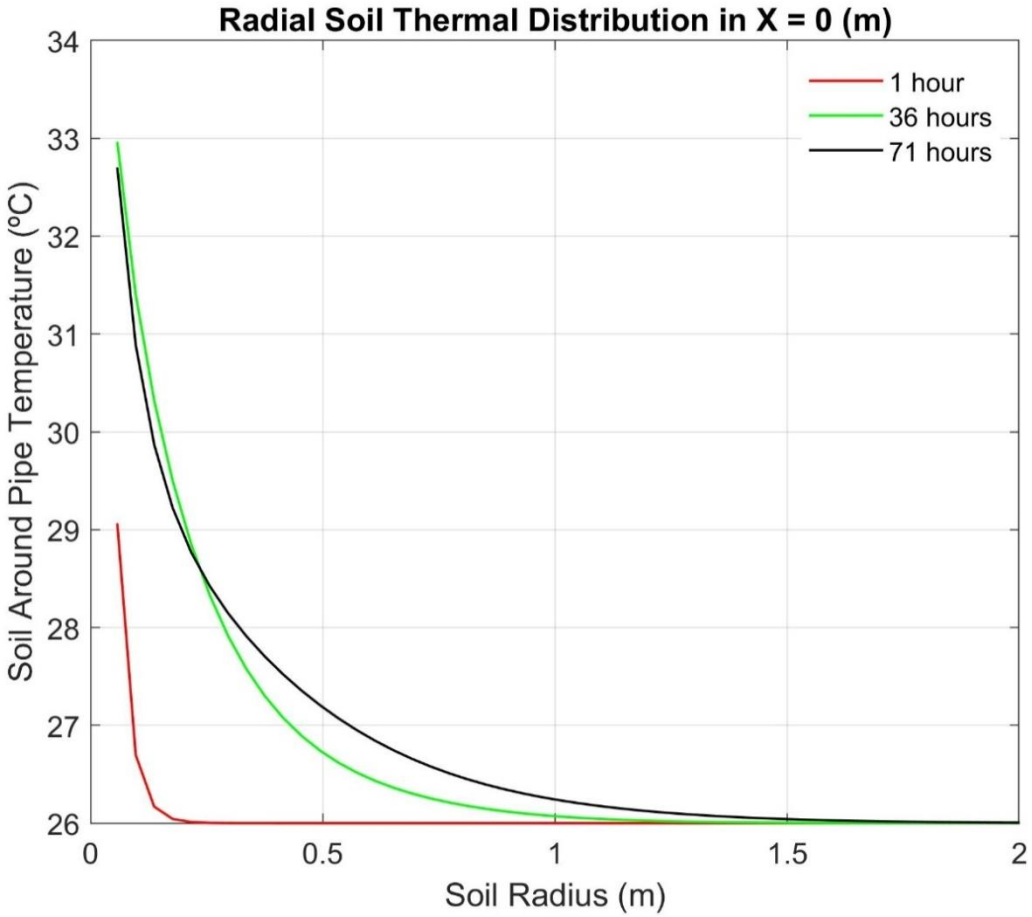

Fig. IV.30 Radial soil thermal distribution in X= 0 (m) at different time during system operation.

Figures IV.29 and IV.30 describe the axial and radial thermal distribution that happen in the soil around pipe during the system operation. In Figure IV.29, the interface (soil-pipe) temperature next to the pipe inlet and outlet has observable decreases after relatively long period of system operation, where the heat stored in the soil at daytime is diffused in all directions and evacuated from the soil control volume through the boundaries $x = 0$ and $x = L$.

IV.5. Conclusion

Through the present study, we aim to model in more details the thermal behavior of an EAHE by investigating the validity of the hypothesis of dominant radial heat conduction in the soil surrounding the pipe, which is commonly assumed in the study of such system. It has been found that axial heat conduction can be neglected from the soil conduction equation only for high air-soil temperature difference; however, for low air-soil temperature difference, the heat

conduction becomes a leading-order term in the soil conduction equation, thus, it should be taken into account. By doing so, the predictability of the previous models can be improved as it was observed from the results above especially for long periods of operation, where the present simulation shows less sensitivity to the duration of operation as well as to the periodic temperature condition at the inlet of the EAHE system in comparison to the previous models. We have published this chapter in separate research paper (HAMDANE et al., 2020).

References

BELLOUFI, Y., BRIMA, A., ZEROUALI, S., ATMANI, R., AISSAOUI, F., ROUAG, A. & MOUMMI, N. 2017. Numerical and experimental investigation on the transient behavior of an earth air heat exchanger in continuous operation mode. *International Journal of Heat and Technology*, 35**,** 279-288.

BEN JMAA DERBEL, H. & KANOUN, O. 2010. Investigation of the ground thermal potential in tunisia focused towards heating and cooling applications. *Applied Thermal Engineering*, 30**,** 1091-1100.

BENHAMMOU, M., DRAOUI, B. & HAMOUDA, M. 2017. Improvement of the summer cooling induced by an earth-to-air heat exchanger integrated in a residential building under hot and arid climate. *Applied Energy*, 208**,** 428-445.

BERGMAN, L., LAVINE, S., INCROPERA, P. & DEWITT, P. 2011. *Fundamentals of Heat and Mass Transfer.*

HAMDANE, S., MAHBOUB, C. & MOUMI, A. 2020. Numerical Approach to Predict the Outlet Temperature of Earth-to-Air-Heat-Exchanger. *Thermal Science and Engineering Progress***,** 100806.

LAURENT, G. 2019. *Real Time Weather Records In Biskra* [Online]. Infoclimat. Available: https://www.infoclimat.fr/observations-meteo/temps-reel/biskra/60525.html.

MEHDID, C.-E., BENCHABANE, A., ROUAG, A., MOUMMI, N., MELHEGUEG, M.-A., MOUMMI, A., BENABDI, M.-L. & BRIMA, A. 2018. Thermal design of Earth-to-air heat exchanger. Part II a new transient semi-analytical model and experimental validation for estimating air temperature. *Journal of Cleaner Production*, 198**,** 1536-1544.

General Conclusion

This thesis is divided into four principal subjects that are related to each other. Several research about soil temperature and outlet air temperature of EAHE system were collected to show the researchers tendencies and our orientation. After that, experimental studies of both recording soil temperature and soil physical analysis in different regions and locations from Algeria and Portugal countries were realized. Then, we talked about the methodology of EAHE system modelling in the horizontal portion of system's pipe. Later, we have developed a mathematical model using the complete ax-symmetric heat conduction equation in the soil domain.

The outcomes of this thesis touch EAHE system parametric as :

- Researchers tendencies about predicting the soil temperature and predicting the outlet air temperature of EAHE system and our orientation.
- Comparison between the model results in predicting soil temperature when using air data / soil data.
- Create soil temperature reference years of three sites in Covilhã-Portugal.
- Use different protocols for analysing soil and define their texture.
- Define the modelling methodology.
- Develop a more detailed mathematical model that can predict outlet air temperature in horizontal portion of EAHE system.
- In practical terms using air data (extracted from the average annual air temperature) in the model allows us predicting soil temperature. This procedure avoids having to measure the soil temperature at greater depths, however the error is higher.
- The average soil temperature of the three years is used as reference year's undisturbed soil temperature. Also, the average value of soil temperature amplitude is used as reference year's amplitude soil temperature. These parameters are used as input in the Equation II.3, where the output shows us the soil temperature prediction of reference year of each site.
- Reference years of soil temperatures allow us selecting the available sites for the wanted function (pre-heating or pre-cooling). For example, the sites B and C have low undisturbed ground temperature. They are good sites to install EAHE as pre-cooler system. Site A has higher undisturbed temperature. It gives better results as pre-heater with EAHE system.

- The ten samples analyzed show five types of soil, which are Silt loam, Sandy loam, Sand, Gypsum and Loam. Samples densities values change between $2077.56\,(\mathrm{m^3.kg^{-1}})$ and $2533.78\,(\mathrm{m^3.kg^{-1}})$, where the lowest value belong to Gypsum soil in Tolga and Silt loam soil in El-Kantara. Silt loam soil does also exist in Biskra but with higher density. The highest density value belongs to Sand soil in Ouargla.
- It has been found that axial heat conduction can be neglected from the soil conduction equation only for high air-soil temperature difference; however, for low air-soil temperature difference, the heat conduction becomes a leading-order term in the soil conduction equation, thus, it should be taken into account. By doing so, the predictability of the previous models can be improved as it was observed especially for long periods of operation, where the present simulation shows less sensitivity to the duration of operation along the pipe as well as to the periodic temperature condition at the inlet of the EAHE in comparison to the previous models.

Future works:

This thesis touches on several topics such as bibliographic studies, soil temperature, soil analysis and EAHE system modelling. These topics could be taken as bases of continue / new study on those domains. As future work, it is suggested:

a. Prepare a review article.
b. Natural soils are composed of more than one type of individual soil, while the tables of soil heat conductivities and soil heat capacities in literature generally have individual elements properties. We suggest developing a model that find the composed soil: i) thermal conductivity ii) heat capacity.
c. Records of soil temperature in the current thesis can be used to validate a new developed model.
d. Develop numerical approaches to calculate the outlet air temperature of EAHE in different system designs.

Annex

14th World Congress in Computational Mechanics (WCCM)
ECCOMAS Congress 2020
11 – 15 January 2021, Paris, France

COMPARISON STUDY BETWEEN USING AIR DATA AND SOIL DATA IN PREDICTING SOIL TEMPERATURE

Samia Hamdane [1], Pedro Dinho da Silva [2,4], Luis Carlos Carvalho Pires [3,4], Abdelhafid Moummi[5]

[1]Laboratory of Mechanical Engineering (LGM), University of Biskra, BP145 Biskra 07000, Algeria.
samia.hamdane@univ-biskra.dz
[2] University of Beira Interior, Rua Marquês d'Ávila e Bolama, 6201-001, Covilhã, Portugal,
dinho@ubi.pt
[3]University of Beira Interior, Rua Marquês d'Ávila e Bolama, 6201-001, Covilhã, Portugal,
pires@ubi.pt
[4] C-MAST - Centre for Mechanical and Aerospace Science and Technologies, Covilhã, Portugal
[5]Laboratory of Mechanical Engineering (LGM), University of Biskra, BP145 Biskra 07000,
Algeria.a.moummi@univ-biskra.dz

Key Words: *Soil Temperature, Reference Year, Depth, Air Data, Soil Data.*

Predicting soil temperature is important study in proceed of installing geosystems as Earth Air Heat Exchanger system (EAHE) and Ground Heat Pomp system (GHP). Mathematical models that used in predicting soil temperature are usually using amplitude and average values of ambient air temperature of reference year in certain place as alternative parameters of soil surface amplitude temperature and soil undisturbed temperature for year, respectively (Larwa and Krzysztof, 2019, Cho and Ihm, 2018, Larwa, 2018).

In present work, authors compare the results of using soil data and air data with soil temperature records to show the preciseness of using each of them in predicting soil temperature. For soil data, it has been utilized the records of soil temperature in three sites (A, B & C) in Covilha (Portugal) for three years in calculating soil surface amplitude temperature and soil undisturbed temperature (soil undisturbed temperatures is define as averages values of soil temperatures for certain year in each depth from 1 to 5 (m)). For air data, it has been utilized a reference year of ambient air temperature in the same city (Aguiar and Carvalho, 2012).

The results show the differences of using average soil temperatures from different depths as undisturbed soil temperature, as compared with using air data in mathematical model to predict soil temperature in the depth five meter. It is showing that using air data gives better agreements with less relative errors as compared with the results of using average soil temperatures of the 1^{st} and 2^{nd} meters, where 24.86 (%) and 21.89 (%) are the relative errors of using soil data and air data, respectively. However, using average soil temperatures of the 3^{rd}, 4^{th} and 5^{th} meters depths, as undisturbed soil temperatures, give better agreements as compared with using air data in mathematical model to predict soil temperature, where 7.86 (%) and 17.97 (%) are the relative errors of using soil data and air data, respectively

Using soil temperature records, authors create soils temperature reference years under 1 to 5 (m), where the average temperature differences in each depth were 2 (°C) in all sites.

As conclusion, it can be saying that air data (annual air temperature) can be used to calculate the needed parameters in analytical model to predict soil temperature. This procedure avoids having to measure the soil temperature however the error is higher.

It is better to use air data if authors need to predict soil temperature in depth equal or less than 2 (m), while if they want to predict soil temperature for higher depth it is better to use soil data.

This study shows that B and C sites are suitable for installing EAHE system as pre-cooler, while site A is suitable for installing GHP system and EAHE system as pre-heater

The created soils temperature reference years are helpful to guess how the soil thermal behaviour is act during any year.

REFERENCES

Aguiar, R. & Carvalho, M. J. 2012. Performance analysis of solar thermal and photovoltaic systems,. Lisbon, Portugal,: Solterm software, National Laboratory of Energy and Geology

Cho, S.-W. & Ihm, P. 2018. Development of a Simplified Regression Equation for Predicting Underground Temperature Distributions in Korea. *Energies,* 11**,** 2894.

Larwa, B. 2018. Heat Transfer Model to Predict Temperature Distribution in the Ground. *Energies,* 12**,** 25.

Larwa, B. & Krzysztof, K. 2019. Study of temperature distribution in the ground. *Chemical and Process Engineering,* 40**,** 123-137.

New Journal and we have not received input yet 21 (2021) 100806

Contents lists available at ScienceDirect

Thermal Science and Engineering Progress

journal homepage: www.sciencedirect.com/journal/thermal-science-and-engineering-progress

Numerical approach to predict the outlet temperature of earth-to-air-heat-exchanger

Samia Hamdane *, Chawki Mahboub, Abdelhafid Moummi

Mohamed Khider University of Biskra, Laboratory of Mechanical Engineering (LGM), BP145 Biskra 07000, Algeria

ARTICLE INFO

Keywords:
Earth/Air heat exchanger
Modelling
Outlet air temperature
Heat conduction

ABSTRACT

It is usually assumed that the heat conduction in the soil surrounding the pipe of an EAHE is one-dimensional in the radial direction which allows one to simplify the mathematics and eventually to obtain an analytical or semi-analytical solution to the problem. For the simulation model proposed in this work, the complete axisymmetric heat conduction equation is solved in the soil domain. The results of the simulation in terms of the air temperature were validated using experimental data available in the literature where they demonstrate an overall superiority over the other models that used one-dimensional heat conduction equations in the soil domain.

1. Introduction

The world population increases every day (it reached 7.6 Billion in 2018 according to Toshiko et al. [19]. This leads to an increase in the energy demand and production, and eventually to an increase in the energy consumption (+2.2% in 2017 according to Bob [8]). The energy consumed worldwide is primarily produced from fossil fuels, which is the main cause of the pollution and global warming of the earth [17]. This drives toward looking for renewable systems technology which could be an alternative to the classical systems technology that requires fossil fuels to operate.

For instance, from the total energy consumed in the residential and service sectors, the energy consumption for space cooling in US, China and EU is less than 10%, while for space heating in the same regions is generally more than 30% in residential sector, and 25% in service sector [9]. It is possible to considerably reduce this energy consumption using renewable systems such as earth-to-air-heat-exchanger (EAHE). This latter is easy to install[10], its energy consumption is very low as compared to the classical systems [16], and it can be integrated to other systems in order to improve their performance [1,2,13].

The modeling of EAHE is of great interest when studying the feasibility of such system. The solution of the mathematical model may provide us with useful information for improving the system design and selecting the conditions that can lead to optimum system performance. This was the subject of many research papers, some of which are reviewed next. All the proposed models are using the one-dimensional energy equation in the fluid region, while different approaches have been adopted to determine the time-dependent temperature field in the soil surrounding the pipe.

Goswami and Dhaliwal [11] presented heat transfer analysis and developed a computer model solution to predict the transient air temperature while passing through an underground pipe. The authors considered a transient one-dimensional (radial) conduction in the soil, for which a semi-analytical solution has been given using an integral method. Hollmuller [12] developed the complete analytical solution for the heat diffusion of a cylindrical air/soil heat-exchanger with adiabatic or isothermal boundary condition, submitted to constant airflow thickness, the harmonic signal is subjected to amplitude dampening and phase-shifting as the air passes through the heat-exchanger. Belatrache et al. [3] presented the modeling and simulation of an earth-air heat exchanger used as air-conditioning device in the climate conditions of the south of Algeria. A parametric analysis enabled selecting the optimal depth of the buried heat exchanger and the length of the pipe allowing the air temperature to reach the soil temperature. Belloufi et al. [4] investigated the thermal performance of an earth-air heat exchanger under transient conditions in cooling mode. Experiments were performed using a PVC pipe of 53.16 m long and 110 mm diameter buried at 3 m depth, continuously for 71 h in summer season at the University of Biskra-Algeria. A mathematical model for EAHE was presented where the air temperature distribution in both horizontal and vertical portions of the pipe is obtained using the implicit finite difference method. Benhammou et al. [6] examined the impact of the thermal insulation of buildings on the cooling effectiveness of the Earth-to-Air Heat Exchanger systems under hot and arid climate. A transient model is

* Corresponding author.
E-mail address: samia.hamdane@univ-biskra.dz (S. Hamdane).

https://doi.org/10.1016/j.tsep.2020.100806
Received 15 August 2020; Received in revised form 4 November 2020; Accepted 3 December 2020
Available online 9 December 2020

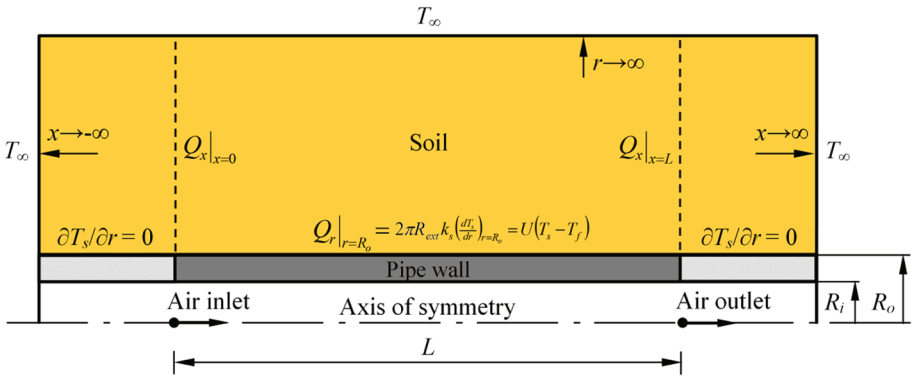

Fig. 1. The physical domain and the boundary conditions.

developed for the whole system (EAHE + building) and solved using the technique of Complex Finite Fourier Transform. Mehdid et al. [15] developed a semi-analytical model to predict the thermal performance of EAHE operating under transient conditions for cooling mode, by subdividing the soil and the pipe into layers and using a transient semi-analytical model developed earlier by Rouag et al. [18] to estimate the temperature and the thermal resistance of the disturbed soil surrounding the pipe.

The aforementioned studies were concerned the most with providing simplified models by neglecting the axial conduction through the soil in comparison with the radial conduction, so that analytical or semi-analytical solutions of these models can be easily obtained. We are, on the other hand, concerned in the present study with providing a more detailed mathematical representation of the system in question so an accurate simulation can be obtained.

2. Theoretical analysis

The problem encountered here concerns the conjugate heat transfer that takes place between the air flowing inside an horizontal pipe of length L(we ignored the effects of elbows/bends) and of inner and outer radius respectivelyR_i and R_o, buried under ground, and the surrounding soil initially at uniform temperature T_∞. The heat conduction and energy equations can be simplified for the present problem by assuming the following hypotheses:

The soil is homogeneous and all its properties are constant;
The heat conduction in the soil is unsteady axisymmetric with no heat source$\dot{Q} = 0$;
The air flow is one-dimensional along the x-axis and all its properties are constant;
The air thermal inertia is neglected (yet the air temperature can vary with time instantaneously due to the variation of the boundary conditions, as it will be seen later);
The pipe thermal inertia is neglected (i.e. the heat transfer through which is instantaneous), while its thermal resistance is taken into account;
The thermal contact between the pipe and the soil is perfect (i.e. there are no air gaps in the pipe-soil interface).

By taking into account the above hypotheses, the heat conduction and energy equations in the two-region (soil-air) domain can be written respectively as:

$$\frac{\partial T_s}{\partial t} = \alpha_s \left(\frac{1}{r} \frac{\partial}{\partial r} \left(r \frac{\partial T_s}{\partial r} \right) + \frac{\partial^2 T_s}{\partial x^2} \right) \tag{2.1}$$

$$\dot{m} c_p \frac{\partial T_f}{\partial x} = U \left(T_{\text{interface}} - T_f \right) \tag{2.2}$$

The present problem described by Eqs. (2.1) and (2.2) must be solved subject to the following initial and boundary conditions:

$$T_s(0, x, r) = T_\infty \tag{2.3}$$

$$T_s(t, x, \infty) = T_\infty \tag{2.4}$$

$$T_s(t, \pm\infty, r) = T_\infty \tag{2.5}$$

and from the heat balance between the soil and the pipe interface, we have:

$$2\pi R_{ext} k_s \left. \frac{\partial T_s}{\partial r} \right|_{\text{interface}} = U \left(T_{\text{interface}} - T_f \right) \tag{2.6}$$

where U is the equivalent heat transfer coefficient given by:

$$\frac{1}{U} = \frac{1}{2\pi R_{int} h} + \frac{1}{2\pi k_p} ln \left(\frac{R_o}{R_i} \right) \tag{2.7}$$

With the convection heat coefficient $h = \text{Nu}\ D_i/k_f$ is calculated from:

$$\text{Nu} = 0.023 \text{Re}^{0.8} Pr^{0.33} \tag{2.8}$$

for turbulent flow, whereas$\text{Nu} = 3.66$ is taken when the flow is laminar [7]. The boundary condition Eq. (2.6) is applied at the soil-pipe interface from the inlet (at $x = 0$) to the outlet (at$x = L$), otherwise the pipe is considered to be insulated (see Fig. 1). And finally the temperature of the air at the inlet is:

$$T_f(t, 0) = T_{in}(t) \tag{2.9}$$

3. Solution method

The previous set of equations is solved using the finite difference method. A uniform mesh is generated for the soil region with N × M (1141 × 201) grid points, in which the following implicit finite difference formula has to be solved:

$$\left(1 + 2\frac{\alpha_s \Delta t}{\Delta r^2} + 2\frac{\alpha_s \Delta t}{\Delta x^2}\right) T^k_{si,j} = \frac{\alpha_s \Delta t}{\Delta x^2} \left(T^k_{si+1,j} + T^k_{si-1,j} \right) + \left(\frac{\alpha_s \Delta t}{\Delta r^2} + \frac{\alpha_s \Delta t}{2 r_j \Delta r} \right) T^k_{si,j+1} + \left(\frac{\alpha_s \Delta t}{\Delta r^2} - \frac{\alpha_s \Delta t}{2 r_j \Delta r} \right) T^k_{si,j-1} + T^{k-1}_{si,j} \tag{3.1}$$

With the corresponding boundary conditions:

$$T^0_{si,j} = T_\infty \tag{3.2}$$

$$T^k_{si,M} = T_\infty \tag{3.3}$$

$$T^k_{s1,j} = T^k_{sN,j} = T_\infty \tag{3.4}$$

Table 4.1
The input parameters.

	Parameter	Belloufi et al. [4]	Benhammou et al. [6]	Mehdid et al. [15]
Air	ρ (kg.m^{-3})	1.2	1.1774	1.225
	Cp (J.kg^{-1}.K^{-1})	1000	1005.7	1005
	k (W.m^{-1}.K^{-1})	0.0242	0.02624	0.0242
	μ (kg.m^{-1}.s^{-1})	1.85e-5	1.983e-5	1.85e-5
Pipe	k (W.m^{-1}.K^{-1})	0.17	0.16	0.16
Soil	ρ (kg.m^{-3})	1450	2050	1340
	Cp (J.kg^{-1}.K^{-1})	880	1840	1800
	k (W.m^{-1}.K^{-1})	1.25	1.16	1.5
Geometry	R_{int} (m)	0.055	0.1	0.055
	R_{ext} (m)	0.0575	0.102	0.0575
	L (m)	47	60	47
Initial conditions	V (m.s^{-1})	3.5	0.6	3.5
	T_∞ (°C)	26	27.43	22
Time step	Δt (min)	15	60	15

at the soil-pipe interface:

$$T_{si,1}^{k} = \frac{T_{si,2}^{k} + \left(\frac{U\Delta r}{2\pi R_{ext} k_s}\right) T_{fi}^{k}}{1 + \left(\frac{U\Delta r}{2\pi R_{ext} k_s}\right)} \tag{3.5}$$

and along the adiabatic length:

$$T_{si,1}^{k} = T_{si,2}^{k} \tag{3.6}$$

The upwind scheme used to approximate the convective term in the Eq. (2.8) leads to the formula:

$$T_{fi}^{k} = \frac{T_{fi-1}^{k} + \left(\frac{U\Delta x}{\dot{m}c_p}\right) T_{si,1}^{k}}{1 + \left(\frac{U\Delta x}{\dot{m}c_p}\right)} \tag{3.7}$$

with the following boundary condition at the pipe inlet:

$$T_{f1}^{k} = T_{in}^{k} \tag{3.8}$$

As we have mentioned earlier the air temperature varies with time as a result of the time-dependent boundary conditions T_{in}^{k} and $T_{si,1}^{k}$. The Eqs. (3.1), (3.5) and (3.7) are solved simultaneously according to the following algorithm:

1. Calculate the air temperature from Eq. (3.7);
2. Calculate the temperature at the soil-pipe interface from equation (3.5);
3. Guess the soil temperature field and solve equation (3.1) to obtain a new soil temperature field, and use it as a new guess for the next iteration;
4. Repeat the previous steps until the convergence criterion $\left|\frac{\varphi_{ij}^{k} - \varphi_{ij}^{k-1}}{\varphi_{ij}^{k-1}}\right| \leq 10^{-10}$ is satisfied.

4. Results and discussion

The results presented below were obtained for an EAHE system that consists of a PVC tube buried under 3 m from the ground surface in a homogeneous soil, and operates in cooling mode with constant air velocity. The geometry of the EAHE, the thermo-physical properties, the operating conditions as well as the duration of the system operation were selected according to the experimental investigations [15,6,4] with which a comparison of the simulation results was performed (see the table below).

A conductive heat flux ratio defined as the ratio between the axial

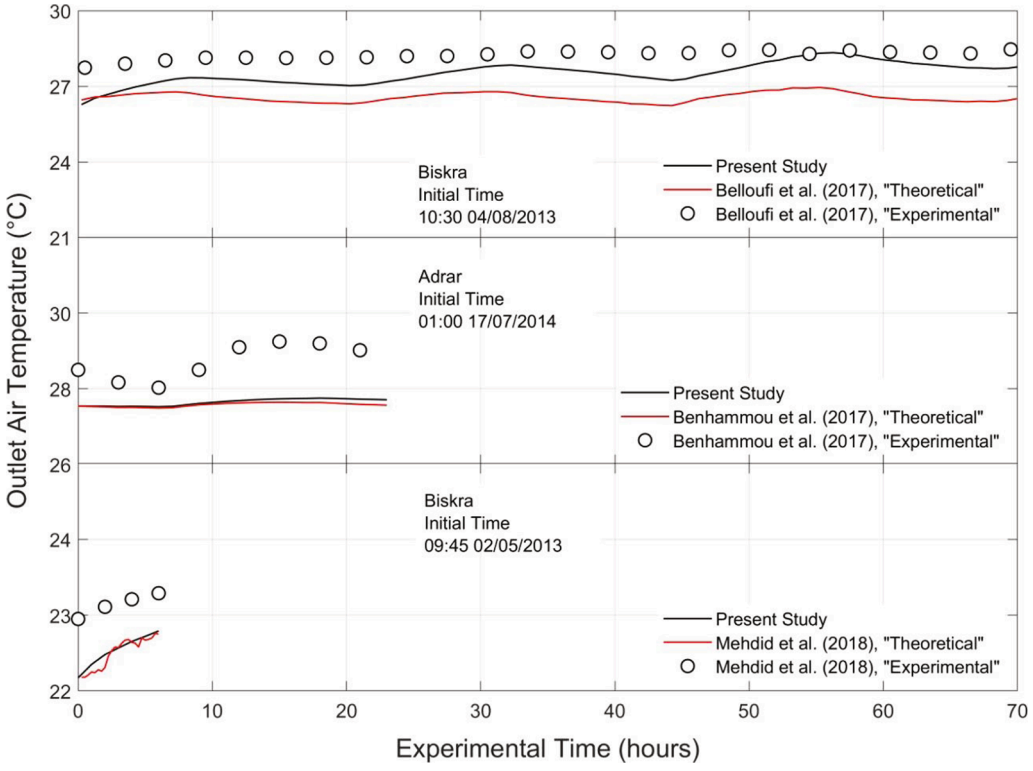

Fig. 4.1. Outlet air temperature according to time variations.

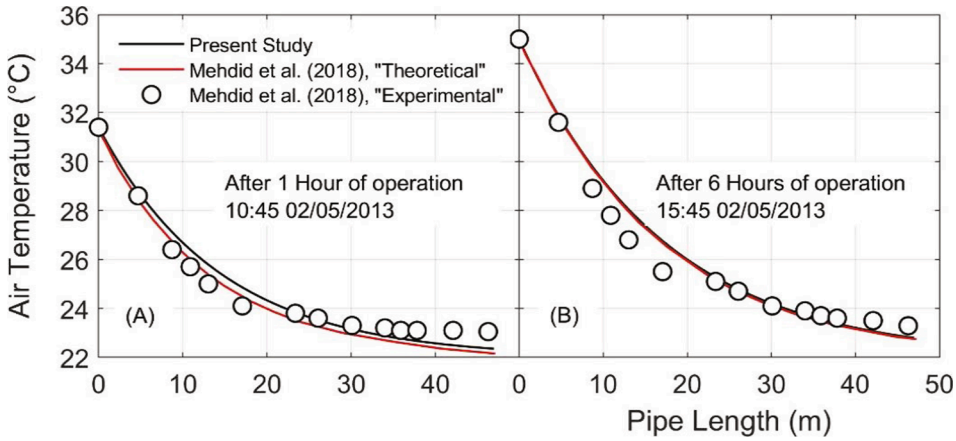

Fig. 4.2. Air temperature function by length after 1 and 6 h of EAHE system operation.

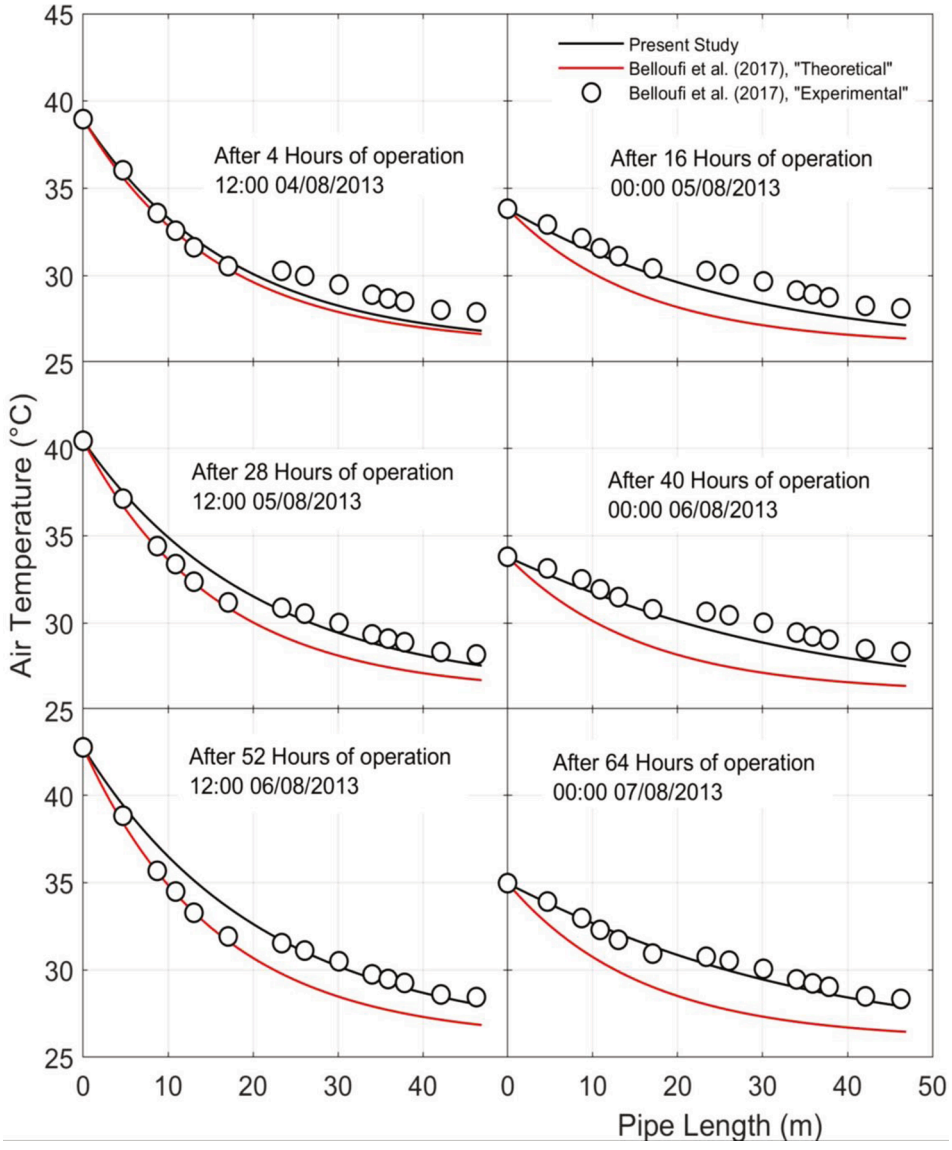

Fig. 4.3. Outlet air temperature function by length.

conductive flux leaving the soil control volume at both boundaries $x = 0$ and $x = L$, and the radial conductive flux entering the soil control volume at the boundary $r = R_o$, is calculated to verify whether or not the assumption of dominant radial (one dimensional) heat conduction in the soil Mehdid et al. [15] is supported (Table 4.1).

The Fig. 4.1 shows the variation of the outlet air temperature

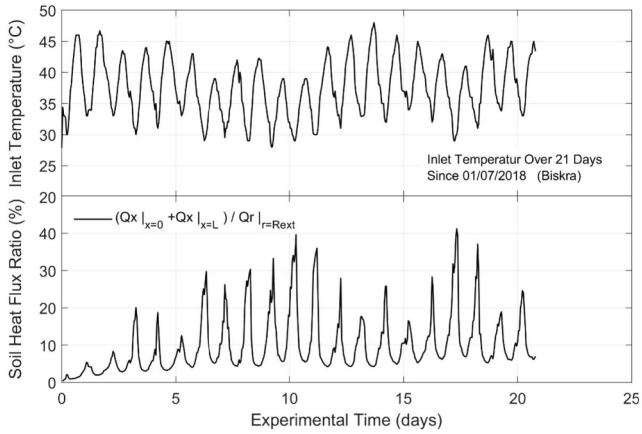

Fig. 4.4. The ambient air temperature variations for 21 days and the conduction heat flux ratio of EAHE operation in that period variations.

obtained from the numerical simulation and the data from experimental investigations Belloufi et al. [4], Mehdid et al. [15], Benhammou et al. [6] carried out in the University of Biskra in August the 4th 2013 (Fig. 4.1A) and in May the 2nd 2013 (Fig. 4.1C), and in the University of Adrar in July the 17th 2014 (Fig. 4.1B).

It can be seen that when the EAHE operates in relatively short period of time (6 and 24 h), the results from the present numerical simulation coincide with those predicted by the analytical and semi-analytical models proposed in the previous investigations; however for relatively long period of time (70 h), the numerical results are more consistent with the experimental data as compared to the analytical model of Belloufi et al. [4].

Fig. 4.2 shows the variation of the air temperature along the pipe, (A) after 1 h of operation and (B) after 6 h of operation. The two models fit well the experimental data where the close agreement between these models is probably attributed to the time of the day in which the measurement have been taken, as well as to the short period of operation of the EAHE system, as it will be better demonstrated below.

Fig. 4.3 shows the variation of the air temperature along the pipe, at daytime and at night. As it was observed for the previous figure, the present model is overall more accurate as compared to the model proposed by Belloufi et al. [4]. At daytime, when the ambient temperature is relatively high, the two models give good results that fit well the experimental data. At night, when the ambient temperature is relatively low, the present model still in very good agreement with the experimental data, while the model of Belloufi et al. [4] tends to underestimate the air temperature.

Fig. 4.4 shows the variation over time of the ambient (inlet) temperature from Laurent [14] and the corresponding numerical results of the conduction heat flux ratio in the soil using the system's thermophysical properties from Mehdid et al. [15] and the undisturbed soil temperature from the semi-finite heat conduction model [5]. The evolution of the ambient temperature is an almost-periodic function, while the evolution of the conduction heat flux ratio resembles multi-peak distribution which has the same frequency as that of the ambient temperature. It can be seen that each peak corresponds to the lowest ambient temperature recorded each day, and the peak value increases as the minimum ambient temperature decreases (the peak reaches a maximum value of approximately 40% for a minimum ambient temperature of about 28 °C between 01/07/2018 and 21/07/2018).

At daytime, temperature difference between air and undisturbed soil is maximum which leads to a maximum radial heat flux at the boundary $r = R_o$ where the greater portion is stored in the soil of initially low temperature, and the other portion is primarily diffused in the same (radial) direction, which allows neglecting the axial heat flux. At night, temperature difference between air and undisturbed soil decreases which leads to a minimum radial heat flux; on the other hand, the heat stored in the soil at daytime is diffused in all directions and evacuated from the soil control volume through the boundaries $x = 0$ and $x = L$ which reflects the contribution of axial conduction term in the soil heat conduction equation during night time.

5. Conclusions

Through the present study, we aimed to model in more detail the thermal behavior of an EAHE by investigating the validity of the hypothesis of dominant radial heat conduction in the soil surrounding the pipe, which is commonly assumed in the study of such system. It has been found that axial heat conduction can be neglected from the soil conduction equation only for high air–soil temperature differences; however, for low air–soil temperature differences, the heat conduction becomes a leading-order term in the soil conduction equation, thus, it should be taken into account. By doing so, the predictability of the previous models can be improved as it was observed from the results above especially for long periods of operation. The present simulation shows less sensitivity to the duration of operation as well as to the periodic temperature condition at the inlet of the EAHE in comparison to the previous models.

CRediT authorship contribution statement

Samia Hamdane: Conceptualization, Software, Validation, Formal analysis, Data curation, Writing - original draft, Methodology, Visualization. **Chawki Mahboub:** Conceptualization, Software, Formal analysis, Data curation, Writing - review & editing, Methodology. **Abdelhafid Moummi:** Writing - review & editing, Supervision.

Declaration of Competing Interest

The authors declare that they have no known competing financial interests or personal relationships that could have appeared to influence the work reported in this paper.

References

[1] V. Bansal, R. Mishra, G.D. Agarwal, J. Mathur, Performance analysis of integrated earth–air-tunnel-evaporative cooling system in hot and dry climate, Energy Build. 47 (2012) 525–532.
[2] V. Bansal, R. Misra, G.D. Agrawal, J. Mathur, Performance evaluation and economic analysis of integrated earth–air–tunnel heat exchanger–evaporative cooling system, Energy Build. 55 (2012) 102–108.
[3] D. Belatrache, S. Bentouba, M. Bourouis, Numerical analysis of earth air heat exchangers at operating conditions in arid climates, Int. J. Hydrogen Energy 42 (2016) 8898–8904.
[4] Y. Belloufi, A. Brima, S. Zerouali, R. Atmani, F. Aissaoui, A. Rouag, N. Moummi, Numerical and experimental investigation on the transient behavior of an earth air heat exchanger in continuous operation mode, Int. J. Heat Technol. 35 (2017) 279–288.
[5] B.E.N. Jmaa DERBEL, H. & KANOUN, O. Investigation of the ground thermal potential in tunisia focused towards heating and cooling applications Applied Thermal Engineering 30 2010 1091 1100.
[6] M. Benhammou, B. Draoui, M. Hamouda, Improvement of the summer cooling induced by an earth-to-air heat exchanger integrated in a residential building under hot and arid climate, Appl. Energy 208 (2017) 428–445.
[7] L. Bergman S. Lavine P. Incropera P. Dewitt Fundamentals of Heat and Mass Transfer 2011.
[8] BOB, D. 2018. Statistical Review of World Energy. BP. 67 ed.
[9] X. Cao, X. Dai, J. Liu, Building energy-consumption status worldwide and the state-of-the-art technologies for zero-energy buildings during the past decade, Energy Build. 128 (2016) 198–213.
[10] GINTING MANIK, S., PANJAITAN, L. & SITORUS, B. 2018. Simulation of fluid flow in an earth-air heat exchanger with the open loop system. IOP Conference Series: Materials Science and Engineering, 420, 012026.
[11] D.Y. Goswami, A.S. Dhaliwal, Heat Transfer Analysis in Environmental Control Using an Underground Air Tunnel, J. Sol. Energy Eng. 107 (1985) 141–145.
[12] P. Hollmuller, Analytical characterisation of amplitude-dampening and phase-shifting in air/soil heat-exchangers, Heat Mass Transf. 46 (2003) 4303–4317.
[13] C.-Y. Hsu, Y.-C. Chiang, Z.-J. Chien, S.-L. Chen, Investigation on performance of building-integrated earth-air heat exchanger, Energy Build. 169 (2018) 444–452.

[14] LAURENT, G. 2019. Real Time Weather Records In Biskra [Online]. Infoclimat. Available: https://www.infoclimat.fr/observations-meteo/temps-reel/biskra/60525.html.
[15] C.-E. Mehdid, A. Benchabane, A. Rouag, N. Moummi, M.-A. Melhegueg, A. Moummi, M.-L. Benabdi, A. Brima, Thermal design of Earth-to-air heat exchanger. Part II a new transient semi-analytical model and experimental validation for estimating air temperature, J. Cleaner Prod. 198 (2018) 1536–1544.
[16] S. Menhoudj, A.M. Mokhtari, M.-H. Benzaama, C. Maalouf, M. Lachi, M. Makhlouf, Study of the energy performance of an earth—Air heat exchanger for refreshing buildings in Algeria, Energy Build. 158 (2018) 1602–1612.
[17] RINKESH. 2019. Fossil Fuels Facts [Online]. Conserve Energy Future. Available: https://www.conserve-energy-future.com/various-fossil-fuels-facts.php.
[18] A. Rouag, A. Benchabane, C.-E. Mehdid, Thermal design of Earth-to-Air Heat Exchanger. Part I a new transient semi-analytical model for determining soil temperature, J. Cleaner Prod. 182 (2018) 538–544.
[19] Toshiko, K., Charlotte, G. & Kaitlyn, P. 2018. World Population Data Sheet [Online]. Population Reference Bureau (PRB). Available: https://www.prb.org/2018-world-population-data-sheet-with-focus-on-changing-age-structures/.

5TH INTERNATIONAL CONFERENCE ON ADVANCES IN MECHANICAL ENGINEERING ISTANBUL 2019, 17-19 DECEMBER 2019

HYBRID GEOTHERMAL HEAT EXCHANGER PERFORMANCE ANALYSIS

Samia HAMDANE[1], Sadam-Houcine SELLAM[1,*], Abdelhafid MOUMMI[1]

ABSTRACT

The integrated geothermal heat exchanger with an evaporative cooling system is new technology; it has been created to decrease the energy consumption of an air conditioner. It is particularly in the arid and semi-arid regions. In this paper, we are going into thermal performance analysis of the hybrid system in the summer period, for different geometrical order with different values of system effectiveness, humidity and air temperature. In certain order and for quite hot weather the system minimizes more than 20°C; this result can reduce/avoid the use of the air conditioner.

Keywords: *Air conditioner, Arid and semi-arid regions, Thermal performance, Hybrid geothermal heat exchanger system, thermal comfort*

[1] *Laboratory of Mechanical Engineering, Faculty of Science and Technology, Mohamed Khider University, Biskra, Algeria*
**E-mail address: sh.sellam@univ-biskra.dz*

Systematic Prediction of Outlet air Temperature of a Buried air/soil Heat Exchanger In arid and semi-arid regions

Conference Paper · December 2017

CITATIONS
0

READS
206

2 authors:

Samia Hamdane
Université de Biskra
2 PUBLICATIONS **0** CITATIONS
SEE PROFILE

Abdelhafid Moummi
Université de Biskra
79 PUBLICATIONS **470** CITATIONS
SEE PROFILE

First Arab Conference on Mechanical Engineering (ARCME'17)
Biskra, Algeria, December 10-11, 2017

Article Topic: **Energy Engineering**

Systematic Prediction of Outlet Temperature of a Buried air/soil Heat Exchanger In arid and semi-arid regions

Samia Hamdane[1,a *], Abdelhafid Moummi[2,b]

[1]*Département de génie mécanique, Université de Biskra, Algérie*
[2]*Laboratoire en Génie Civil, Hydraulique, Développement Durable et Environnement, Université de Biskra, Algérie*
[a] hamdane.samia5@gmail.com
[b]moummi.abdelhafid@gmail.com

Abstract. In this work, we studied the systematic prediction of the outlet air temperature in a PVC air/soil heat exchanger buried to a depth of 03 m, designed to cooling the air in summer and heating it in winter for the arid and semi-arid regions. The dynamic and thermal behavior of the system is governed by three mathematical models, ambient temperature model, soil temperature model and model of the outlet air temperature of the buried exchanger. A calculation code was written under Matlab 9.0, which allowed following as a function of time, the evolution of the outlet temperature of the air as a function of the outside and the soil temperatures.

Keywords: Systematic prediction, simulation, buried exchanger, air / soil, refreshment, heating, arid, thermal comfort.

INTRODUCTION

Cooling of the air using a buried air/soil heat exchanger or a geothermal exchanger is a technique traditionally used in the southern Algerian regions, particularly in Sahara. People build their homes in the form of cellars in order to benefit from the freshness contained in the underground during the summer period, where the heat can reach high temperatures up to 50 °C for a very long period of the month From May to October.

This new, economical, non-polluting technique consists in feeding a habitat with fresh air which is conveyed through a tube, usually made of high pressure PVC, buried at a certain depth underground, which, whatever the climatic conditions. The geothermal exchanger provides inside the habitat with fresh air during the summer and less cool air relative to the ambient temperature during winters, the thermal air inertia, air takes the role of heat transfer fluid and the pipe as a heat exchanger channeling air to the habitat.

In this work, we will start a numerical simulation study, which allowed us to predict the outlet air temperature in a PVC air/soil heat exchanger, buried to a depth of 03 m and a length of 55 m. Theoretical analysis allowed us to identify the parameters involved in the dynamic and thermal behavior of the exchanger, which are governed by three mathematical models that describe the physical phenomena that occur ; the ambient temperature model, Model of the soil temperature and model of the outlet air temperature in the buried air/soil heat exchanger.

For the prediction of the outlet air temperature in the EAHE, a calculation code was developed under Matlab 9.0, which allowed to observe the variation of the air outlet temperature as a function of the temperature evolutions of the outside air and the soil one in the 15th day of every month during a year, where the air mass flow, the exchange surface and the depth of our system for the three regions that made the context of our study are the same.

OUTDOOR TEMPERATURE MODEL

To monitor the evolution of the outlet air temperature in an air/soil heat exchanger buried during a whole day, it is important to know the daily variation of the ambient temperature, which represents, in our case, Inlet of the air in the geothermal exchanger, the thermal behavior which depends substantially on this parameter in continuous fluctuation.

The outdoor ambient temperature, also known as the outside dry temperature, is affected by several factors, such as incident solar radiation in the site, the duration of the day, the latitude and the altitude of the place under consideration, the surrounding weather conditions, Wind, close proximity to the sea and lakes as well as mountains and vegetation. In order to simulate the outside ambient temperature during a day, a prediction model was adopted, based essentially on the minimum temperature data T_{min} and the maximum temperatures T_{max} which are generally based on experimental surveys carried out over several years by meteorological stations in a geographic site considered.

In this work, a semi-empirical model has been used which was recently published by F.Chahane et al. [**1**]. This model makes it possible to observe the variations of the ambient temperature $T_{air(amb)}$ (°C), whose values are determined numerically hour by hour using the minimum and maximum values of the ambient temperature, the values of which are given by measurement stations on the web [**2**]. We took the result of the maximum and minimum ambient temperature in different region of those Curves.

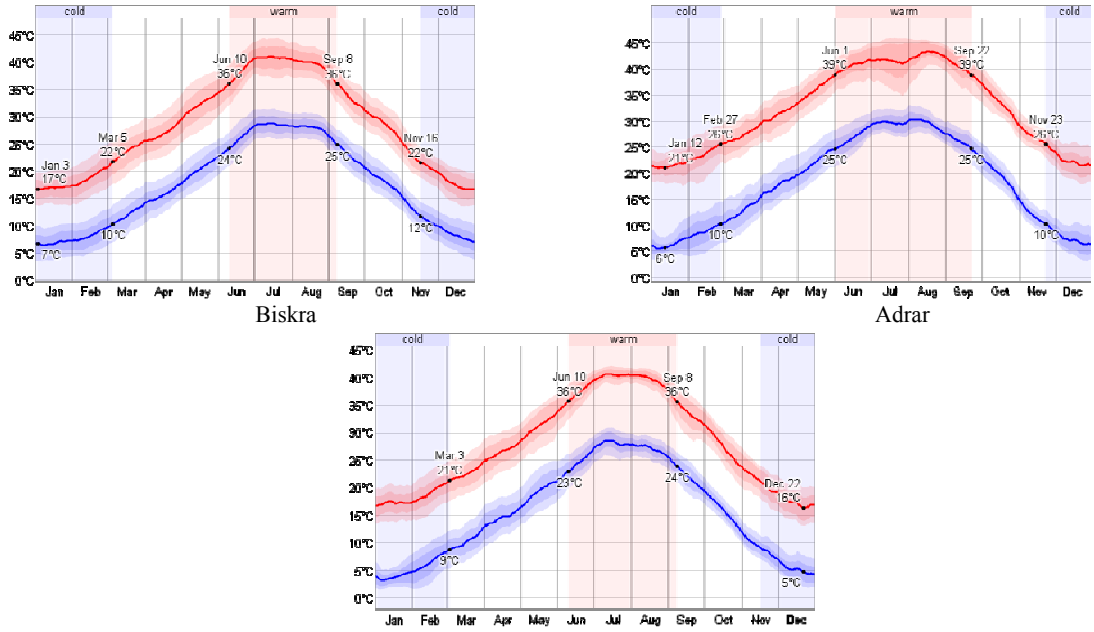

FIGURE 1. Evolution of maximum and minimum ambient temperature in Biskra, Adrar and Bechar regions. [**2**]

Ambient temperature is given by this equation [**1**]

$$T_{air-amb}(t) = T_2 + T_1 \cos\left(\frac{(14-t)\pi}{12}\right) \quad (1)$$

With, T_1 : the amplitude of the soil surface temperature variation calculated as follows (°C) :

$$T_1 = \frac{T_{\max} - T_{\min}}{2} \quad (2)$$

T_2 : the mean annual temperature calculated as follows (°C) :

$$T_2 = \frac{T_{\max} + T_{\min}}{2} \quad (3)$$

T_{max} and T_{min} respectively represent the maximum and minimum temperature of the 15th day of each month for one year. In our simulation study, Matlab was used to show the evolution and variation of the ambient temperature for the 15th day of each month, during one year using equation (1), respectively for the regions of Biskra Adrar and Behar, which are arid and semi-arid zones, characterized by a hot and dry climate in summer and very cold days In winter periods.

The simulation by Matlab showed in the form of curves the evolution of the external ambient temperature for the Biskra, Adrar and Bechar regions, respectively presented in the following Figure (2).

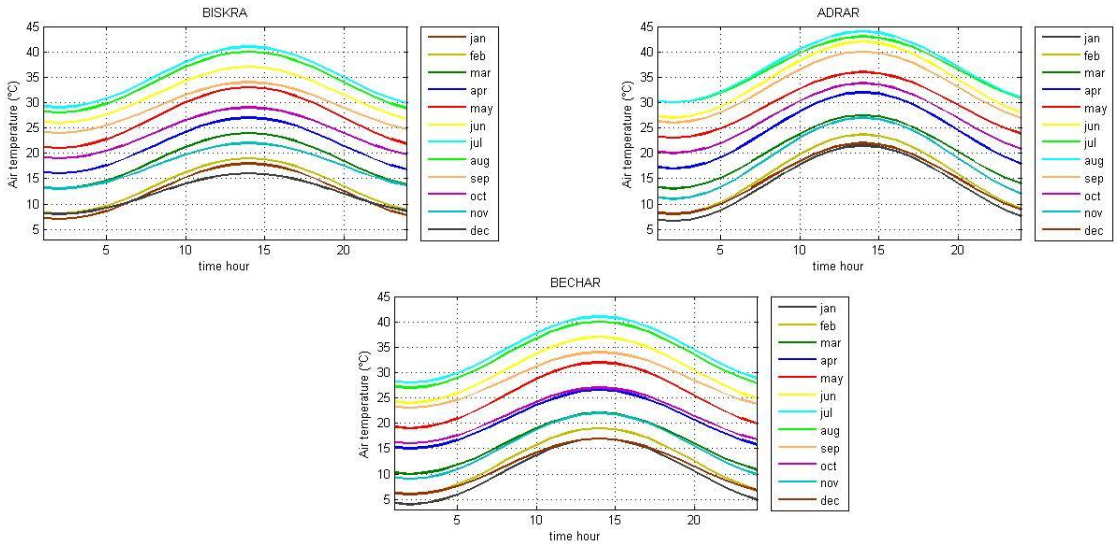

FIGURE 2. Variation of the air temperature as a function of time for Biskra, Adrar and Bechar regions.

SOIL TEMPERATURE MODEL

The assessment of the potential surface geothermal energy using buried air/soil exchanger technology requires the determination of changes over the year from soil temperature to different depths. These variations are obtained by simple modeling, which takes into account the properties of the soil and the ambient temperatures. The evolution of the soil temperature is also a function of the time (days), described by a semi-empirical relation as shown in the preceding paragraph.

The soil temperature model adopted in this work considers that the transfer of heat to the soil is one-dimensional, taking place solely by a dominant conduction, while considering that it is a homogeneous medium. The governing relation the variation of the temperature in the soil is given by the following expression [**3**]:

$$T_{soil}(z,t) = T_2 + T_1.e^{-Z\sqrt{\frac{\pi}{365\,a}}}\left[\cos\left(\frac{2.\pi}{365}.(t-t_0) - \frac{z}{2}.\sqrt{\frac{365}{\pi.a}}\right)\right] \qquad (4)$$

Where, T_{soil} : Soil temperature (°C).
Z : The depth of burial from the surface of the air/soil heat exchanger (m)
A : The thermal diffusivity (m2. days $^{-1}$)
t_0 : the day that has maximum temperature in the year (days)

A soil is characterized by three main parameters that directly influence the thermal behavior of the buried air/soil heat exchanger, mainly the evolution of the temperature of the injected air, the thermal conductivity, the density and the calorific capacity of the soil. In this simulation study we considered three types of soil that are the most responsive in Algeria, which allowed to follow the variation of the soil temperature for a depth of 03 m as a function

of time for one year (365 days) Figure.(3). The thermophysical properties of the three soil types considered in this simulation study are presented in Table (1), clay soil measurement is used for Biskra region, gypseous soil measurement is used for Adrar region and dry sand measurement is used for Bechar region.

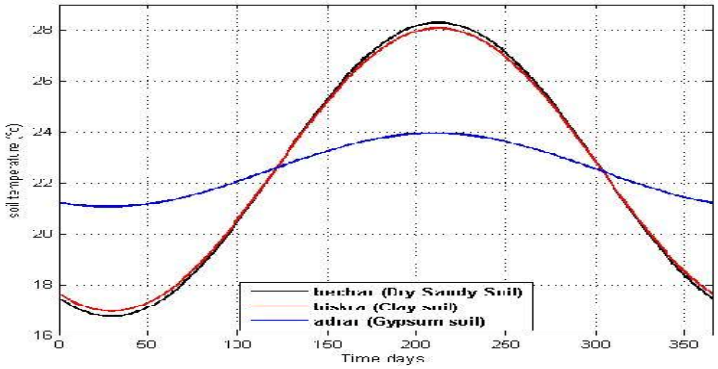

FIGURE 3. Soil temperature as a function of time for three types of soil at a depth of 03m.

OUTLET AIR TEMPERATURE MODEL

The evolution of the outlet air temperature conveyed inside the buried air/soil exchanger is obtained from the elementary thermal balance through a section of length dx of the exchanger tube. Integration from input to output gives the expression of the theoretical air temperature at a certain distance traveled by the fluid, which is described by the following mathematical model [**4**].

$$T_{air-outlet}(L) = T_{soil} + \left(T_{air-inlet} - T_{soil}\right) \cdot e^{\frac{-U}{\dot{m} \cdot C_{pair}} L} \tag{5}$$

Where , U : Total thermal resistance between air and soil ($w.m^{-1}.k^{-1}$)
Cp_{air} : Mass calorific capacity of the air ($J.kg^{-1}.k^{-1}$)
$\dot{m}$: Mass flow of air in the pipe ($Kg.s^{-1}$)
$T_{air\text{-}inlet}$: Outside ambient temperature (°C)
L : Length of tube heat exchanger (m)

$$U = \frac{1}{R_{soil} + R_{tub} + R_{conv}} \tag{6}$$

R_{soil} : is the thermal resistance between tube and soil [m.k.w-1], expressed by :

$$R_{soil} = \frac{1}{2.\lambda_{soil}.\pi} \ln\left(\frac{r_{soil}}{R}\right) \tag{7}$$

R_{tub} : is thermal resistance of buried tube [m.k.w-1] calculated by the relation next :

$$R_{tub} = \frac{1}{2.\lambda_{tub}.\pi} \ln\left(\frac{R}{r}\right) \tag{8}$$

R_{conv}, is the thermal resistance convection between air and tube [m.k.w-1], given by :

$$R_{conv} = \frac{1}{2.h_{conv}.\pi.r} \tag{9}$$

Where, r_{soil} : Radius of the adiabatic soil layer (m)
R : External radius of buried tube (m)
r : Internal radius of buried tube (m)

λ_{tub} : Thermal conductivity of the buried tube ($w.m^{-1}.k^{-1}$)
λ_{soil} : Thermal conductivity of soil united by ($w.m^{-1}.k^{-1}$)

h_{conv}, Is the convection exchange coefficient expressed by the following Nusselt relation, for a turbulent flow with in a circular duct cross-section, expressed by :

$$h_{conv} = \frac{Nu.\lambda_{air}}{2.r} \quad (10)$$

Where, λ_{air} : Thermal conductivity of the air ($w.m^{-1}.k^{-1}$)
r : internal radius of buried tube (m)

The Nusselt number is given by the following relation [**4**]:

$$Nu = 0{,}026 \cdot \mathrm{Re}^{0,8}\,\mathrm{Pr}^{0,33} \quad (11)$$

Re is the Reynolds number $\mathrm{Re} = \frac{\rho_{air} V_{air} D_{inner-tube}}{\mu_{air}}$, and Pr is the Prandtl number $\mathrm{Pr} = \frac{\mu_{air}.Cp_{air}}{\lambda_{air}}$

Where, ρ_{air} : Density of air ($Kg.m^{-3}$)
V_{air} : Average air flow rate inside the buried air /soil exchanger ($m.s^{-1}$)
μ_{air} : Dynamic viscosity of the air ($kg.m^{-1}.s^{-1}$)
$D_{inner-tube}$: Inside diameter of buried exchanger pipe (m)

To simulate the evolution of the outlet air temperature conveyed in the geothermal exchanger buried by equation (5). We consider the thermo-physical and geometrical proprieties for air, soil, and the buried exchanger which are given in the following table (1).

Table.(1) : *Thermo physical heat exchanger tube proprieties* [**3,4,5**].

	λ_{tube} (w/m.k)[a]	λ_{soil} (w/m. k)[b]	r (m)[c]	R (m)[d]	R_{soil} (m)[e]	L (m)[f]
Biskra region	0,17	1,5	0,11	0,113	0,125	55
Adrar region		0,52				
Bechar region		2,1				

[a]: Thermal conductivity of the buried tube ($w.m^{-1}.k^{-1}$).
[b]: Thermal conductivity of soil ($w.m^{-1}.k^{-1}$).
[C]: Internal radius of buried tube (m)
[d] : External radius of buried tube (m)
[e] : Radius of the adiabatic soil layer (m)
[f] : Length of tube heat exchanger (m)

RESULTS AND DISCUSSION

The numerical simulation was executed using Matlab 9.0 software, which is possible to observe the variation of the outlet air temperature as a function of the ambient air and the soil temperatures, at 15th day of every month during one year, where the air mass flow rate $\dot{m}$ = 0,05 kg/s, the exchange length L = 55 m, the burial depth Z = 03 m are kept constant for the three regions that made the context of our study. In this paper we present only the results of December and July, which are a coldest and hottest periods of the year.

In winter, during the months of December and January outdoor ambient air temperatures range from 5 to 22 ° C figures(4,5,6) during the day. However, the outlet air temperature at the buried exchanger is at a constant value about 17 to 20 ° C during the day. The geothermal heat exchanger functions as an air heating device, despite the disturbances surrounding it, especially during very long night periods where the outside temperatures are very low.

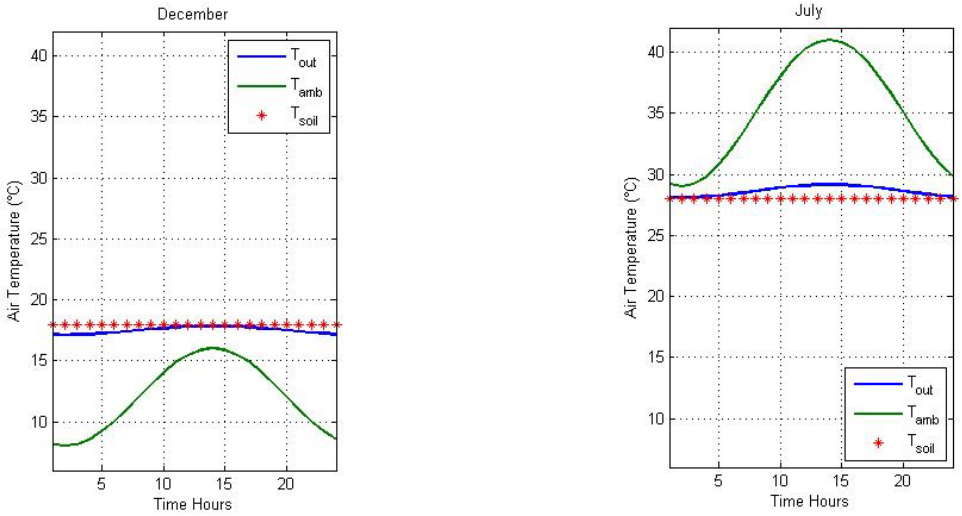

FIGURE 4. Evolution of the outlet temperature for the 15th days of December and July in Biskra region.

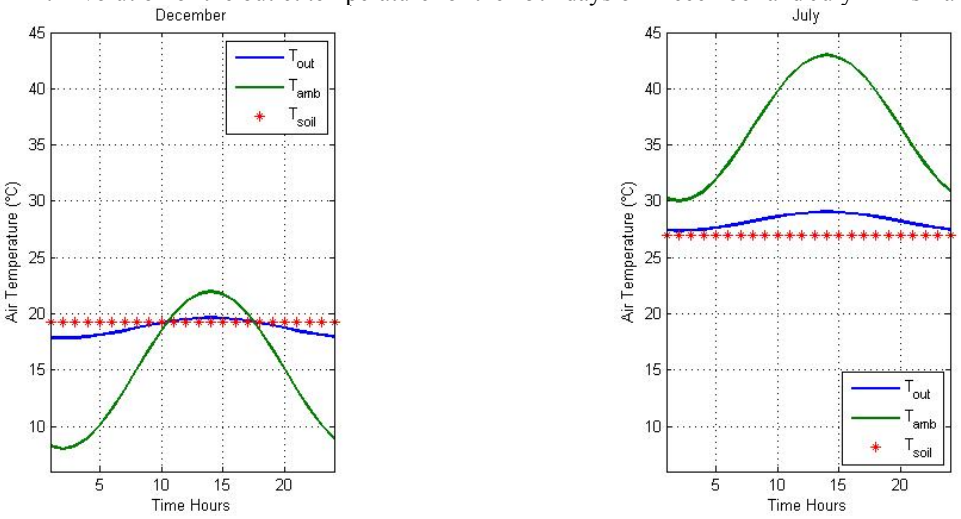

FIGURE 5. Evolution of the outlet temperature for the 15th days of December and July in Adrar region.

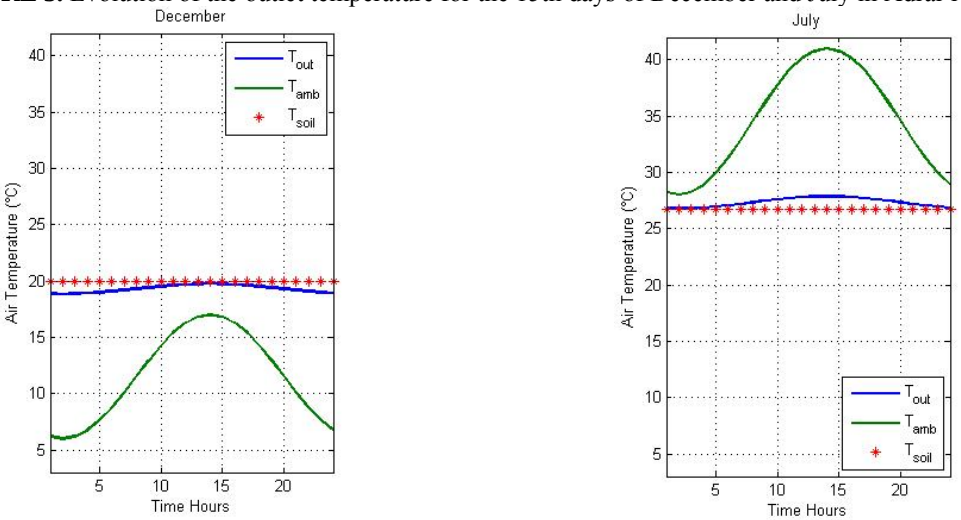

FIGURE 6. Evolution of the outlet temperature for the 15th days of December and July in Bechar region.

In summer, outdoor ambient temperatures are generally between 25 and 45 °C, especially during the months of June, July and August. The geothermal heat exchanger allowed fresh air to be supplied at constant temperatures throughout the day from 26 to 28 °C. The system operates as an air freshening device, which corresponds to the thermal comfort conditions inside the houses located in the arid and semi-arid areas, especially during periods of high temperature.

CONCLUSION

In this theoretical study, a systematic prediction of the outlet air temperature in a buried air/soil heat exchanger is realized, respectively in 03 arid and semi-arid regions Biskra, Adrar and Bechar. A numerical code has been written in Matlab, based on three theoretical models the ambient, soil and the outlet air temperature.

The analysis of the obtained curves shows that the outlet air temperature of the heat exchanger reaches the soil temperature, in winter and in summer, this observation shows that the buried air/soil exchanger functions as a device for heating in winter, where the temperature of the air supplied is in the vicinity of 17 to 23 ° C, relative to that of the outside generally less than 5 °C at night and at about 15 °C on day. Furthermore, it ensures favorable cooling conditions during the summer period, where the air temperature is between 23 and 28 ° C, relatively lower than the ambient temperature during the day between 28 and 45 °C.

REFERENCES

1. F.Chabane, N.Moummi, A.Brima, A.Moummi, Prediction of the theoretical and semi-empirical model of ambient temperature, Front. Energy, 10, 3, 268-278, (2016).
2. https://weatherspark.com/y/51506/Average-Weather-in-Biskra-Algeria, Web site viewed on 04 Mars 2017
3. D.Belatrache, S. Bentoub and M.Bourouis, Numerical analysis of earth air heat exchangers at operating conditions in arid climates, International Journal of hydrogen energy, 42, 13, 8898-8904, (2017).
4. Salah Eddine.AD, Dimensionnement d'un échangeur air/sol enterré destiné au rafraichissement de l'air, mémoire de Master, Université de Biskra, 2015, Algérie.
5. N.Hatraf, F.Chabane,N.Moummi, A.Brima, A.Moummi, Parametric Study of to Design an Earth to Air Heat Exchanger with Experimental Validation, Engineerin Journal, 18, 2, 41-54, (2014).
6. A. Sehli, A.Hasni, M.Tamali, The potential of earth-air heat exchangers for low energy cooling of buildings in South Algeria, Energy procedia, 18, 496-506, (2012).
7. N. Moummi, H. Benfatah, N. Hatraf , A. Moummi et S.Youcef Ali, Le rafraîchissement par la géothermie: étude théorique et expérimentale dans le site de Biskra, 'revue des Energies renouvelables' Vol. 13 N°3 pp399-406, (2010).

ملخص :

في هذا العمل، قمنا بدراسة العوامل المؤثرة لمبادل حراري هوائي/ أرضي مدفون مخصص للتسخين شتاءا وللتبريد صيفا، خاصة في المناطق القاحلة وشبه القاحلة. بعد دراسة ببليوغرافية لبعض الأعمال المتعلقة بالموضوع. تم تقديم دراسة نظرية، حيث حاولنا من خلالها استعمال ثلاثة نماذج رياضية يمكنها تتبع و وصف تطور درجة حرارة الهواء من مدخل المبادل الحراري إلى المخرج. الدراسة التجريبية تتكون من جزأين، دراسة الخصائص الفيزيائية والكيميائية لبعض أنواع التربة في المناطق القاحلة وشبه القاحلة في الجزائر، ثم من خلال المعلومات المسجلة من درجة حرارة التربة السنوية التجريبية ودرجة حرارة الهواء السنوية، تمكنا من متابعة التغير في درجة حرارة التربة على أعماق مختلفة مما جعل من الممكن معرفة الفرق بين استخدام بيانات التربة وبيانات الهواء في النموذج الرياضي للتنبؤ بدرجة حرارة التربة. أخيرًا، قمنا بتطوير نموذج رياضي يمكنه تنبأ بدرجة حرارة الهواء الخارج من المبادل الحراري، لتوضيح أهمية الانتشار الحراري الأفقي حول أنبوب المبادل أثناء عملية الانتشار الحراري، والتي تم تجاهلها بشكل عام في الأعمال العلمية السابقة.

الكلمات المفتاحية : دراسة العوامل المؤثرة، مبادل هواء / تربة مدفون، تدفئة، تبريد، جاف، راحة حرارية.

Abstract:

In This Work, we are interested in a parametric study of a buried air/soil heat exchanger intended for heating in winters and cooling in summer the habitat, particularly in arid and semi-arid regions. After a bibliographical study devoted to certain works in relation to the theme. A theoretical study was presented, where we tried through three main governing models to describe the evolution of the air temperature from the heat exchanger inlet to the outlet. The experimental investigation consists of two parts, a physicochemical characterization study of some soil types took from the arid and semi-arid regions of Algeria, then through parameters recorded from the experimental annual soil temperature and annual air temperature, we were able to follow the variation of the soil temperature at different depths, what made it possible to observe the difference between using soil data and air data in the mathematical model to predict the soil temperature. Finally, we have developed a mathematical model predicts the outlet air temperature of the heat exchanger, to illustrate the importance of horizontal thermal diffusion around the system pipe during the heat exchange process, which has been generally overlooked in previous scientific work.

Keywords : Parametric Study, Buried air / soil Exchanger, Heating, Cooling, Arid, Thermal comfort.

Résumé :

Dans ce travail on s'intéresse à une étude paramétrique d'un échangeur de chaleur air/sol enterré destiné aux réchauffement en hivers et le rafraîchissement en été des locaux, notamment dans les régions arides et semi-arides. Après une étude bibliographique consacrée à certains travaux en relation avec le thème. Une étude théorique a été présentée, où on a essayé à partir de trois principaux modèles gouvernants de décrire l'évolution de la température de l'air de l'entrée de l'échangeur jusqu'à la sortie. L'étude expérimentale comporte deux parties, une étude de caractérisation physico-chimique de quelques types de sol dans les régions aride et semi-aride de l'Algérie, ensuite à travers des mesures expérimentales annuelles, on a pu suivre la variation de la température du sol à différentes profondeurs ce qui a rendu possible la prédiction par un modèle mathématique les données de la température du sol et de l'air. Enfin, on a développé un modèle mathématique qui prédit la température de l'air sortant de l'échangeur de chaleur, pour illustrer l'importance de la diffusion thermique horizontale autour du conduit enterré pendant le phénomène d'échange thermique généralement négligé dans les travaux scientifiques antérieurs.

Mots clés : Etude paramétrique, Echangeur Air/ Sol enterré, Réchauffement, Rafraichissement, Arides, Confort thermique.